EFFECT OF DIMENSIONAL VARIATION, MANUFACTURING PROCESS, AND MATERIAL ON PERFORMANCE OF FLUDIC OSCILLATOR

A Dissertation
Presented to
The Academic Faculty

by

Viyat Viral Jhaveri

In Partial Fulfillment
of the Requirements for the Degree
Master in Mechanical Engineering in the
School of Mechanical Engineering

Georgia Institute of Technology
May 2017

EFFECT OF DIMENSIONAL VARIATION, MANUFACTURING PROCESS AND MATERIAL ON PERFORMANCE OF FLUDIC OSCILLATOR

Approved by:

Dr. Jonathan Colton, Advisor
School of Mechanical Engineering
Georgia Institute of Technology

Dr. Ari Glezer
School of Mechanical Engineering
Georgia Institute of Technology

Dr. Tequila Harris
School of Mechanical Engineering
Georgia Institute of Technology

Date Approved: January 5, 2017

ACKNOWLEDGMENTS

I would like to thank all those who have helped me throughout this project and this thesis, without whom I would not a have been able complete this work.

First, I would like to thank Dr. Jonathan Colton (Georgia Tech) for giving me the opportunity to do research with him, work on this project, and for providing invaluable advice through the entire process. Under his advisement, I have become a better researcher and engineer. I would like to thank the GT-Boeing Strategic University Partnership Program for funding this project. I would like to thank Dr. Pete George (Boeing), Dr. Abe Gissen (Boeing), Dr. Debbie Radasch (Boeing), and Dr. Howard Appelman (Boeing) for providing the scope, guidance, and support for the project. I am grateful for the incredible support I received from individuals at Georgia Institute of Technology (Georgia Tech) and at The Boeing Company (Boeing).

I would like to thank Dr. Ari Glezer (Georgia Tech) and Dr. Michael DeSalvo (Georgia Tech), for their support throughout the project. I would like to thank Dr. DeSalvo for performing the tests on the fluidic oscillators, discussing the results of the tests and providing guidance on the analysis. Additionally, I would like to thank Dr. Glezer and Dr. Tequila A.L. Harris (Georgia Tech) for serving on my committee. I would like to thank the members from my research group, including Jason Li and Ahmed Aly, for getting the project started and providing thoughtful discussions. I would like to thank members of the Georgia Tech ME Machine Shop, Steven Sheffield, Louis Boulanger, and Brandon Royal, for manufacturing the fluidic oscillators for testing. I would like to thank Chris White (Georgia Tech) for providing access to instruments that I used to measure the fluidic oscillators.

Finally, I would like to thank my family and friends who made this experience possible and memorable.

TABLE OF CONTENTS

LIST OF TABLES

LIST OF FIGURES

LIST OF SYMBOLS AND ABBREVIATIONS

A	Area
AFC	Active Flow Control
ANOVA	Analysis of Variance
APU	Auxiliary Power Unit
b	Jet Slot Width
C_1	Constant for Pressure Model
C_2	Constant for Pressure Model
CF	Carbon Fiber
CNC	Computer Numeric Control
EDM	Electric Discharge Machining
f	Oscillation Frequency
$f+$	Dimensionless Frequency
FDM	Fused Deposition Molding
FO	Fluidic Oscillator
γ	Specific Heat Ratio
I_j	Time Average Jet Momentum
L/D	Lift to Drag Ratio
L_{noz}	Nozzle Width
L_{sh}	Shoulder Width
M	Mach Number
P_{atm}	Atmospheric Pressure
P_{pl}	Plenum Pressure

P_r	Pressure Ratio
PEKK	Polyetherkeytonekeytone
R	Gas Constant
Re	Reynolds Number
ρ_j	Jet Air Density
Q	Flow Rate
SDBD	Single Barrier Dielectric Discharge
SLA	Stereolithography
SLS	Selective Laser Sintering
t	Time
τ	Time Period / 2
u_j	Phase Averaged Jet Velocity
ν	Kinematic Viscosity

SUMMARY

The use of active flow control (AFC) on civil transport aircraft flaps can delay stall at low aircraft speeds. This can lead to reducing the size of flaps or removing them from aircraft, which can reduce the part count, weight, and manufacturing cost of the aircraft. In addition to these changes, the cruise drag can also be reduced, which leads to lower fuel burn, hence lower costs and emissions. This technology works by energizing the boundary layer using an AFC device, a fluidic oscillator (FO) in this thesis, to prevent flow separation. However, the effects of material, manufacturing process, and dimensional variation on these parts is not entirely known.

In this work, the key performance characteristics, also referred to as the functional requirements of the FO, were identified to be the coefficient of momentum and the oscillation frequency. The operational requirements of the FO were identified to be the fluidic power requirement and the ability to withstand pressure, significant temperature variations, and fluctuations in humidity. The materials that are explored include aluminum and carbon fiber PEKK. The manufacturing processes that were explored include machining, selective laser sintering (SLS), stereolithography (SLA), and injection molding. Variations in the dimensions were explored: nozzle width, nozzle length, nozzle radius, nozzle symmetry, nozzle curvature, and interaction chamber width. These were tested using a bench test setup.

It was concluded that material had no impact on the performance of the FO, given stiff enough materials and those that can be manufactured to the required tolerances. The manufacturing process did affect the performance of the FO as it caused changes in the

geometry of the FO. The changes included the inability of SLS, SLA, and injection molding to produces edges as sharp as can be produced by machining. As a result, the devices had lower pressure drops and higher oscillation frequencies, which are beneficial. It was also identified that nozzle width, shoulder width, and nozzle radius affected the oscillation frequency and that the nozzle width and nozzle radius affected the pressure drop. Nozzle symmetry and nozzle length did not affect the oscillation frequency and pressure drop; however, they did affect the jet profile. Lastly, the nozzle curvature did not have any effect on the performance of the FO. Additionally, the point at which the performance of the FO deviates from the model was identified, which corresponds to where the oscillation frequency is no longer dependent on the flow rate. Using this information, a dimensionless model was developed that can be used by FO designers to predict the pressure drop and oscillation frequency of the FO based on the dimensions of the FO.

CHAPTER 1. INTRODUCTION

The field of flow control began after the discovery of the boundary layer by Prandlt in 1931 (Gad-el-Hak et al. 1998). This discovery provided a deeper understanding of flow over surfaces and paved the way for advancements in flow control devices, which include flaps. Recently, active flow control (AFC) devices have gained popularity due to the potential benefits of applying AFC technology to civil transport aircraft. It was determined by McLean et al. (1998) that integrating flow control into aircraft flaps could reduce the part count by 2.9%, empty weight by 3.3%, recurring manufacturing costs by 1.3%, and cruise drag due to weight by 1.9% when using a Boeing 737-700 aircraft as the reference. A further 1.3% reduction in cruise drag can be achieved due to the decrease in the size of fairings. Thus, integrating this technology would not only reduce the aircraft manufacturing cost, but also reduce fuel consumption leading to lower emissions.

Extensive research has been done on utilizing a type of AFC device called a fluidic oscillator (FO) to delay flow separation. A fluidic oscillator works by two jets interacting in an interaction chamber which creates unsteady jet oscillations, as can be seen in Figure 1. This jet is expelled onto the boundary layer of the wing, providing energy to prevent the jet from detaching before it reaches the trailing edge of the airfoil. The Boeing 757 ecoDemonstrator showed the benefits of using FOs on the vertical tail in a full-scale flight test (Lin et al. 2016). Extensive research has also been conducted through a collaboration between The Boeing Company (Boeing) and Georgia Institute of Technology (Georgia Tech) to test the benefits of using this technology on trailing edge flaps (DeSalvo et al. 2011, Kuchan 2012, DeSalvo et al. 2014, Li 2016). They have quantified the benefits

through bench and wind tunnel testing and evaluated the manufacturing and integration of this technology. However, work still needs to be done to fully quantify the effects of the material, manufacturing process, and variation in geometry that are expected due to manufacturing tolerance. This work serves as a continuation of the work done by Li (2016) into the testing of FOs.

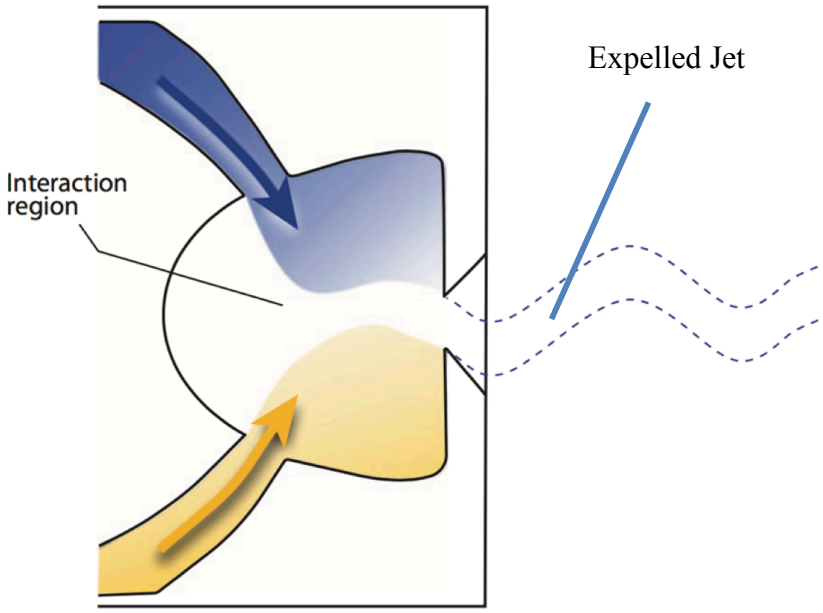

Figure 1 - Fluidic Oscillator Schematic (Cattafesta and Shelpack 2011)

The primary objective of this work is to understand the effects of geometric variation, material, and manufacturing process on the performance of a fluidic oscillator. Performance refers to the oscillation frequency of the oscillator, pressure drop across the oscillator, and the jet profile of the oscillator. The performance will be determined by bench testing the oscillator. The effect of geometric variation will be tested by varying critical dimensions of the oscillator and correlating that to a change in performance of the

oscillator. The effect of material changes will be tested by producing oscillators from different materials and comparing their performance. The effect of the manufacturing process will be determined by producing oscillators using different manufacturing processes and comparing their performance. These data will be used to develop a design tool that can be used for the FO designer to understand the effect of varying the critical dimensions. By collecting these data and understanding the operating conditions, the FO designer can utilize wind tunnel tests that have already been conducted to predict the control authority of the FO. In addition to this, functional and operational requirements of the FO are also discussed.

In this work, Chapter 2 covers the background of Active Flow Control, the different types of AFC devices, how they operate, and how they can be manufactured and assembled. Chapter 3 covers the functional and operational requirements of the FO and the materials and manufacturing processes that are considered for producing the FO. The critical dimensions of the FO are also explored. Chapter 4 covers the different test specimens that are produced and the experimental design and methodology. Chapter 5 presents the data from these tests, determines the critical dimensions, and develops a model to characterize the performance of the FO using these dimensions. Chapter 6 discusses the critical parameters of the FO including the limits of the model, the sensitivity of the critical dimensions, and the effect of material and manufacturing process on the FO. Lastly, Chapter 7 provides the concluding remarks for this work and recommendations for future work.

CHAPTER 2. BACKGROUND

To gain a better understanding of the scope of the project and to identify the knowledge gaps and challenges in integrating active flow control devices into aircraft, it is important to review the research that has been conducted in this field. The two main areas explored include:

1. AFC Technology: the benefits of using AFC devices, the different types of AFC devices and previous work done to understand feedback-free FOs.

2. FO Manufacturing: the different materials and manufacturing process that have been used to make the FOs and common materials and processes used in the aerospace industry.

This will help guide the scope of this thesis. It is assumed the reader has basic knowledge of aerodynamic concepts, such as lift and drag, and aerodynamic terminology, such as angle of attack and leading edge.

2.1 AFC Technology Review

2.1.1 AFC Performance Benefits

Aircraft flaps exist to improve lift during low speed flight, allowing for slower take-off and landing speeds. This is achieved by actuating the flap to increase the angle of attack of the wing, hence improving its lift characteristics (Lan and Roskam 1981). However, if

the flap angle is severely increased or speed is greatly reduced, then the flow can detach from the flap, stalling the aircraft. To prevent this, more complicated, and as a result heavier flaps such as slotted and fowler flaps have been utilized by aircraft designers (Lan and Roskam 1981). Boundary layer control devices, which include FOs, have been shown to delay flow separation, allowing the flap to generate more lift by keeping the flow attached to the surface (Dole and Lewis 2000). To gain a better understanding of how this technology works, it is important to understand the boundary layer.

2.1.1.1 Boundary Layer

A boundary layer exists because a fluid that is close to an object moves slower than the free stream due to viscous effects (Munson et al. 2013). This can be seen in Figure 2**,** where the fluid near the plate is moving at the same velocity as the object and the fluid at the edge of the boundary layer is moving at 99% of the free stream velocity. This boundary layer determines the maximum lift a wing can generate and the stall characteristics of the aerodynamics surface (Dole and Lewis 2000).

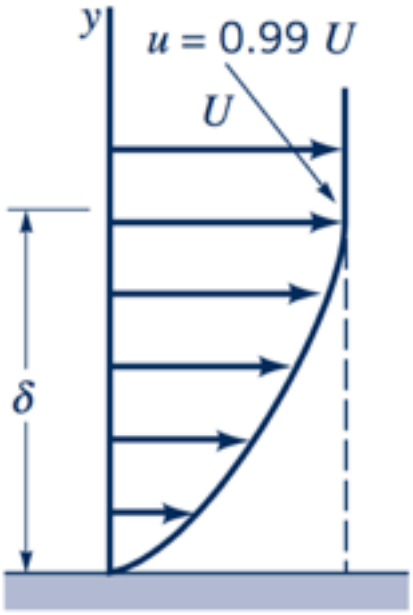

Figure 2 - Laminar Boundary Layer (Munson el al. 2013)

A typical airfoil surface has a low-pressure region on the top surface and a high-pressure region on the bottom surface (Dole and Lewis 2000). The pressure of the air stream that passes over the top and under the bottom of the wing is the same at the leading and trailing edges of the airfoil, thus there exists a point of minimum pressure on the top surface of the wing. As the air approaches this point of minimum pressure, it accelerates by Bernoulli's principle, and once it passes this point, it decelerates until it reaches the trailing edge. The jet stream loses energy as it travels along the adverse pressure gradient, and if the stream depletes its energy before it reaches the trailing edge, then the flow will detach from the surface (Dole and Lewis 2000). If this occurs, the wing will stop producing lift and the aircraft will stall (Lan and Roskam 1981).

There are two main reasons for stall - reduced velocity of the aircraft and increased angle of attack (Dole and Lewis 2000). During take-off and landing, both occur as the flaps

are deployed and the aircraft is moving at a slower speed than at cruise. Many devices can be used to prevent flow separation, which are explored in the next section.

2.1.1.2 Flow Control

The field of flow control began to take shape after Pranldt's discovery of and experiments with boundary layers (Gad-el-Hak et al. 1998). It is a very broad field; hence, it will not be explored in the thesis. The aspect that is of interest is flow control to manipulate the boundary layer for aerodynamic benefits. Within the scope of this thesis, a flow control device is any device that can delay, transition or postpone separation, increase lift, reduce skin-friction and pressure drag, augment turbulence, enhance heat transfer, or suppress noise (Gad-el-Hak et al. 1998). The oscillators explored in this thesis are used to delay flow separation on flaps to improve lift at low speeds during take-off and landing. These devices fall into two main categories - passive flow control and active flow control.

A passive flow control device achieves the goal without expending energy. An example of a passive flow control device is a slotted flap. This is currently used on Boeing 787 aircraft and allows for air from under the wing to flow over the flap. This energizes the boundary layer, thereby delaying flow separation (Dole and Lewis 2000). Other examples of passive flow control devices include vanes, slats, and fins. As this thesis focuses on active flow control, these will not be explored.

Active flow control can be described as the addition of energy via an oscillator (Cattafesta and Shelpack 2001). Hence, any device that meets this definition is an AFC device. These devices can be placed in various locations including the leading edge of the wing, wing main bodies, and trailing edge flaps. They are typically placed on the leading

edge of a flap (Dole and Lewis 2000). There are two main types of AFC devices that can be used to delay flow separation - suction and blowing devices.

Suction devices work by removing the layer of air closest to the aerodynamic surface, allowing for higher energy air to replace the removed air. As this air has more energy, there is a greater likelihood for it to reach the trailing edge before separation occurs (Lan and Roskam 1981). The second type are blowing devices that work by adding a layer of energized air to the surface, keeping the flow attached to the surface of the wing (Lan and Roskam 1981). They provide the air stream with energy to reach the trailing edge of the wing without separating from the airfoil.

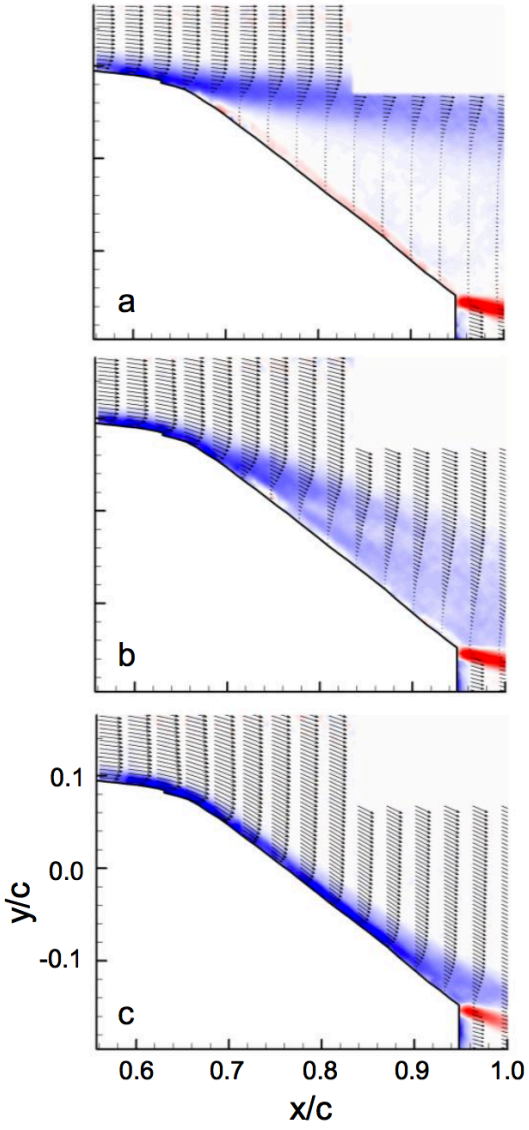

Figure 3 – Flow field on δ = 20o flap; span wise oscillators 26^{o} above the local surface tangent. Cμ = 0 (a), 0.3% (b), 1.6% (c) (DeSalvo 2015)

Figure 3 shows the effect of utilizing a FO by visualizing the flow field over a flap with and without the FOs. Figure 3a shows that the flow separates from the aerodynamic surface when the FOs are not activated. Whereas Figure 3c shows that the flow stays attached to the aerodynamic surface.

2.1.1.3 Performance Benefits

It is understood that these devices can delay flow separation, however it is important to quantify these effects. This can be used to determine if the system is beneficial at a high level. Therefore, it is important to explore the work that has been done to quantify the benefits of AFC devices.

The simplest type of actuators that have been utilized are blown flaps. This technology was utilized on the Hunting H.126, Balls- Bartoe Jetwing (Mason 2012), C-8A De Havilland Buffalo (Gologan 2010), and V/STOL applications, such as the ShinMaywa US-1A and the Lockheed F-104 "Starfighter" (Meyer et al. 2014). These tests used steady state blowing of air over the flap of a wing to achieve the desired benefits of flow control. Although these devices had benefits, it has been shown that there are significant advantages to using unsteady forced jets as opposed to steady state blowing (Greenblatt and Wygnanski 2000).

FOs have been tested on the vertical tail of an aircraft at several scales. The first set of tests was done by Rathay et al. (2014) during a 1/19th scale wind tunnel test. They showed that the using FOs can increase the side slip force on the vertical tail by a maximum of 20% when no side slip angle exists and 34% when side slip angle does exist. They also discovered that the oscillators in the midsection were the most effective at moderate rudder deflections and the oscillators at the base were most effective at large rudder deflections. As the separation propagates from the tip to the base, this finding suggests that the oscillators closer the point of flow separation are the most effective.

Another full-scale test was conducted at the NASA Ames Research Center wind tunnel (Lin et al. 2016). This test showed that side force increased by up to 20% at 0º and -7.5º side slip angles. They also discovered that the momentum coefficient is a useful parameter for scaling the oscillators. The data from these tests were used to successfully test this technology on the 757 ecoDemonstrator (Lin et al. 2016). The full-scale test showed a side force increase of 13% to 16% at an estimated 30º rudder deflection.

The primary objective of the oscillator that is explored in this thesis is to improve lift on wing flaps for take-off and landing. Although no large scale testing has been done for this application, testing has explored the effects of using FO to delay flow separation and improve lift by DeSalvo et al. (2014). They attached an array of oscillators on the leading edge of a fowler flap and showed that using fluidic oscillators increased the coefficient of lift from 2.37 to 2.83. This suggests that there are potential benefits of utilizing the technology on aircraft flaps.

This section provided an overview of the physics behind active flow control and the basic principles that explains how it works. Additionally, previous studies that utilize active flow control are also explored and have shown that there are clear aerodynamic benefits in utilizing active flow control. The next section explores the parameters that characterize the performance of active flow control devices, which are useful to characterize their performance in a bench test.

2.1.2 Key Performance Characteristics

To effectively compare different oscillators, it is important to understand the key performance characteristics and how they affect the control authority of the oscillator when

installed on an airfoil. Control authority is a metric of oscillator performance and refers to the velocity momentum vorticity flux and body force (Cattafesta and Shelpack 2011). This allows for independent testing of the oscillator. The two main performance characteristics of the jet includes the jet momentum and the oscillation frequency.

2.1.2.1 Coefficient of Momentum

The momentum flux of the jet is a measure of its thrust. The jet momentum coefficient is calculated using Equation 1,

$$I_j = \frac{1}{\tau}\rho_j b \int_0^\tau u_j^2(t)dt \quad (1)$$

where I_j is the time average jet momentum, τ is half the time period, ρ_j is the jet air density, b is the jet slot width, and u_j is the phase averaged velocity at the jet exit plane. Hence, increasing the velocity of the jet will increase the momentum coefficient of the jet. Additionally, increasing the slot width will also increase the jet momentum coefficient; however, that might affect the velocity of the jet.

Experiments performed by Goodfellow et. al. (2013) varied the frequency and the jet momentum coefficient of fluidic oscillators. It was shown that the jet momentum coefficient is the governing factor in the performance of the jet. They showed that increasing the jet momentum coefficient while controlling the frequency shifted the separation point further down the airfoil. They also showed that there is a threshold for the jet momentum coefficient which causes a large change in the separation point and that large changes above and below that point do not create significant changes in the separation location. Similar observations were made with drag reduction, where a large reduction in

drag was seen when the jet momentum coefficient threshold was crossed, which was similar to the threshold for moving the jet separation point. This suggests that a certain amount of energy is required to gain benefits from utilizing FOs and this could be the energy required by the air stream to reach the trailing edge of the airfoil.

As the oscillator that was used in the study was a piezo-electric synthetic jet oscillator, there was a resonant frequency at which the momentum coefficient peaks. Although the jet momentum coefficient is the governing characteristic for the performance of an oscillator, this coefficient was largely dependent on the jet oscillation frequency due to this resonant behavior (Goodfellow et al. 2009). Therefore, it is important to understand the behavior between the jet momentum coefficient and the frequency of oscillation.

One major disadvantage of utilizing the jet momentum coefficient as a parameter to predict performance is the difficult to measure it. This is because the momentum coefficient is dependent on the airfoil on which the FO is installed; hence, it is not a useful parameter to measure during bench testing. As a result, the mass flow rate is used to characterize the FO instead of the momentum coefficient of the jet (Li 2016). If the mass flow rate, along with other operation conditions of the FO, are known, then existing wind tunnel tests can be used to predict the performance of the FO.

In summary, it is important to maximize the jet momentum coefficient as this is the amount of energy that jet adds to the stream and governs the effectiveness of the fluidic oscillator. However, for the scope of this thesis, due to the difficulty of measuring the coefficient of momentum, the mass flow rate will be used. As this is an input parameter during testing of this thesis, no work can be done to optimize this parameter; however, the

relationship between the mass flow rate and the pressure drop across the AFC can be observed.

2.1.2.2 Oscillation Frequency

The oscillation frequency of the jet is another important parameter. There are two major frequency bands that have been used in testing (Goodfellow et al. 2009). The first frequency is the dominant wake frequency, also known as the shedding frequency, and the second is the range of frequencies an order of magnitude greater than the shedding frequency. Studies have shown that the two different frequency ranges have different effects on the boundary layer.

Amitay et al. (2001) showed that at frequencies closer to the shedding frequency (lower frequency regime), the boundary layer is deflected towards the airfoil and a vortex trail is advected from the surface. For frequencies an order of magnitude higher than the shedding frequency (higher frequency regime), the flow was completely attached to the surface and a vortex trail can be seen. They also discovered that the lift to drag ratio (L/D) increases from 2.65 to 3.2 for the higher frequency regime when compared to the lower frequency regime. They also noted that in the lower frequency regime, the L/D ratio was dependent on the frequency and it decreased with increasing frequency; however, it was independent of the frequency at the higher frequency regime. This tells us that if the FO is operating in the higher frequency regime, variations in the oscillation frequency are not significant, as they will not affect the performance of the FO.

This section provided an overview of the two main characteristics of an AFC device. It is important to maximize the coefficient of momentum of the jet, as it is a good

indicator of the control authority of the device when installed on an airfoil surface. The frequency of oscillation is another important factor to control as the frequency regime of an oscillator can affect its performance.

2.1.3 Oscillator Types

An oscillator is any device that adds energy to the boundary layer. As a result, there are many ways of achieving this goal and much work has been done to explore different technologies that can be used to create an oscillating jet. Although much work has been done in the lab to develop oscillators, there has been less success in applying the technology to real world applications (Cattafesta and Shelpack 2011).

There are many ways of organizing flow control devices. The classification used by Cattafesta and Shelpack (2001) has three major categories - fluidic, moving object, and plasma. These can be characterized based on their function and are shown in Figure 4. There are many different types of oscillators within each category. This section will explore the different categories and provide an overview of the different technologies that can be used.

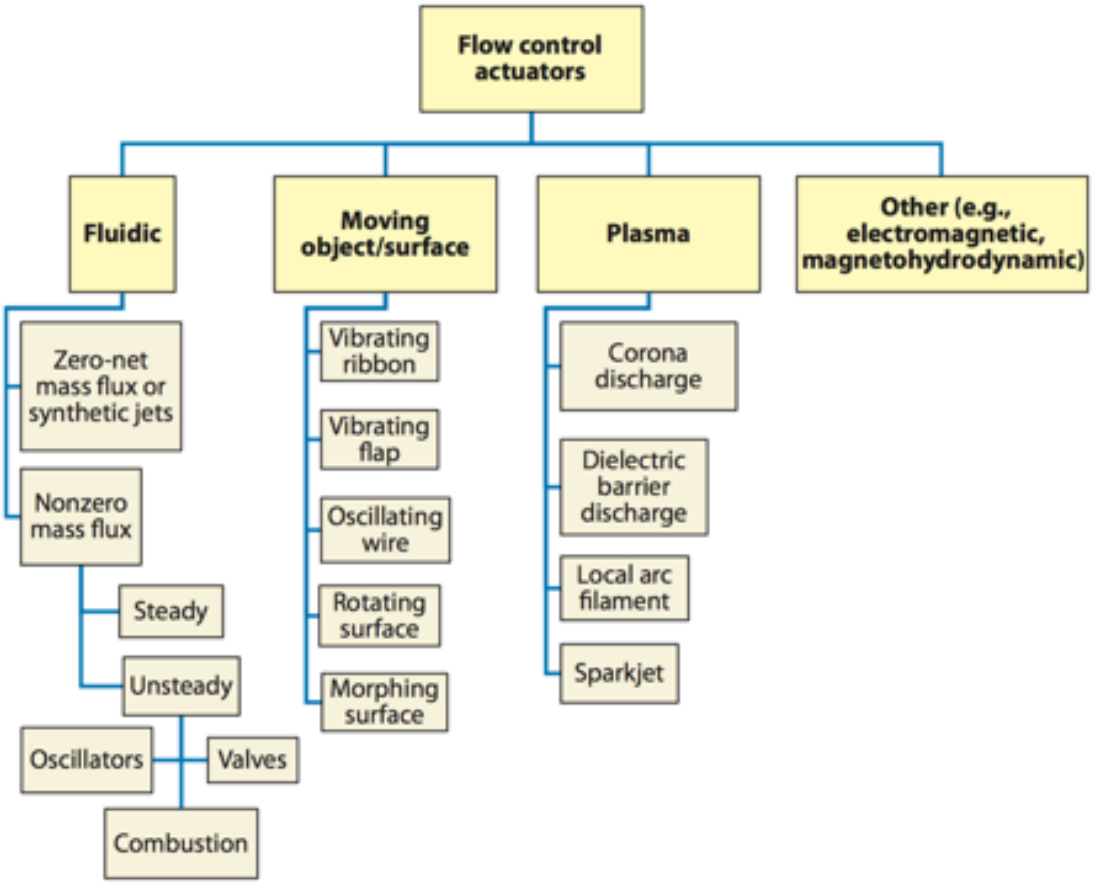

Figure 4 - Classification of Flow Control Devices (Cattafesta and Shelpack 2011)

2.1.3.1 Fluidic Actuators

Fluidic actuators can be divided into many categories. The characteristic feature of a fluidic actuator is the use of a fluid to add energy to the boundary layer. The major categories into which they fall are zero net flux mass actuators, pulsed jet actuators, powered resonance tube actuators, combustion actuators, and fluidic oscillators.

Zero Net Mass Flux (ZNFM)

One type of actuator is the zero net mass flux actuator. It operates using a diaphragm that oscillates about an equilibrium position (Cattafesta and Shelpack 2011). This causes it to inject and expel air through the orifice into a cavity. This oscillator movement can be achieved through piezo-electric or electrodynamic systems. Figure 5 shows schematics of the two different types of actuation methods. The major advantage of this type of actuator is that it does not require an external fluid source, which allows these actuators to be easily integrated into the plane without requiring piping for air. Additionally, these actuators can be easily scaled and are suitable for feedback control. However, their disadvantages are that they are typically limited to low and moderate speeds and have to be operated near the resonant frequency of the device. This limits the variation that can be achieved in the oscillation frequency. They are also complicated and require advanced manufacturing techniques.

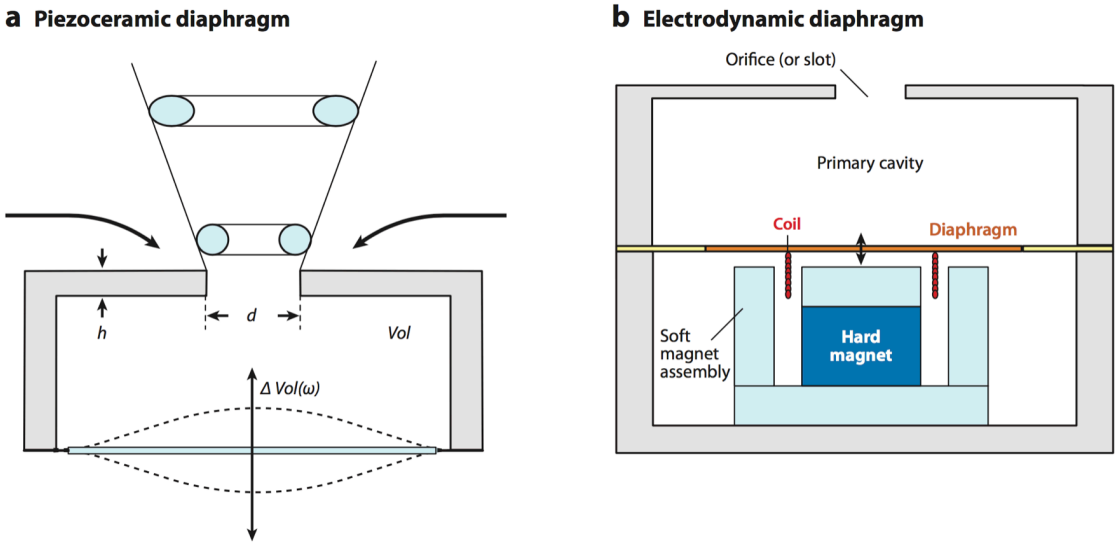

Figure 5 - Zero Net Mass Flux Actuator (Cattafesta and Shelpack 2011)

Pulsed Jets

A pulsed jet actuator is similar to a simply blown flap, however the jet can be varied between on and off states, which is usually characterized by a square wave. This jet can be achieved using a fast acting solenoid, a high speed rotating screen valve, or a rotating orifice assembly (Cattafesta and Shelpack 2011). The advantage of this type of actuator is that it can produce high air velocities with either fast response time or high bandwidth. However, its disadvantages include the fact that it requires an external air source, which can add complexity and weight to the system. Additionally, the use of a valve or solenoid is required to create the pulsed jet, which adds to the cost and complexity of the actuator.

Fluidic Oscillator

A fluidic oscillator is a device that generates a pulsed jet when high-pressure fluid is supplied. It is similar to a pulsed jet actuator; however, it has the advantage of having no moving parts. This reduces the complexity of the device and the potential modes of failure, and improves the reliability and ease of assembly of the actuator. It also simplifies the manufacturing process and reduces the number of components, thereby reducing the overall cost of the system. Additionally, the frequency of the jet can be controlled through the flow rate of the actuator (Cattafesta and Shelpack 2011). However, that can also be seen as a disadvantage as it couples the two operating parameters of the actuator. There are two main types of fluidic actuators - feedback and feedback-free – and are shown in Figure 6.

The first type of fluidic oscillator is a feedback actuator. This works on the principle of wall attachment, also known as the Coanda effect (Kirschner 1966). As the air is

supplied into the actuator, the flow attaches to one of the two walls in the actuator, this causes the pressure to increase in the feedback tube. This increase in pressure is propagated to the inlet of the air supply. This increase in pressure on the attached side forces the air to detach from that wall and attach to the opposing wall. This process repeats itself, thus creating an oscillating jet.

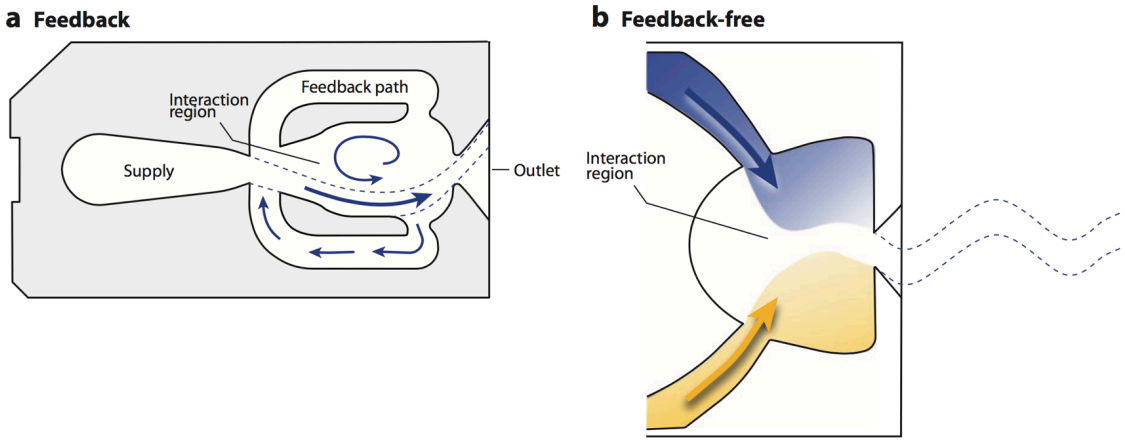

Figure 6 - Feedback and Feedback-Free Fluidic Oscillators (Cattafesta and Shelpack 2011)

The second type of fluidic oscillator is feedback-free. This can be seen by the lack of feedback tubes in the design. Instead of using the feedback to switch the jet, this oscillator works through jet interaction. As the air enters from both sides, the jets interact in the interaction chamber. This interaction creates vortices in the interacting chamber, creating a sweeping jet pattern. This is the type of oscillator explored in this thesis. This oscillator is chosen due to the work that has been done by DeSalvo (2011, 2014), Kuchan (2012), and Li (2016) in testing and integrating this device into a composite wing flap.

Although the basic principle of these jets are well understood, an in-depth understanding of the physics is still not present. Much work has been done by Gregory et

al. (2004) to utilize various imaging techniques to picture the oscillators. Additionally, Gokoglu et al. (2009) have developed numerical models to simulate the oscillators. As there is still a lack of understanding on the exact physics behind these oscillators, it is important to develop tools that designers can use to design oscillators for their specific application.

Combustion Actuators

The output of a combustion actuator is similar to that of a pulsed jet actuator. However, instead of using a valve to create the pulses, they are created by igniting a mixture of fuel and an oxidizer in a small combustion chamber (Cattafesta and Shelpack 2011). This mixture is injected into a combustion chamber and ignited, which creates a pressure rise and forces air out of the chamber and creates a high velocity pulsed jet. The advantage of this system is the ability to create high velocity flows; however, these are limited to low frequencies up to a few hundred Hertz. Additionally, they require combustion, which can increase the potential for failure in the system.

2.1.3.2 Moving Object Actuators

In addition to the fluidic actuators, there are actuators that utilize moving objects in the flow stream to create oscillations. The most common method is to utilize a cantilevered piezo-electric beam that oscillates near the nozzle of the beam (Gregory and Raghu 2009). This can be seen in Figure 7. The frequency of the jet oscillation is determined by the electrical signal that is supplied to the piezoelectric oscillator. This is desirable as it allows for a decoupling of the operating frequency of the jet from the flow characteristics. It can also be applied to different frequency ranges and is suitable for feedback control. However,

as these are resonant devices, they need to be operated near the resonant frequency to achieve large free tip displacements. This limits the variability that can be achieved in the oscillation frequency. Experiments have shown that that frequencies in the range of 1-2 kHz can be achieved (Kegerise et al. 2007).

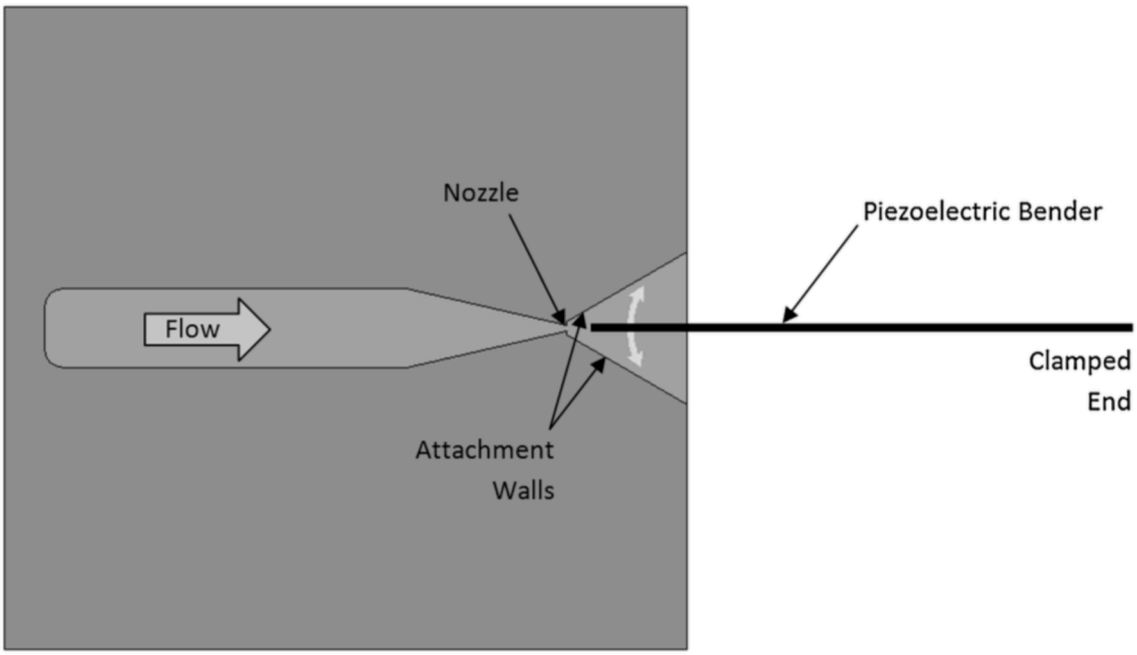

Figure 7 - Piezoelectric Blender (Gregory and Raghu 2009)

2.1.3.3 Plasma Actuators

The last major category of actuators is a plasma actuator. The leading type of plasma actuator is a single dielectric barrier discharge (SDBD). A SBDB consists of an asymmetric pair of electrodes with a sandwiched dielectric material (Cattafesta and Shelpack 2011). AC voltage on the order of 1-30 kV and frequency of 5-20 kHz is supplied to the exposed electrode. This creates an electric field that ionizes the surrounding air,

transferring momentum to the surrounding air. Their major advantages are the lack of moving parts, easy installation, low mass, and fast response time. However, they are unable to generate large velocities and require a high voltage system.

To summarize, this section provided an overview of the different types of actuators, how they operate, and their advantages and disadvantages. It is clear that no single actuator is perfect, and the right type of actuator has to be chosen for a specific application. The actuator that is explored in this thesis is a feedback-free fluid oscillator, due to the preceding work that has been completed using this actuator. The next section explores the work that has been done regarding this particular type of actuator.

2.1.4 Feedback-Free Fluidic Oscillator

This section explores the feedback-free FOs and the research that has been done to understand this particular type of oscillator.

2.1.4.1 Effects of Operating Conditions

Studies have been conducted on the effect of operating conditions on the performance of FOs. The primary control variable for an FO is the mass flow rate. Studies have shown that increasing the mass flow rate increases the pressure in the interaction chamber (Li 2016). This results in an increase in the oscillation frequency of the FO and the relationship is continuous with no local peaks. It was also noted that the relationship between the flow rate and the oscillation frequency was not linear but parabolic. This suggests that after a certain flow rate, further increases in flow rate will not increase the oscillation frequency of the oscillator. The location at which this occurs will be explored.

2.1.4.2 FO Geometric Variation

As there are no moving parts in this type of FO, the operating characteristics are largely dependent on the geometry of the FO. Studies have been done to explore the effects of variations in these geometries.

Tomac and Gregory (2012) explored how the variation of the aspect ratio - the nozzle width divided by the nozzle height - and the overall scale of the FO affected its performance. When comparing oscillators of different sizes, they showed that increasing the size of the FO decreases the oscillation frequency for a particular flow rate. Additionally, a comparison of the dimensionless frequency with the Reynolds numbers for oscillators of different sizes showed that increasing the size of the FO increases the dimensionless frequency for the same Reynolds number. Regarding the aspect ratio, they showed that increasing the aspect ratio increases the oscillation frequency, which might be due to 3D effects becoming more prominent at larger FO depths. In short, the studies showed that the aspect ratio and size of the FO affect the oscillation frequency of the FO and are important parameters to explore.

Another study by Koklu (2016) explored the effect of changing the nozzle length of the FO. They showed that increasing the length of the nozzle increased the jet width, while reducing the max jet velocity. The results also showed that increasing the nozzle length reduces the momentum coefficient required to achieve similar control authority by 50%. This suggests that the nozzle length is a critical dimension and can greatly affect the performance of an FO. It is important to note that this was observed using a feedback FO,

hence this test would have to be repeated with a feedback-free FO to see if the same performance benefits can be observed.

There are many more dimensions and radii in the nozzle area that can be controlled and that have not been explored by other studies. This thesis aims to explore variations in those dimensions to determine if they are critical, and if so, how the affect the oscillation frequency and jet momentum coefficient.

2.1.4.3 Material and Manufacturing Process

As the end goal of this project is to determine the feasibility of large-scale integration of FOs, it is important to consider the effects of material and manufacturing process on the performance of FOs. Work has been performed by Li (2016) on the effects of manufacturing process and material on the performance. Various materials, such as aluminum, carbon fiber PEKK, polypropylene, and resin, and manufacturing processes, such as machining, selective laser sintering, stereo-lithography, fused deposition molding, and injection molding, were considered. The study looked into the effects of surface roughness on performance. Variations in the oscillation frequency and pressure drop of the FO were found, but were not the result of the surface roughness within the range produced by the processes used in his study. This suggests that dimensional variations were the cause of these variations. This means that it is important to consider the effect of dimensional variations on the performance of FOs and will be a focus of this thesis.

2.2 Fluidic Oscillator Manufacturing Review

A key aspect of this project is to determine if the manufacturing process or materials affect the performance of FOs. Thus, this section provides an overview of different materials and processes that have been used to manufacture FOs. It is also useful to discuss manufacturing of micro-fluidic devices as their geometry is similar to FOs.

2.2.1 Fluidic Oscillator Design

A typical design of a feedback-free FO has hollow channels in a polymer part. Due to this geometry, it is difficult to manufacture the entire FO as a single part using traditional manufacturing processes. Therefore, most FO designs consist of two separate pieces, where the fluid channel is in one part and the second part serves as a cover (Schultz et al. 2008). However, with the advancement of additive manufacturing techniques, it is possible to create the entire part as one piece if one uses a removable support material. Additive manufacturing has been successfully used to manufacture FOs for research purposes and is being considered for full-scale manufacturing (DeSalvo 2011, Kuchan 2012, Li 2016). The main benefits include reducing the number of steps to manufacture the part and that they do not need to be assembled or sealed together; however, drawbacks include increased cost and cycle time.

2.2.2 Manufacturing Processes

Becker and Gartner (2008) provide a thorough overview of manufacturing processes used to make micro-fluidic devices from polymers. These devices are similar to FOs; therefore, advancements in manufacturing of those devices can be used to guide

manufacturing of FOs. Their overview covers manufacturing techniques including precision machining, injection molding, injection compression molding, stereolithography, thermoforming, hot embossing, and laser ablation. From these methods, injection molding, injection compression molding, thermoforming, and hot embossing are suitable for large-scale manufacturing. Laser ablation can also be used for large-scale manufacturing; however, due to its depth of cut limitation, it is not appropriate for manufacturing of FOs (Becker and Gartner 2008). Precision machining is also a viable method for manufacturing FOs; however, due to its long processing times, it is recommended only for prototyping purposes. Thermoforming and hot embossing are similar processes where a sheet of plastic is inserted into a system, heated, pressurized, and pressed onto a mold. It is then cooled to produce the final part. Hot embossing is recommended for low to medium scale production due to its cycle time (Becker and Gartner 2008). Finally, injection molding is better suited for large production rates due to its short cycle time. Cycle time can also be reduced by using injection compression molding; however, this adds complexity to the mold geometry.

The focus of this thesis is to observe the effect of variation in dimensions on the performance of FOs. Therefore, it is important to consider the achievable tolerances using various manufacturing techniques. Figure 8 shows those typically possible. Polymer parts can achieve tolerances of 0.004 in, while machining operations can achieve tolerances closer to 0.001 in. Therefore, if a tolerance tighter than 0.004 in is required, injection molding might not be a suitable choice and machining or post-machining would be necessary to meet the required tolerance. The results of this thesis can help guide the manufacturing process selection. Figure 9 shows the relative price of the part when compared to the manufacturing tolerance. The price begins to increase sharply after a

tolerance tighter than 0.01 in. This is because tighter tolerances require greater care while manufacturing and result in lower yield rates, which increase the cost of the part. Therefore, it is important to determine the required tolerance of the part to avoid overpaying for tighter tolerances.

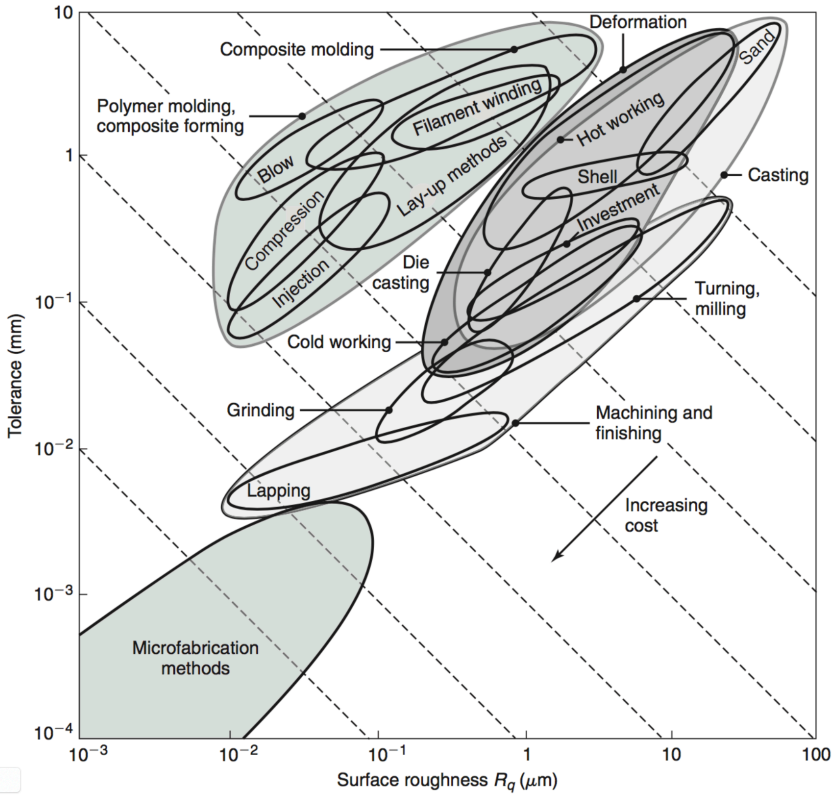

Figure 8 - Surface Roughness vs. Tolerance for Manufacturing Methods (Kalpakjian and Schmid 2008)

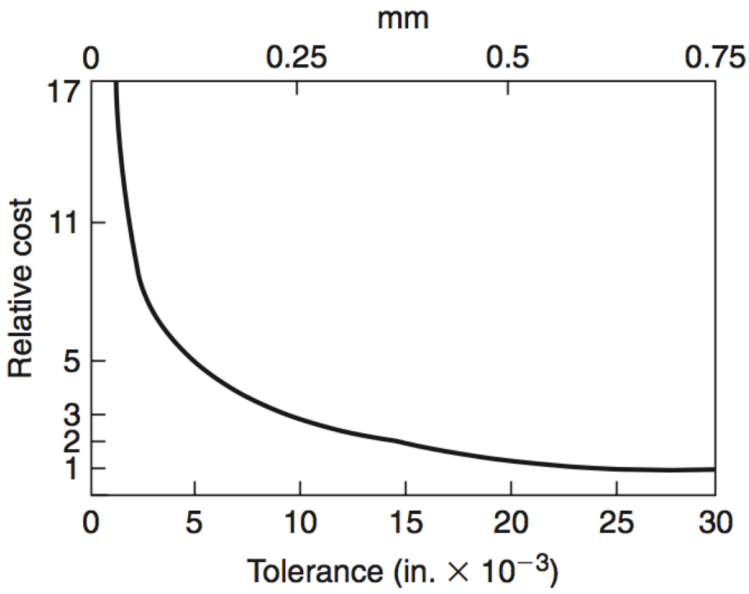

Figure 9 - Part Tolerance vs. Relative Cost (Kalpakjian and Schmid 2008)

With the advent of additive manufacturing, more processes have become available to manufacture FOs. These processes have also become more economically viable due to the extensive research that has been done in additive manufacturing. Stereolithography (SLA) has been successfully used for research purposes by DeSalvo (2011), Kuchan (2012), and Li (2016). SLA works by selectively curing a photopolymer resin using UV light. This is done layer by layer to create the desired 3D geometry. Similarly, Selective Laser Sintering (SLS) works by using a laser to sinter power in the desired locations, layer by layer to create the desired geometry. Li (2016) proposed a single piece FO design using SLS, where the entire FO and fastening mechanism are printed together. Additionally, the tolerances on additive manufactured parts are very similar to those of injection molded parts. Tightest possible tolerances of 0.005 in can be achieved in the x- and y-directions, while tolerances of 0.01 in can be achieved in the z-direction for both SLS and SLA parts

(3D Systems 2016). Therefore, injection molding and additive manufacturing can be used interchangeably when only considering tolerances.

2.2.3 Assembly Process

As most manufacturing processes require the oscillator to be manufactured in two separate parts, it is important to consider methods that can be used to assemble the two halves. Before assembling the parts, any waste must be removed, which could include removing the sprue from injection molded parts or trimming the remaining material after a hot embossing process (Becker and Gartner 2008). Multiple methods can be used to bond thermoplastics including thermally fusing the parts together, adhesive bonding, Clearweld, mechanical joining, and magnetic fastening (Kalpakjian and Schmid 2008).

Thermally fusing the parts together is a common method to join thermoplastics. Heating the plastic causes it to soften and melt. When the parts are in this state and pressure is applied, they can fuse together and create a bond (Kalpakjian and Schmid 2008). With certain materials, oxidation is a problem; however, this can be prevented by using an inert shielding gas. The heat required for bonding the parts can be generated using internal and external sources. Methods that utilize external heat sources include heated tools, lasers, and electrical resistance. Methods that use internal heat sources include ultrasonic welding, friction welding or orbital welding.

Other methods include adhesively bonding the parts; however, it can be difficult to create an adequate bond on plastics without surface treatment due to their low surface energy (Kalpakjian and Schmid 2008). Solvents can also be used to bond the parts together as they can temporarily soften the parts to bond them together. Similarly, the Clearweld

process works by applying toner on the bond surfaces and heating the toner using a laser. The laser heats the part where the toner is applied and fuses the pieces together (Kalpakjian and Schmid 2008).

The two halves can also be attached using non-permanent methods. One option is to fasten the parts together using fasteners or self-tapping screws. Snap fasteners can also be used to connect the two halves together. Although these methods can be used to attach the two pieces, there is no need to take the FO apart after it has been assembled. These methods would add complexity to the design of the FO, such as threaded holes, with no added benefit; therefore, the other methods discussed above would be preferable.

2.3 Chapter Summary

This chapter explored the fundamentals of active flow control technology and how using flow control devices adds energy to the boundary layer to delay flow separation. The key performance characteristics of a FO are the coefficient of momentum and the frequency of oscillation. Different FO devices and their advantages and disadvantages were explored. Also, research performed in the field of feedback-free fluidic oscillators was highlighted to outline the scope of this thesis. In addition to the AFC technology review, manufacturing techniques were reviewed. This included a review of the design of fluidic devices, different manufacturing techniques that could be utilized, and different assembly methods to join FOs manufactured from multiple parts. The development of additive manufacturing and its effects on the research and manufacturing of FO devices were also discussed. In the next chapter, the design of the FO is discussed.

CHAPTER 3. FLUIDIC OSCILLATOR DESIGN

This section explores the design of the FO. The goal of this thesis is to determine the effects of material, manufacturing process, and dimensional variation on the performance of the FO. Therefore, it is important to understand what parameters characterize its aerodynamic performance. These are referred to as the functional requirements of the FO because it must meet these requirements to fulfill its function, which is to delay flow separation. There also exist operational requirements of the FO that must be met for it to remain operational during the life of the FO. In addition to these requirements, there are multiple aspects of the FO design that can be varied. These include the material, the manufacturing process, and the critical dimensions. These are varied to better understand their effects on the performance of the FO and develop a tool that can be used to design an FO.

3.1 Functional Requirements

There are several requirements that the FO must meet to achieve the benefits of utilizing FO technology. They include the coefficient of momentum, and the oscillation frequency of the jet. These are the dependent variables that are affected by changes in the design of the FO.

3.1.1 Coefficient of Momentum

In the review of FO devices, it was shown that the coefficient of momentum is an important factor to consider when designing FOs. There is a strong correlation between the momentum coefficient and the effectiveness of an oscillator as increasing the momentum coefficient increases the coefficient of lift of the airfoil and improves its L/D ratio. As the momentum coefficient is dependent on the airfoil being used, no specific target needs to be met. Therefore, the goal of this thesis is to characterize the effects of the material, manufacturing process, and variation in the critical dimensions on the momentum coefficient. The materials, manufacturing processes and critical dimensions will be explored in greater detail in this chapter. In general, increasing the phase averaged velocity of the jet increases the coefficient of momentum, hence it is preferred to increase its value. This will provide the designer a tool to design an FO that will achieve the desired coefficient of momentum based on the airfoil on which the system will be installed.

One disadvantage is the difficulty to measure the momentum coefficient as it requires many measurements and can change depending on the airfoil on which the FO is installed. As a result, it is not an appropriate parameter to use for bench tests. Instead, the mass flow rate will be used. If the operating conditions of the FO are known, they can be correlated with existing wind tunnel tests to estimate the performance benefits of the FO. Hence, the thesis will aim to characterize the relationship between the mass flow rate and other parameters that describe the operating conditions of the jet, including the oscillation frequency and pressure drop.

3.1.2 Oscillation Frequency

From the background discussion, it is understood that an oscillation frequency that is an order of magnitude larger than the shedding frequency is preferred as it decouples the L/D ratio from the oscillation frequency. Therefore, the goal of the FO is to operate in this range. If the oscillator is operating in this range, the variations in oscillation frequency will not affect the performance of the FO. It is preferable for the FO to operate in the lower band of this requirement as increasing the frequency requires increasing the mass flow rate and the fluidic power requirement. As the frequency is dependent on the dimensions of the wing, the required frequency will change depending on the airfoil on which the FO is installed. Therefore, the goal of this thesis is to characterize the effects of the material, manufacturing process, and variation in the critical dimensions on the frequency of oscillation. This will provide the designer with a tool to design an FO that will achieve the desired frequency based on the airfoil on which it will be installed. In short, variations in the oscillation frequency will not affect the aerodynamic performance of the FO as it is being operated at an order of magnitude greater than the shedding frequency; however, it is useful to know if the parameters explored do have an effect on the oscillation frequency.

3.2 Operational Requirements

For the FO to operate as intended, it must meet certain operational requirements. These are not linked directly to the main functional requirements of the device, but represent additional requirements it must meet to achieve the functional requirements.

They include the fluidic power requirement, the ability to withstand pressure, temperature and humidity, and the weight of the system.

3.2.1 Fluidic Power

One major consideration for a FO device is the fluidic power. Fluidic power is the product of mass flow rate and pressure drop. These oscillators require an air source; hence, a system has to be in place to provide air. This air can be sourced from multiple locations including engine bleed or the Auxiliary Power Unit (APU). However, there is a limit to how much air can be retrieved from these locations. Therefore, it is important to minimize the fluidic power requirements of the FO devices. It is observed that increasing the mass flow rate increases the frequency of oscillation; hence, is it important to pick an FO design that achieves the minimum oscillation frequency required with the lowest fluidic power. It is important to note that increases in the mass flow rate and the pressure drop will both increase the fluidic power requirement of the FO; however, increasing the mass flow rate will also increase the momentum coefficient of the jet. Therefore, for a given mass flow rate, the goal should be to minimize the pressure drop across the FO. As there are many variables affecting the power requirement and momentum coefficient, it is important to understand the relationship between these variables so appropriate tradeoffs can be made.

3.2.2 Pressure

A pneumatic FO operates by forcing air out of its nozzle. The rate at which the air flows out of the FO is determined by the difference in pressure between the plenum and the atmosphere. It is important that the device withstand the pressure without breaking. Li (2016) used a plenum pressure of 30 psi while testing the oscillators. Under extreme

conditions, the nozzle could also be blocked, which could elevate the pressure in the FO and cause it to fail. Hence, it is important the FO be designed to withstand worst-case scenario pressures.

Additionally, the pressure could cause deflections in the wall geometry, which could alter the flow characteristics of the oscillator. Hence, when selecting a material, it is not only important that the FO does not break but that it does not expand past a certain value and cause significant changes in the flow profile.

3.2.3 Temperature

A pneumatic FO requires an air source. There are several locations on an aircraft from which this air can be retrieved. One of these locations is bleed from the jet engine. This air is suitable because it is pressurized. This air can have temperatures up to 300ºC (Adib et al. 2007). Therefore, it is important that the FO can withstand temperatures in this range without permanently deforming or else a heat exchanger will have to be included in the system. Additionally, elevated temperatures will cause the FO to expand, which can change its flow characteristics of the FO. Hence, it is important that it doesn't expand past a certain value.

In the case that the air source is not the engine, but a lower temperature source, the FO may still be heated from the jet engine exhaust. It has been shown that temperatures inside a flap can reach up to 127ºC due to its proximity to the engine, especially in the flaps-down position (Mixon et al. 1975).

Additionally, there will be large temperature variations over the FO's life due to the temperatures of the destinations visited by the aircraft, exhaust gasses, and cold temperatures at cruise altitudes. These temperatures can range from -50ºC to 300 ºC. Hence, when picking the material for the FO, it is important that the material does not fatigue or crack due to temperature variations.

3.2.4 Humidity

Humidity is another environmental factor that must be considered when selecting the material. As the aircraft travels, it is subjected to a large variety of environmental conditions and significant fluctuations in humidity. Certain materials are not resistant to humidity and can swell over time. Therefore, it is important to pick a material that will be able to resist changes in humidity over time.

3.2.5 Weight

Weight is last factor that will be considered when picking the material. As multiple FOs will be placed along the span of the flap, it is important to minimize the weight of the system. Therefore, a lighter FO is preferred if it meets the other functional and operational requirements.

3.3 Material

There are several materials that can be used to manufacture the FO. It is important that the material can meet the operational requirements described above. This section

covers the different materials that are explored and the reasons for their selection. These materials include carbon fiber reinforced PEKK and Aluminum. It is important to note that the material should not affect the performance of the FO as that is primarily governed by the geometry of the FO, as long as it is stiff enough not to deflect significantly. An aspect that would affect the performance is the way the material responds to the manufacturing process and that is explored in the thesis. Previous work done by Li (2016) showed that the surface roughness within the limits that he tested, which are the same as those in this thesis, did not have an effect on the performance of the FO.

3.3.1 Carbon Fiber PEKK

The most likely material that will be used to manufacture the FO is carbon fiber reinforced polyetherkeytonekeytone (CF PEKK). Traditional polymer manufacturing methods can be used to manufacture the part. In addition, it can be used with the SLS process, making the material versatile. The addition of carbon fiber, 15% filled, reinforces the base PEKK material and increases the in-plane tensile strength from 76 MPa to 110 MPa and the out of plane strength from 62 MPa to 69 MPa (Oxford Performance Materials 2016). These increases allow it to better handle the pressures and forces that are expected during operation. It also has a glass transition temperature of 155 ºC and melting temperature of 307 ºC (Oxford Performance Materials 2016). This means that it can withstand the temperatures in the flap area and will not melt when exposed to the engine bleed air. It also has a low coefficient of thermal expansion 29 x 10^{-6}/ºC, limiting the changes in geometry expected at higher operating temperatures. These properties make CF PEKK an ideal material to use for manufacturing FOs.

3.3.2 Aluminum

Aluminum is commonly used in the aerospace industry. Its main advantages are its strength to weight ratio and its ability to resist temperature and humidity variations. This makes it an ideal material based on operational requirements. Its strength enables it to withstand the expected pressures and forces, and its material properties allow it to operate at the expected high temperatures, temperature variations, and changes in humidity. One disadvantage of using aluminum is its density. Aluminum adds weight to the system and if a lower density material can fulfill the requirements, it will be preferred. Aluminum FOs are used for prototyping due to its machinability, availability and cost; however, they are not likely to be selected for the final FO design. Other metals were not considered due to their higher density.

3.4 Manufacturing Process

As these devices are manufactured, it is important to consider the manufacturing methods that can be used to produce them. Additionally, manufacturing methods have their limitations. Hence, it is important to consider the effects of these on the performance of the FO.

3.4.1 Machining

Machining is prominently used in this thesis due to its tight tolerance and low cost per part when prototyping. This allows several different FOs with geometric variation to be manufactured at low cost. In addition, sharp external edges can also be produced using

this process. These edges exist in certain areas of the FO and can be produced by machining. Although it is unlikely that machining will be used as a large-scale manufacturing process due to its cycle time and cost, it is a useful method for creating test pieces. However, if it is determined that certain tolerances cannot be met using other manufacturing methods, a post-fabrication machining process might be required. As it is thought that the material and manufacturing process should not affect the FO performance, the data collected using FOs should transferable to other manufacturing methods. In short, machining is a preferred manufacturing method for prototyping in this thesis due to its low cost and ability to fabricate critical dimensions accurately.

3.4.2 Injection Molding

Injection molding is a popular large-scale manufacturing method. Its major advantages are short cycle time, low cost, and high volume. This method can also produce FOs from Carbon Fiber PEKK, which is important, as it is the most likely material to be used. However, there are some limitations of this process. These include the inability to produce corners as sharp as machining, which could have an impact on the performance of the FO as the orifice design has a sharp edge. Li (2016) tested an injection molded polypropylene FO and observed that the performance was similar to that of a machined FO. The molds used for that injection molding process were manufactured using electric discharge machining (EDM) to make the edges as sharp as possible; however, the edges were not as sharp as those that can be made using a machining process. Additionally, sharp edges can cause molded-in stresses and make the part difficult to eject, possibly leading to fracture of the part. Thus, sharp edges should be avoided when injection molding parts. An FO will be machined to mimic an injection molded part to determine the effects of sharp

and rounded edges. The orifice widths will be controlled to ensure that they do not affect the data.

3.4.3 Additive Manufacturing

Additive manufacturing is also an option for manufacturing the FOs. Its major advantages are the ability to manufacture a single piece FO. This would mean that the FO does not include several parts that need to be sealed together. This reduces the processing time by eliminating assembly. The geometry of the FOs can be varied without additional cost in contrast to injection molding. This allows the designer to utilize different FO geometries depending on the location on the flap. This could be done to optimize the performance because certain locations might require different oscillation frequencies or momentum coefficients. This process also allows for sharp internal edges to be manufactured, when compared to the machined parts. However, there are disadvantages to this process including the high cost of production especially for large scale production and the long cycle times.

SLS is the most likely additive manufacturing method to be used as it can process CF PEKK. This is important due to the operating temperature requirements of the FO. However, CF PEKK is not suitable for SLA or FDM processes and the suitable materials for them may not meet the operational temperature requirements. Li (2016) utilized SLS, SLA, and FDM test pieces and showed that they had similar performances to machined parts. This thesis will retest FOs produced by SLS and SLA in a new jig to validate those results and determine if the variations that were observed were due to the manufacturing process or geometric variations.

3.5 Geometry

A significant aspect of the design of an FO is its geometry. As a feedback-free oscillator has no moving parts, its performance is highly dependent on its geometry. As a perfect part cannot be manufactured, it is important to consider the effect of variation in critical dimensions of the FO. The section covers the different dimensions that are explored in this thesis including nozzle length, nozzle width, nozzle radius, nozzle curvature, nozzle symmetry, interaction chamber width, and shoulder radius, and the motivation behind exploring them. This thesis only explores small variations in the dimensions of an FO. Large changes, such as changing the scale of the FO, are not explored.

3.5.1 Nozzle Length

Figure 10 shows the dimension referred to as the nozzle length. The motivation behind exploring the nozzle length lies in previous studies that have explored this dimension. As seen in the study by Koklu (2016), increasing the nozzle length reduced the required momentum coefficient and achieved performance benefits. This study was conducted on feedback oscillators; therefore, replicating this result on a feedback-free oscillator can be useful. Li (2016) explored changes in the nozzle length for a feedback-free oscillator and concluded that there might be an upper and lower limit for this dimension to operate correctly. Therefore, further exploration could help find its limit and help choose an appropriate manufacturing method to remain within this tolerance band.

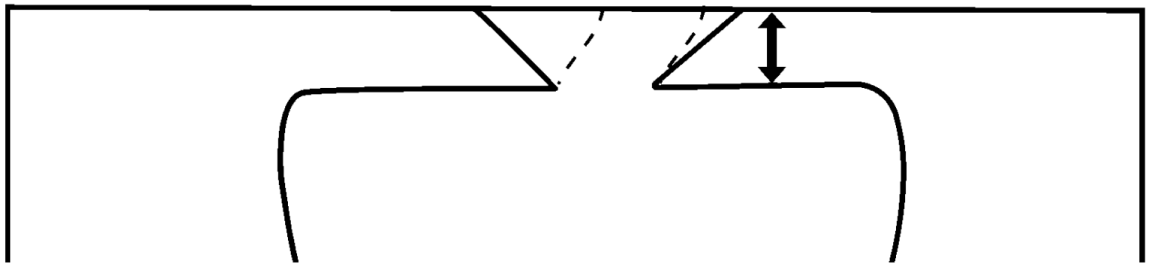

Figure 10 - Nozzle Length Dimension (Cattafesta and Shelpack 2011)

3.5.2 Nozzle Width

Figure 11 shows the dimension referred to as the nozzle width, which is another important dimension of the oscillator. It governs the amount of air that is expelled from the oscillator, thus governing the pressure inside the interaction chamber. This means that reducing the nozzle width increases the pressure in the interaction chamber and the pressure requirements from the air source. This is an important consideration as it may be difficult to achieve the required pressure. Therefore, if increasing the width of the nozzle has no effect on the oscillation frequency of the jet and only affects the pressure in the interaction chamber, it would be beneficial to increase the nozzle width. Additionally, it will also provide an insight into the sensitivity of the pressure and oscillation frequency to changes in the nozzle width and help choose an appropriate manufacturing method to achieve this tolerance.

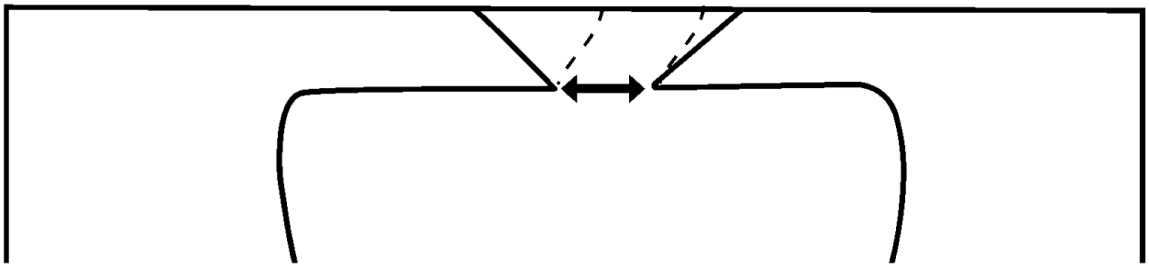

Figure 11 - Nozzle Width Dimension (Cattafesta and Shelpack 2011)

3.5.3 Nozzle Radius

Nozzle radius refers to the radius of the sharp edge at the orifice, as seen in Figure 12. As it is difficult to produce sharp edges using injection molding, it is important to consider the effect of this radius. If it is found that this edge affects the performance of the FO, then it might be inappropriate to use manufacturing processes such as injection molding. This dimension could influence the performance of the FO as the sharp edge could increase the pressure as there will be more losses when the air flows out of the chamber. Rounding this edge could also be used as a mechanism to reduce the pressure in the interaction chambers, hence reducing the pressure required from the air source. For these reasons, it is important to consider the effect that this radius has on the performance of the FO and to help to choose an appropriate manufacturing method to achieve this radius.

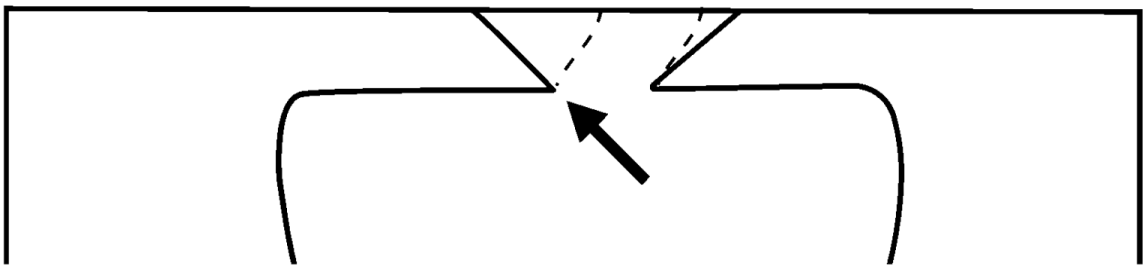

Figure 12 - Nozzle Radius Dimension (Cattafesta and Shelpack 2011)

3.5.4 Nozzle Symmetry

Nozzle symmetry refers to the difference in shoulder lengths on the FO, which can be seen in Figure 13. It is possible that the nozzle is not centered within the FO, which could result in uneven peaks in its jet profile and hinder the performance of the FO. Therefore, it is important to determine how far from the center that the nozzle can be before

performance is severely affected. This study will help to determine the sensitivity of the jet profile to nozzle symmetry and to choose an appropriate manufacturing method to achieve the required tolerance.

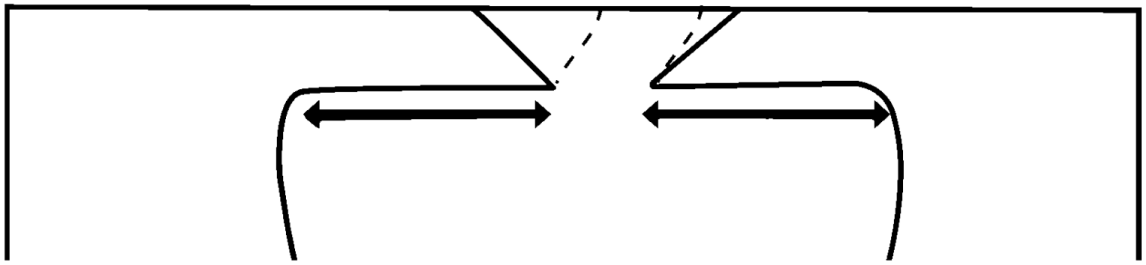

Figure 13 - Nozzle Symmetry Dimension (Cattafesta and Shelpack 2011)

3.5.5 Interaction Chamber Width

Figure 14 shows the dimension referred to as the interaction chamber width. This dimension governs the size of the interaction chamber. As the interaction chamber is where the jets interact and produce the vortices, it is important to consider the effect of changing this dimension, especially on the oscillation frequency. If this dimension is found to be critical to the oscillation frequency, then it is important to understand how changes in this affect the performance of the FO and can help choose an appropriate manufacturing method to achieve the required tolerance.

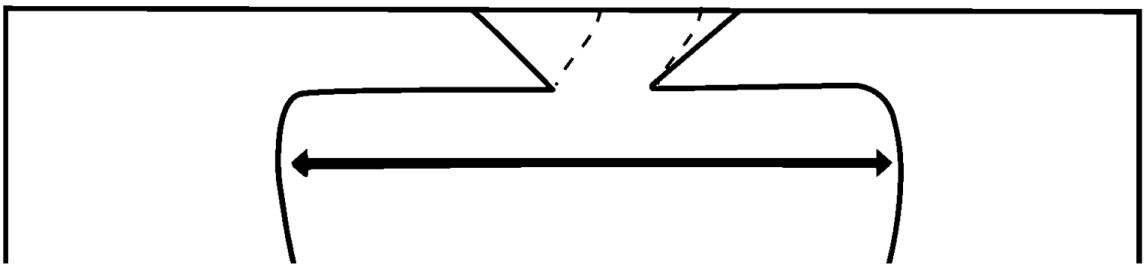

Figure 14 – Interaction Chamber Width Dimension (Cattafesta and Shelpack 2011)

3.5.6 Shoulder Radius

Figure 15 illustrates the shoulder radius. Similar to nozzle radius, it can be difficult to produce a sharp corner here with certain manufacturing methods. Therefore, it is important to consider the effect that this radius has on the performance of the FO. This radius also affects the interaction chamber width. A larger radius will effectively narrow the interaction chamber. Therefore, it is important to consider the effect of both these factors and determine if it is the radius or the interaction chamber width that is responsible for changes in performance of the FO. If it is determined that this radius has an effect on the performance of the FO, then it will help to choose an appropriate manufacturing method to achieve the required radius.

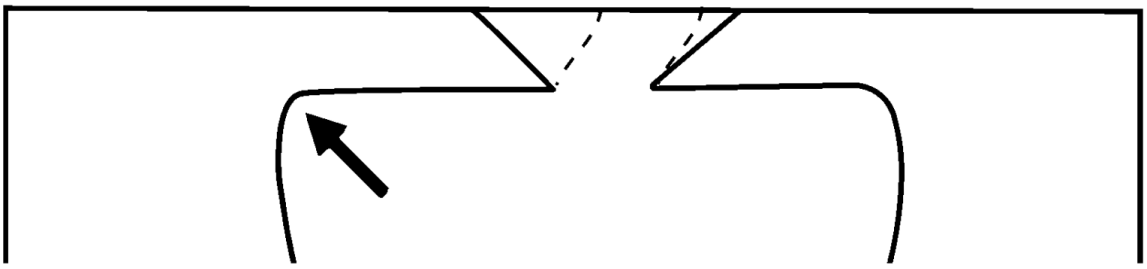

Figure 15 - Shoulder Radius Dimension (Cattafesta and Shelpack 2011)

3.5.7 Nozzle Curvature

Lastly, Figure 16 illustrates the nozzle curvature. As this dimension could affect the flow of the air coming out of the nozzle, it is important to consider its effects if this curvature is changed or removed. If it is determined that the feature has no effect on the performance of the FO, then it does not need to be controlled during manufacturing.

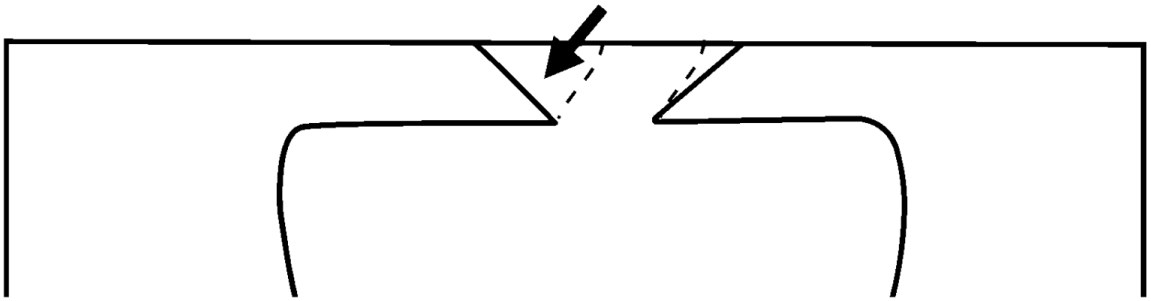

Figure 16 - Nozzle Curvature Feature (Cattafesta and Shelpack 2011)

3.6 Chapter Summary

This chapter covered the different functional and operational requirements that the FO must meet to achieve the benefits of using active flow control and continue to operate properly over the life of the device. The functional requirements include the coefficient of momentum, which should be maximized, the oscillation frequency, which should be maximized within in limits, and the fluidic power, which should be minimized. The operational requirements include the ability to withstand the operating pressures, temperature variations, and changes in humidity, and to reduce the weight of the device.

There are also several design variables that were considered that could affect the performance of the FOs. They fall into three main categories including material, manufacturing process, and variations in critical dimensions. The materials that were considered are CF PEKK and aluminum. CF PEKK is advantageous due to the range of manufacturing processes that can be employed and its ability to withstand the expected temperatures and forces. Aluminum also has those benefits, however, due to its density, it might not be an appropriate material for this application. Various manufacturing processes

that were also considered included machining, injection molding, and additive manufacturing. Machining is an ideal process for prototyping due to its tight tolerances and low cost, but can be expensive and slow for large scale production. Injection molding is an ideal process for large scale manufacturing; however, the effects of its ability to produce sharp edges needs to be characterized. Additive manufacturing is advantageous due to its ability to produce a single piece FO and vary the FO geometry; however, it can be expensive and slow for large-scale production. Finally, the critical dimensions were also identified and include the nozzle length, nozzle width, nozzle radius, nozzle symmetry, FO width, and shoulder radius. This thesis will characterize the effects of variations in these dimensions. In the next chapter, the FOs that were manufactured and the testing process will be described.

CHAPTER 4. EXPERIMENTAL METHODOLOGY

This chapter describes the FOs that were produced for testing. The experimental setup and procedures that are used are also described.

4.1 FO Fabrication

To test the effect of the different parameters discussed in the previous section, several test pieces were manufactured using various materials and manufacturing processes. Several dimensions were also varied to higher and lower values. This section describes the different FOs that were created and the reasons for their selection.

4.1.1 Effect of Material

The effects of material on the performance of the FO are explored. If the material has no impact on the performance, then it would give the designer the freedom to pick a material that is best for the operating conditions of the FO. This assumes that the features produced by machining creates equivalent dimensions and tolerances in the two materials, and that the two materials are similar enough in stiffness so that the FOs perform the same. To test this, two FOs were machined using the same machine and CNC code. One of the FOs was manufactured from aluminum, while the other was manufactured from a billet of CF PEKK produced by selective laser sintering. If the material does not affect their performance, then these two FOs should have the same performance characteristics.

4.1.2 Effect of Manufacturing Process

Another aspect that was explored was the effect of manufacturing process on the FO. The manufacturing processes that were compared include machining, SLS, SLA, and injection molding. The effect of manufacturing processes can be difficult to compare directly as different manufacturing processes use different materials and certain processes are subject to geometric variations. To account for these variations, the critical dimensions were measured and input to a numerical model to determine if the variation is due to the manufacturing process or the geometric variation.

One material-controlled test that was performed included comparing a machined CF PEKK FO to a SLS produced CF PEKK FO. This ensured that the material did not affect the performance. There were differences in surface roughness; however, these were ignored based on the findings of Li (2016) that the surface roughness of the processes that he studied did not affect FO performance. This work used the same processes with the same resulting surface finishes. However, the different manufacturing processes were subject to geometric variations and were accounted for in the analysis.

Another test specimen that was manufactured was a machined aluminum FO with rounded edges. This simulates the roundness of an injection molded FO because sharp edges are difficult to produce using the injection molding process. This provides a better understanding of whether this limitation of the injection molding process affects the performance of the FO, or if it is solely dependent on the geometric variation.

4.1.3 Geometric Variation

A major requirement when manufacturing a part is its dimensional tolerance. It can be difficult and expensive to control a dimension; therefore, it is important to understand which are the critical dimensions of the FO. This will allow the designer to determine which dimensions need to be controlled, so to be able to reduce the cost when manufacturing the part. It will also give the designer a tool to determine which dimensions affect the functional characteristics of the FO, which can be used to optimize its design.

This thesis focuses on the dimensions near the nozzle of the FO. A single FO body was manufactured and nozzles were attached to it using screws, reducing the variation between the different FOs and the manufacturing time and cost. The setup can be seen in Figure 17. A baseline nozzle was also created to serve as a control. Table 1 lists the dimension that were varied and the nozzles that were manufactured. Refer to chapter 3 for explanation of these dimensions.

Table 1 - Changes in Dimensions

Dimension	Changes
Nozzle Length	35% and 18% in longer and shorter than nominal
Nozzle Width	17% narrower and wider than nominal
Nozzle Symmetry	2.3% and 5.8% offset
Nozzle Radius	1/32 in radius and 1/16 in radius
Nozzle Curvature	Straight Nozzle

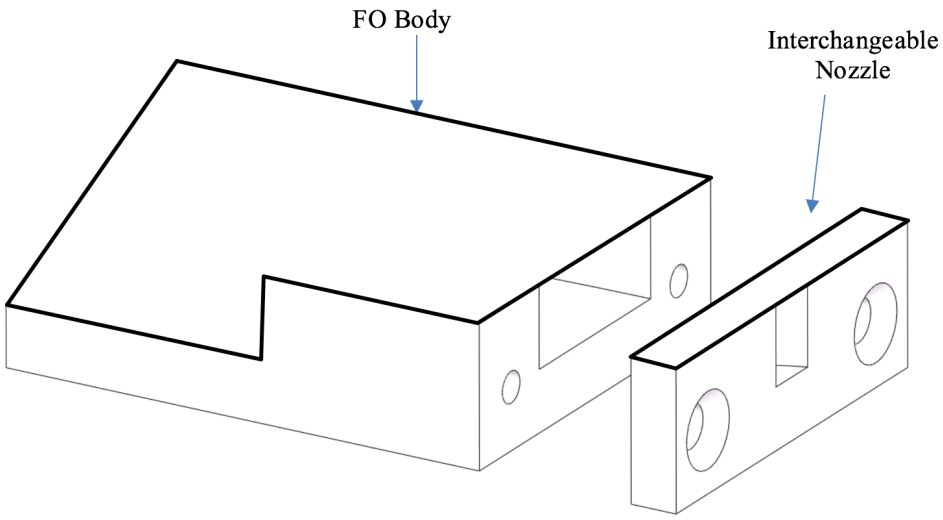

Figure 17 - FO with Nozzle Insert

In addition to these variations, the shoulder radius was varied between the different FOs with different manufacturing techniques. This was because square internal edges cannot be produced using machining. Changing the radius effectively changed the width of the interaction chamber due to the angle of the FO. This allowed for testing of the FOs with different interaction chamber widths, which is thought to be a critical dimension.

Table 2 outlines all the FOs that were manufactured and their characteristics. It also gives identifiers to each test piece used to describe the particular test pieces for the rest of the thesis.

Table 2 - FOs Test Specimens

Identifier	Material	Mfg. Process	Internal Radius	Nozzle
M-MR-AL	Aluminum	Machining	Machining	Nominal
M-IR-AL	Aluminum	Machining	Injection Molding	Nominal
M-MR-CF	CF PEKK	Machining	Machining	Nominal
SLS-NR-CF	CF PEKK	SLS	None	Nominal
SLA-N	Resin	SLA	None	Nominal
AL1	Aluminum	Machining	Machining	35% Shorter
AL2				Nominal
AL3				35% Longer
M-AL-VND				Nominal
M-AL-VNDL2				Nominal
M-AL-VN50S				35% Shorter
M-AL-VN25S				18% Shorter
M-AL-VN25L				18% Longer
M-AL-VN50L				35% Longer
M-AL-VNS				No Nozzle Curvature
M-AL-VN20N				17% Narrower
M-AL-VN20W				17% Wider
M-AL-VNSRN				1/32” Nozzle Radius
M-AL-VNLRN				1/16” Nozzle Radius
M-AL-VN10-O				2.3% Offset
M-AL-VN25-O				5.8% Offset

4.2 Test Procedure

The goal of this thesis is to determine the effects that material, manufacturing process, and dimensional variation have on the performance of an FO. To do this effectively, it was important to create a test setup that allowed FOs to be tested in a

controlled experiment. As the test FOs are designed to fit into a housing and are not standalone devices, a test rig was designed to house the FOs.

The main requirements of the rig were to provide laminar airflow to the entrance of the FO and to ensure that the only outlet for the air is through the FO nozzle. It was also important that air did not leak between the different parts of the FO. There are several components that were required to test the FO. They are explored in detail below.

4.2.1 FO Top Cover

Most manufacturing techniques require that a FO be manufactured in two parts due to its internal cavity. Therefore, a top cover for the FO had to be created. Several sealing options were considered including using a gasket or a plate.

It was decided that a plate would be attached to the top of the FO. This plate would be manufactured using the same material and manufacturing process as the rest of the FO to ensure that the material or manufacturing process did not affect the results of the tests. The plate was attached to the FO using a cyanoacrylate adhesive, also known as "super glue." This allowed the glue to fill any gaps and create an airtight seal between the top and bottom parts of the FO. One disadvantage of this method is the possibility for the adhesive to seep into the cavity and modify the geometry. To minimize this, care was taken when assembling the parts. Mechanically fastening the two half together was considered; however, there was a chance for air to leak if the mating surfaces were not flat. Mechanical fastening would also further complicate the design of the FO, requiring screw holes to be drilled into the parts; hence, this method was not chosen.

Another option that was considered was to use a gasket for the top surface. This would create a seal between the top surface and the FO, thereby ensuring a single path for the air flow. Several materials were considered; however, wrinkles and droops were observed in past gasket usage (Li 2016), which at times blocked the orifice of the FO. This resulted in inaccurate results because it altered the flow characteristics; hence, this option was not selected.

4.2.2 Air Source

The air was supplied to the plenum from the building's air compressor. As the flow rate, temperature, and pressure of the air were measured, the specifics of the air source are not important.

4.2.3 Plenum

An existing plenum was used to test the FOs. This plenum was manufactured using a large pipe and two plates on either end, as seen in Figure 18. The plenum has an inlet on one end of the device and an opening for the FO rig on the other. There was also a port to measure the pressure and the temperature of the air in the plenum.

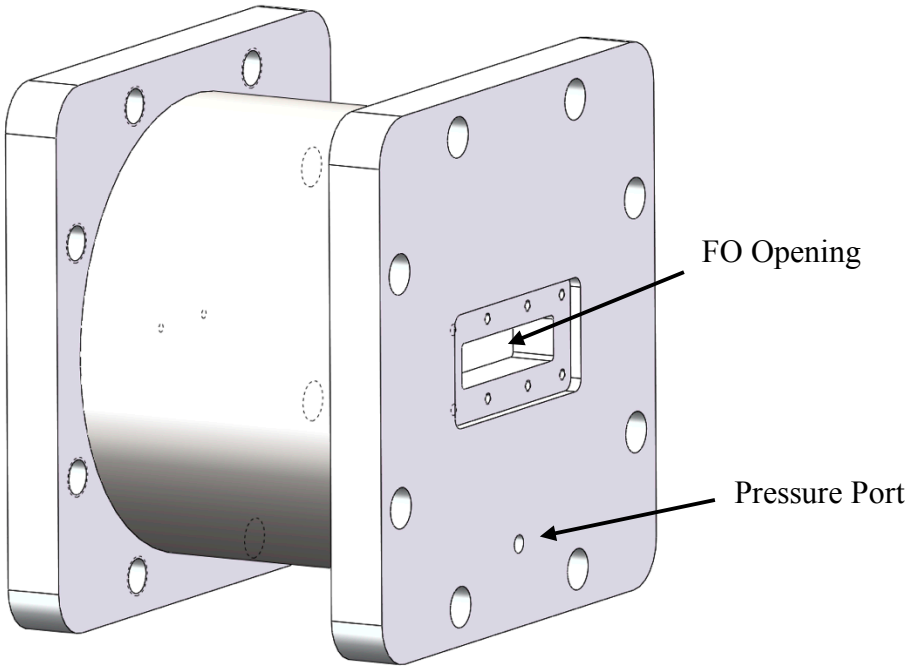

Figure 18 – Plenum

An earlier iteration of the design, as seen in Figure 19, utilized a different plenum to hold the FO. This plenum was much smaller and utilized gaskets to seal the plenum and provided an opening in the front to insert the FO. This design was not selected because the size of this plenum might not provide laminar airflow into the FO. No formal test was done to test if the flow was laminar; however, it was assumed that a larger plenum would increase the possibility that the flow is laminar.

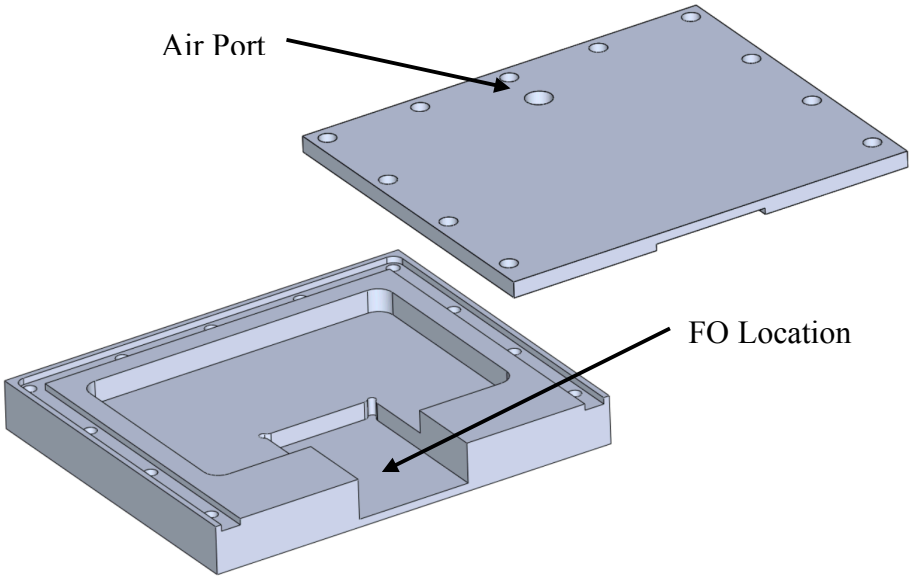

Figure 19 - Old Plenum Design

4.2.4 FO Holder

Another major component of the testing jig is the FO holder. This component is shown in Figure 20**.** This component holds the FO in position for testing and can be inserted into the plenum, which supplies the air to the FO. There are three major components of the FO holder: the main body, the bell-mouth, and the gaskets.

The main body holds the FO in place and provides a mechanism for attaching it to the plenum, using the screws on the outer flange. The opening in the front exposes the nozzle and allows air to flow out. This opening is sealed using a gasket around the outer edges of the FO. On the interior side of the holder is a bell-mouth, which guides the air from the plenum to the FO inlet without creating turbulence. This piece is bolted onto the

main frame of the holder to secure the FO and provide a clamping force for the gasket in the front.

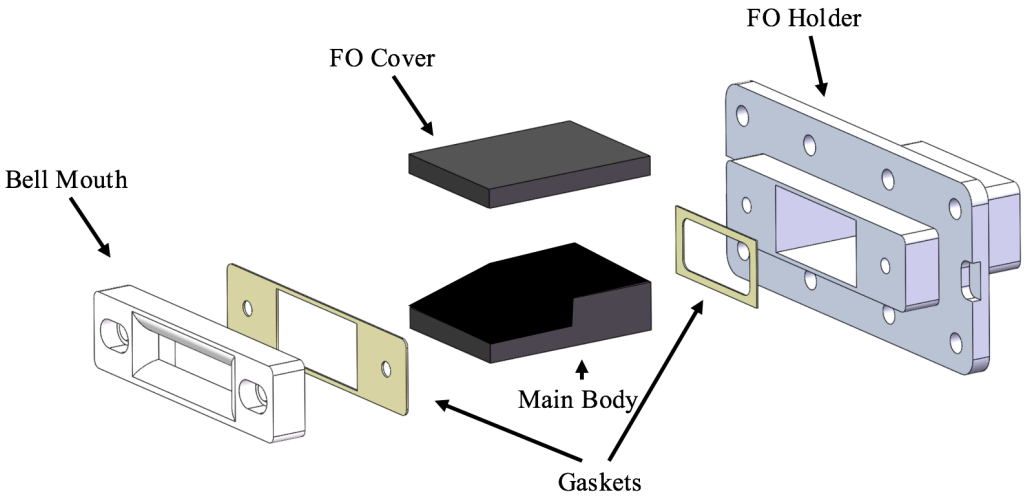

Figure 20 - FO Holder

This holder worked well during the testing. However, at pressures in excess of 30 psi, the gasket in the front blew out, thereby creating an air leak. To counteract this, a thicker gasket material was used to create the seal, which worked effectively at higher pressures.

Multiple materials were considered to manufacture the holder. Aluminum was considered due to its strength and machinability. This would allow it to easily withstand the pressures that were seen in the plenum and minimize the risk of stripping the threads where fasteners are used. However, this was not selected due to time constraints and the difficulty to machine the pocket to hold the FO due to its depth. Additionally, the bell mouth could not be machined due to its complicated geometry and had to be manufactured using rapid prototyping.

The process that was ultimately chosen to prototype the rig was SLA. Xtreme White 200 was selected as the material due to its mechanical properties, allowing it to withstand the expected pressures. This part succeeded in accomplishing the required task; however, swelling of the part was observed over time most likely due to moisture. This made it difficult to insert and remove the part from the plenum and caused one of the rigs to break. Sanding the part temporarily solved the problem; however, the part is expected to expand further. This suggests that SLA is not an ideal process to manufacture this part because it is intended to be used over time. The part was redesigned to be machined from aluminum using wire EDM to create the pocket.

4.2.5 Measuring Equipment

Several parameters were measured during the testing of the FOs to characterize their performance. The entire setup can be seen in Figure 21. Below is a list of all the measurements that were taken and the instrumentation that was used to measure the values.

- Flow Rate: The flow rate of the air was measured using a mass flow meter connected between the air source and the inlet to the plenum. This provided a measurement of the mass flow rate that was being passed through the FO. This is useful in calculating the coefficient of momentum of the jet and determining the air flow requirements for the FO design.

- Pressure: Another important characteristic of the FO that was measured was the pressure drop across the FO. To determine this, a pressure gauge was placed in the plenum. This is another important characteristic of the FO as a lower pressure drop is preferred.

- Temperature: This was also measured in the plenum of the FO using a thermocouple. This was measured to ensure that the temperature of the air between the different tests was similar and did not affect the results of the tests.

- Jet Velocity: This was measured using a hot wire anemometer.

- Oscillation Frequency: This was also measured using a hot wire anemometer. The anemometer was placed on one side of the FO and as the air reached that side, a spike in velocity was measured. The frequency of these spikes corresponded to the frequency of the jet oscillation.

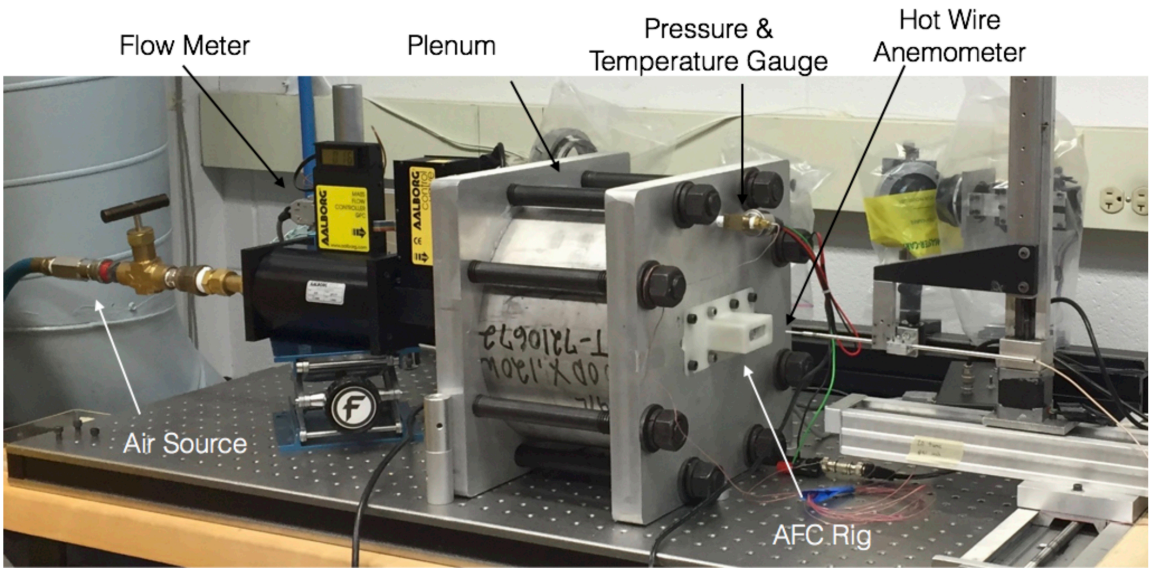

Figure 21 - Test Setup

4.2.6 Procedure

Below is the procedure for testing the FO.

1. Once the FO was manufactured, it was bonded to the top cover plate to create a test module.

2. This module was inserted into the FO holder, sealed using gaskets, and inserted into the plenum.

3. The air supply was turned and set to a specific flow rate to activate the FO. The flow rates were increased in 50 L/min increments up to 500 L/min.

4. At each flow rate, the pressure, oscillation frequency, and temperature were measured. The oscillation frequency was measured 3 mm away from the orifice opening.

5. For flow rates of 50 L/min to 150 L/min, the span wise velocity distribution was measured at 3, 8, 15, and 25 mm from the orifice opening.

4.3 Geometric Measurements

In addition to measuring the flow characteristics of the FOs, the geometric dimensions of the oscillators were also measured. This allowed for accurate assessment of the critical dimensions that were modulated during testing. Three different methods were used to measure the different dimensions of the oscillator.

4.3.1 Micrometer

To measure certain external dimensions, a micrometer was used. This was primarily used to measure the nozzle length. This proved to be an accurate method to measure this dimension as it required clamping the part between the calipers and no effort had to be made to ensure that calipers were parallel to the surface of the oscillator. However, this method was not suitable to measure internal dimensions such as the nozzle width and the interaction chamber width because there was no way to ensure the calipers were perpendicular to the wall. There was also a chance to damage the nozzle during measurement. Hence, other methods were used to measure these dimensions.

4.3.2 Zeta Optical Profiler

Initially, measurements were taken using a Zeta 3D Optical Profiler using a 5x zoom lens. The part was placed under the lens and multiple photos were taken to stitch together. Once the photos were stitched, the software was used to measure the geometric dimensions. Here the limitation in accuracy of the measurements was determined by how accurately the endpoints were placed.

4.3.3 Camera and MATLAB

In an attempt to use more readily available equipment to measure the dimensions, a phone camera and MATLAB were used to measure the geometric dimensions. A pair of calipers were set to a reference distance and were placed on the same plane as the dimension being measured. This setup was then photographed using a phone camera. This photograph can be seen in Figure 22.

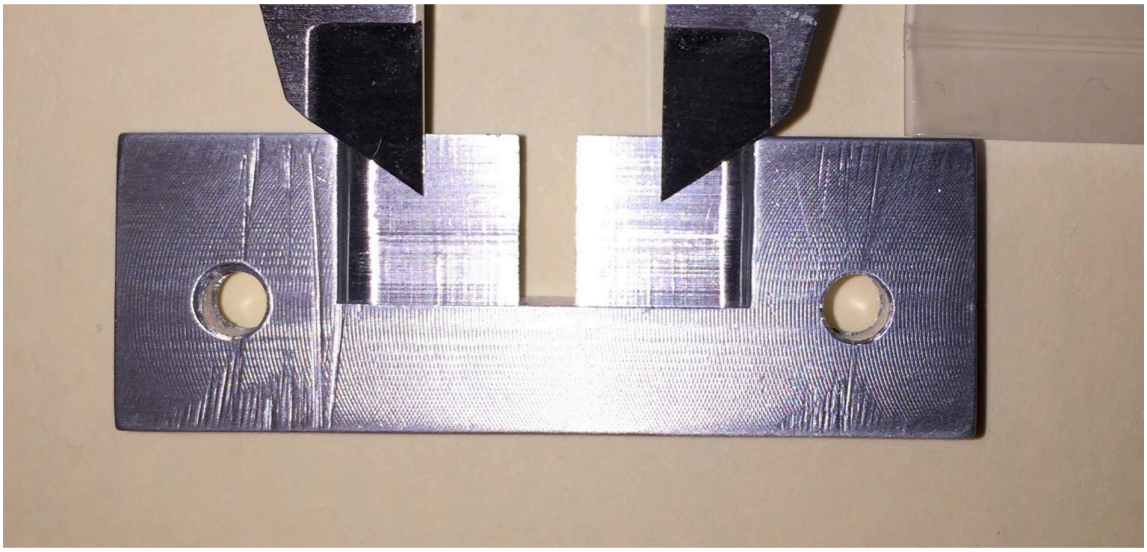

Figure 22 - Image of Test Nozzle with Reference

Once this photo was taken, the image was imported into MATLAB, converted to a gray scale image and edge detection was performed on the image. This image was then displayed. Utilizing the distance measurement tool in MATLAB, the reference distance was measured to determine the distance per pixel. Multiple distances were measured along the nozzle opening and converted to inches using the distance per pixel measurement. The accuracy of this measurement was within 0.001 inches, which is acceptable for the required use. The processed image can be seen in Figure 23 and the code is attached in the Appendix A1.1.

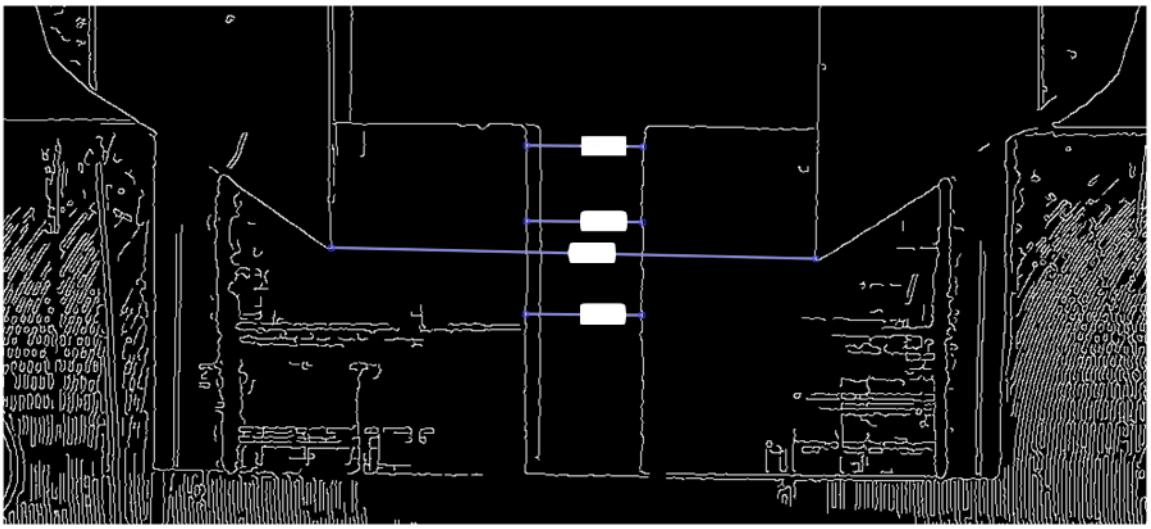

Figure 23 - Processed image used to measure dimensions

Table 3 list the dimensions that were measured for all the FOs. One important factor to note is that the interaction chamber width is the same for all the FOs tested with different nozzles. This is because the nozzles were split at the edge of the fillet, which is the widest part of the interaction chamber. The numbers are listed as percentages to protect proprietary information. A negative percentage means that that dimension was that percentage smaller than the nominal dimension while a positive percentage means that the dimension was that percentage larger than the nominal dimension.

Table 3 – Variation in Geometric Measurement of all FOs in percentage

Identifier	Nozzle Width	Nozzle Length	Interaction Chamber Width
M-MR-AL	1.2%	1.0%	-0.4%
M-IR-AL	0.3%	3.8%	-0.4%
M-MR-CF	1.2%	1.0%	-0.4%
SLS-NR-CF	27.1%	-5.3%	0.4%
SLA-N	7.7%	-0.6%	0.1%
AL1	0.5%	-35.3%	-0.4%
AL2	0.9%	0.1%	-1.3%
AL3	2.9%	41.0%	-0.1%
M-AL-VNDL	-1.2%	5.9%	-2.2%
M-AL-VNDL2	-0.8%	1.3%	-2.2%
M-AL-VN50S	6.7%	7.9%	-2.2%
M-AL-VN25S	6.4%	-36.3%	-2.2%
M-AL-VN25L	2.4%	-12.2%	-2.2%
M-AL-VN50L	4.1%	14.1%	-2.2%
M-AL-VNSN	0.0%	42.1%	-2.2%
M-AL-VN20N	-20.6%	-0.8%	-2.2%
M-AL-VN20W	16.1%	0.6%	-2.2%
M-AL-VNSRN	-2.6%	-0.8%	-2.2%
M-AL-VNLRN	-1.8%	1.3%	-2.2%
M-AL-VN10-O	-3.1%	-1.1%	-2.2%
M-AL-VN25-O	-1.3%	-0.4%	-2.2%

4.4 Chapter Summary

This chapter provided a description of all the FO test specimens. One test studied the effect of material on the performance of FOs by machining an FO from two different

materials. Test specimens were also created to observe the difference between manufacturing processes. Finally, multiple nozzles were created where dimensions including nozzle length, nozzle width, nozzle radius, nozzle curvature, and nozzle symmetry were varied.

In addition to the test specimens, the testing rig was designed to include an FO holder that held the test specimens and could be inserted into the plenum to create an airtight seal. Parameters including flow rate, temperature, pressure, jet velocity, and oscillation frequency were measured.

Lastly, the method used to measure the geometric dimensions of the test specimen was also detailed, where a phone camera and MATLAB software were used to measure critical dimensions. In the next chapter, the data from the experiments are presented.

CHAPTER 5. RESULTS

This chapter presents the results of the experiments. First, the relationships between the different critical dimensions and the performance of the FO are characterized using the machined aluminum FOs. Statistical analysis is then used to determine which dimensions are critical to the performance of the FO. These results are used to develop a model that can predict the oscillation frequency and the pressure drop for the FO based on the geometry and the operating conditions. These are factored into the results for varying material and manufacturing process in Chapter 6.

5.1 Geometric Variation

This section explores the qualitative relationships between the different variables that are measured. Specifically, the effects of these variables on the pressure drop, oscillation frequency, and the jet profile are characterized.

5.1.1 Nozzle Width

The graph on the left in Figure 24 shows the relationship between the frequency and flow rate. Initially, the frequency is dependent on the flow rate; however, at increasing flow rates the frequency starts to become independent of the flow rate. For the narrower nozzle, VN-20N, this begins to happen at a much lower flow rate, around 0.004 m^3/s. This is delayed for the larger nozzle, indicating that a larger nozzle width delays when the frequency becomes independent of the flow rate. This will also be referred to as the knot

point in this thesis and will be explored in greater detail in Chapter 6. The figure on the right shows the relationship between flow rate and the pressure in the plenum. It can be seen that reducing the nozzle width increases the pressure in the plenum. This is expected as reducing the nozzle width will constrict the flow; hence, it increases the pressure drop for the same flow rate.

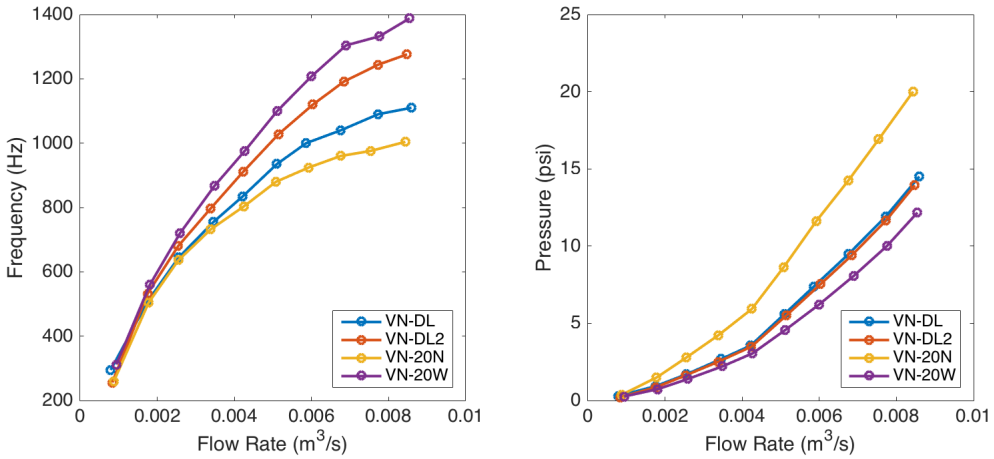

Figure 24 - Frequency vs. Flow Rate (left) Pressure vs. Flow Rate (right) for Nozzle Widths: -1.2% (VN-DL), -0.8% (VN-DL2), -20.6% (VN-20N), and 16.1% (VN-20W)

Figure 25 shows the relationship between pressure and frequency. It can be seen that the wider nozzle can reach higher frequencies at the same pressure. The change in gradient with relation to pressure is similar for all the nozzles after the initial incline, indicating that pressure is the governing factor in determining when frequency becomes independent of the operating conditions. For this oscillator design, this begins to occur around 7.5 psi.

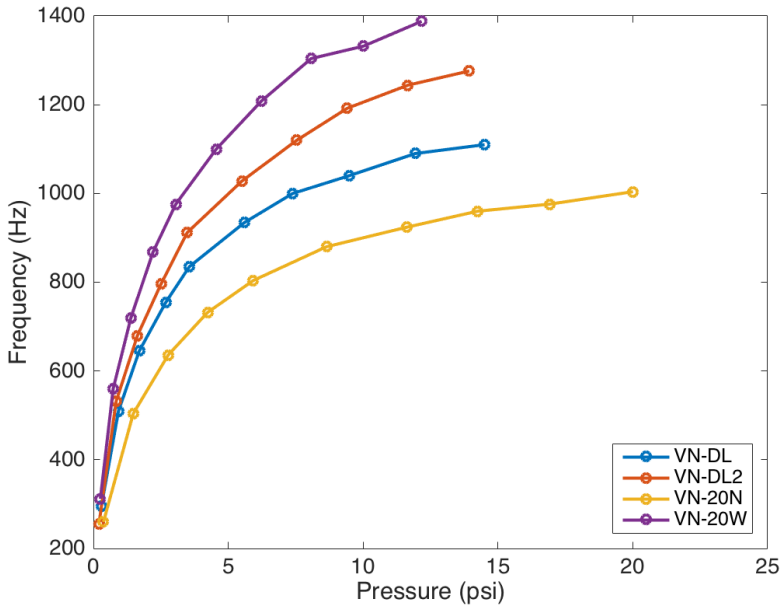

Figure 25 - Pressure vs. Frequency for Nozzle Widths: -1.2% (VN-DL), -0.8% (VN-DL2), -20.6% (VN-20N), and 16.1% (VN-20W)

5.1.2 Nozzle Length

In Figure 26, the graph on the left plots the relationship between flow rate and oscillation frequency for the various nozzle lengths. It can be seen that all the curves are similar and the oscillation frequencies are within 15% of each other. Additionally, the curves are not ordered according to nozzle length, which indicates that the nozzle length has no effect on the oscillation frequency of the FO.

The chart on the right in Figure 26 plots the relationship between flow rate and pressure. It can be seen that all of the FOs have the same flow rate versus pressure relationship. This indicates that the nozzle length has no effect on the pressure drop across the FO. This is expected as the nozzle width was found to be the governing factor and the geometry outside the FO should not affect the pressure.

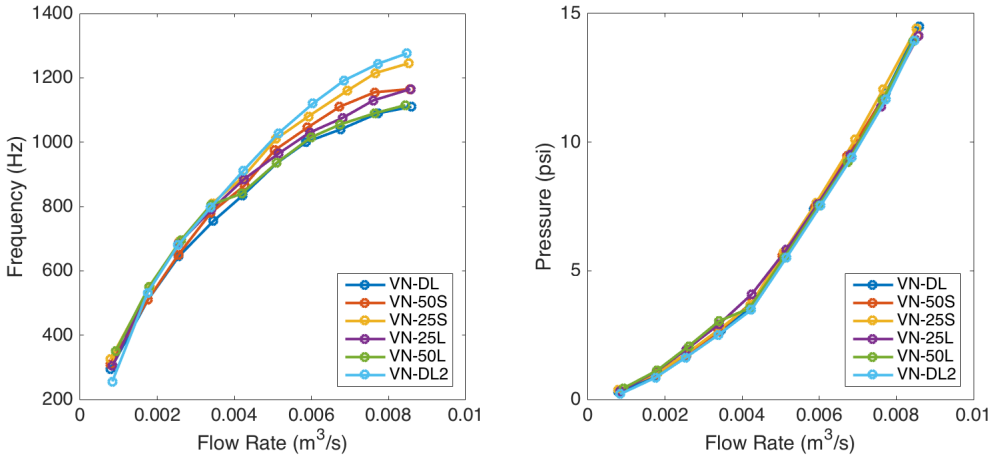

Figure 26 - Flow Rate vs. Frequency (left) Flow Rate vs. Pressure (right) for Nozzle Lengths: 6% (VN-DL), 1% (VN-DL2), -35% (VN-50S), -12% (VN-25S), 14% (VN-25L), and 42% (VN-50L)

Another aspect of the nozzle length that was explored in the background section of this thesis was the effect of varying nozzle length on the jet profile. Figure 27 shows the span-wise distance versus the normalized jet exit velocity for the different nozzle lengths at 0.00083 m^3/s flow rate and measured 8 mm from the FO. The jet exit velocity was normalized by setting the maximum velocity of each jet to one (1). This was required as the jet velocity varies with respect to the height of the hot wire anemometer, which was not controlled during testing. It can be seen that increasing the nozzle length increases the jet width. This is true for increases up to the nominal length. However, there is no noticeable increase in jet width between the VNDL nozzle and the VN25L nozzle. Another set of data that can be used to determine effect of nozzle length on jet profile is the set for the Al 1, 2, and 3 oscillators, as their nozzle lengths were also varied. Figure 28 plots the normalized jet profile for Al 1, 2, and 3 at 0.00083 m^3/s flow rate and measured 8 mm from the FO. It can be seen that increasing the nozzle length increases the jet width, up to the nominal

length, after which point there is no further increase in the jet width. Increasing jet width by increasing the nozzle length is similar to the changes in the jet profile observed by Koklu (2016), indicating that a longer nozzle length would provide similar control authority with a lower momentum coefficient. These FOs would have to be tested in a wind tunnel to fully characterize these effects. Another feature to note is the asymmetry of the jet profile. This is likely due to the manufacturing defects; however, to fully quantify the effect of this asymmetry, wind tunnel tests would have to be conducted.

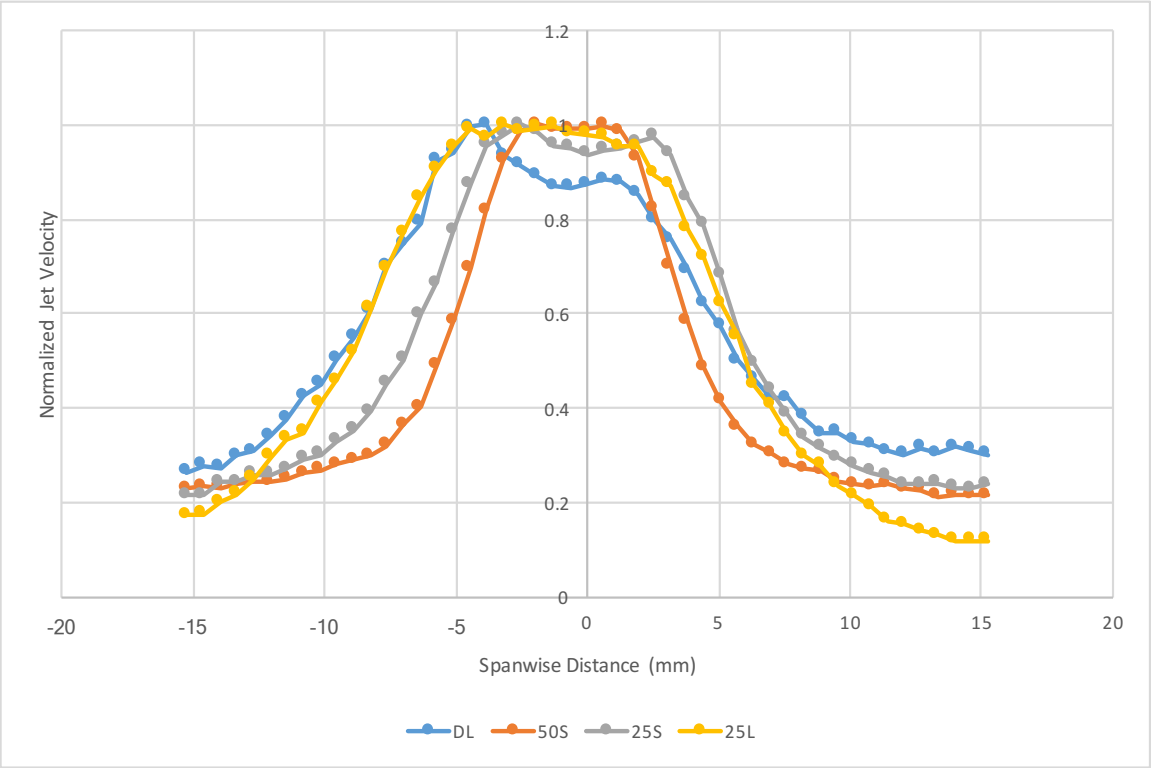

Figure 27 - Span-wise variation of the normalized jet speed along the exit plane for Nozzle Lengths: 6% (VN-DL), -35% (VN-50S), -12% (VN-25S), and 14% (VN-25L)

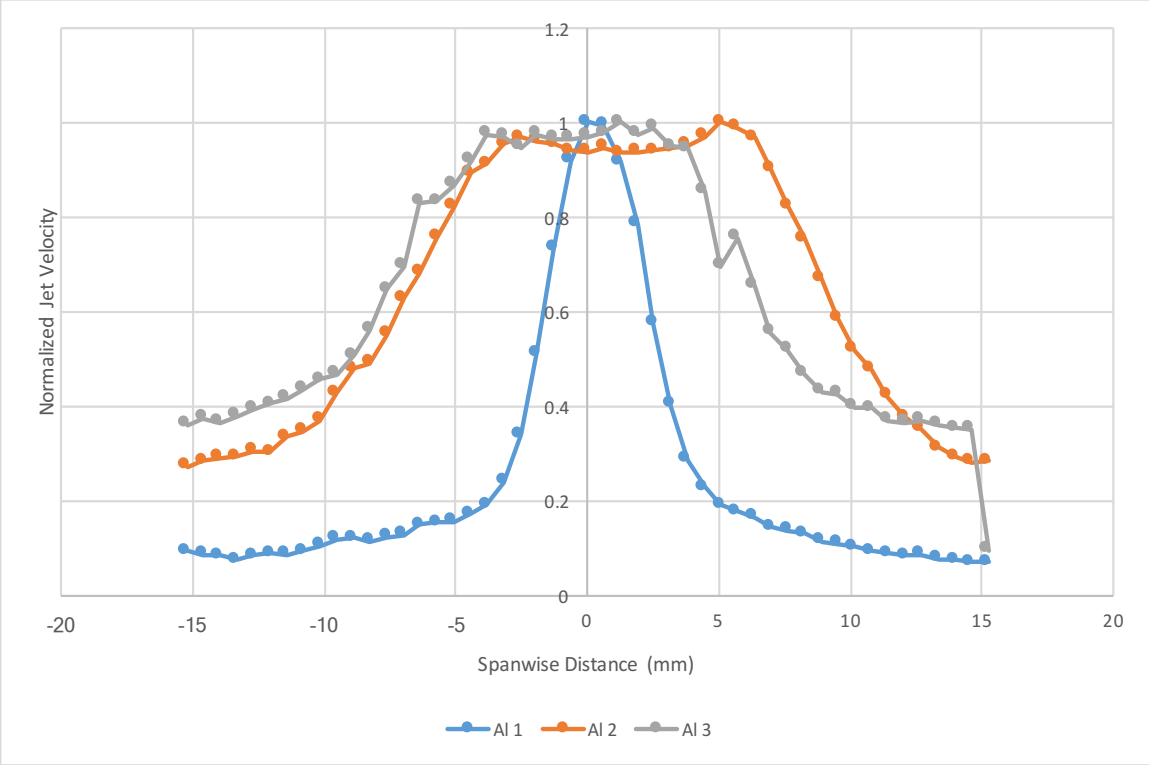

Figure 28 – Span-wise variation of the normalized jet speed along the exit plane for Nozzle Lengths: -35% (Al 1), 0%(Al 2), and 41% (Al 3)

5.1.3 Nozzle Radius

In Figure 29, the graph on the left plots the flow rate versus the oscillation frequency for nozzles with different radii. The VNDL nozzle has a sharp edge, which is the nominal design. The SRN and LRN nozzles have radii of 1/32 in and 1/16 in, respectively. It can be seen that nozzle with sharp edge has a lower oscillation frequency than nozzles with rounded edges. This could be due to flow being affected at it leaves the interaction chamber. This suggests that the radius of the nozzle affects the oscillation frequency of the FO and that a rounded FO will have a higher oscillation frequency.

The graph on the right in Figure 29 plots the flow rate versus the pressure in the plenum. As can be seen, increasing the radius decreases the pressure drop across the FO. This is expected as there are greater losses near sharp corners; hence, the rounded corners reduce these losses, and as a result, there is a lower pressure drop. It is important to note that the SRN had a slightly narrower nozzle than LRN, which could explain the higher pressures observed while testing the SRN oscillator and suggests that the radius does not matter as long as one exists. This suggests that if the designer wants to reduce the power requirements of the FO, a radius could be added to the nozzle edge while keeping the nozzle width the same.

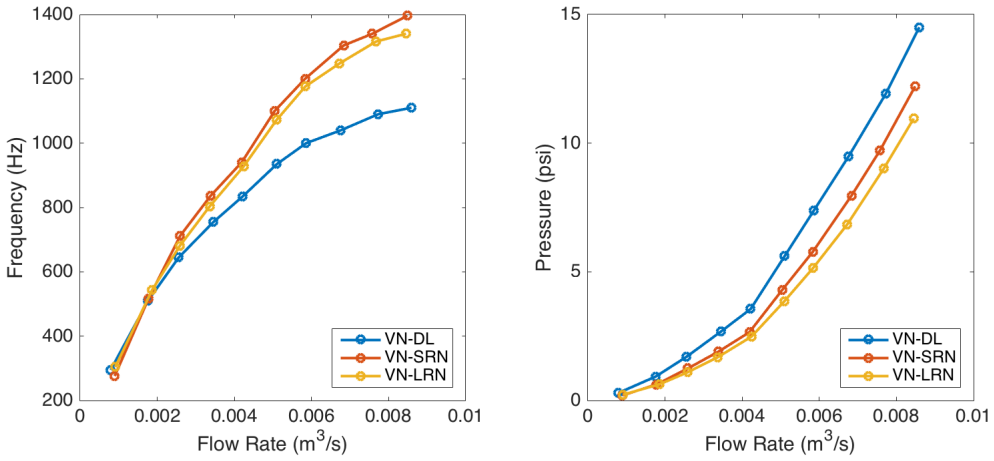

Figure 29 - Flow Rate vs. Frequency (left) Flow Rate vs. Pressure (right) for Nozzle Radii: sharp (VN-DL), 1/32in (VN-SRN), and 1/16in (VN-LRN)

5.1.4 Interaction Chamber Width

In Figure 30, the graph on the left plots the flow rate versus the oscillation frequency for nozzles with different interaction chamber widths. It is worth noting that M-MR-AL had the widest FO and VNDL had the narrowest. It can be seen that the narrower interaction

chamber has a larger oscillation frequency. This indicates that the width of the interaction chamber affects the oscillation frequency of the FO and that a wider interaction chamber will produce a lower oscillation frequency. This could be because a smaller interaction chamber means that the FO takes less time to reach the conditions that cause the jet to flip; however, the detailed physics behind this behavior is not known.

The graph on the right in Figure 30 plots the relationship between flow rate and pressure. It can be seen that the flow rate and pressure relationship for the different FOs are very similar. This indicates that there is no relationship between pressure drop and the interaction chamber width. This is expected as the geometry inside the FO should not affect the pressure drop across the orifice as it is mostly governed by the nozzle area and the nozzle radius.

Another observation that can be made from these figures is that the use of a nozzle plate did not affect the results of the FO performance. The pressure drops across the FOs are the same for the full body and the FO insert specimens and their frequencies are similar. The VN-DL2 nozzle did have an oscillation frequency that was greater than the other three oscillators. This could be due to manufacturing defects in the VN-DL2 nozzle that could have created geometric variations in the part. In short, there are no major differences between the full body and nozzle insert specimens, and any variations caused by using a removable nozzle insert can be ignored.

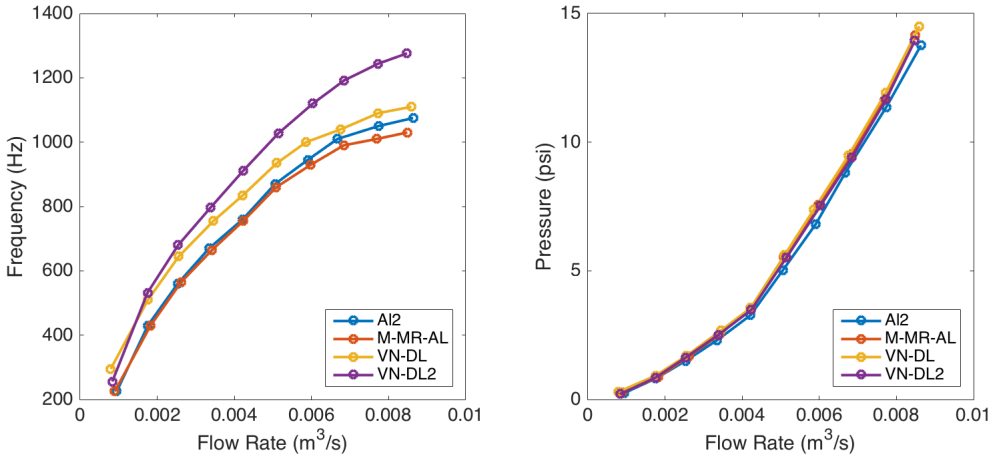

Figure 30 - Flow Rate vs. Frequency (left) Flow Rate vs. Pressure (right) for Interaction Chamber Widths: -0.4% (Al 2), 0.4% (M-MR-AL), -2.2% (VN-DL), and -2.2% (VN-DL2)

5.1.5 Nozzle Symmetry

In Figure 31, the graph on the left plots the relationship between flow rate and oscillation frequency for the various nozzle offsets. It can be seen that all the curves are very similar and the oscillation frequencies are within 15% of each other. The variation between the VNDL and VNDL2 nozzles is greater than the variation between the VN10-O and VN25-O nozzles. This indicates that nozzle symmetry has no effect on the oscillation frequency of the oscillator within the range of values that were tested. This tells us that having an off-center orifice means that the jet spends more time on one side of the orifice, biasing the jet profile to that side. It also indicates that the location of the nozzles does not affect the interaction of the jet within the interaction chamber which governs the oscillation frequency.

The graph on the right in Figure 31 plots the relationship between flow rate and pressure. It can be seen that all the oscillators have very similar pressures. The VN10-O nozzle has a slightly higher pressure than the rest of the FOs, however, this FO also has a narrower nozzle which is likely the cause of the variation. This indicates that the nozzle offset has no effect on the pressure drop across the oscillators. This is expected as the nozzle width was found to be the governing factor and the location of the nozzle should not affect the pressure drop.

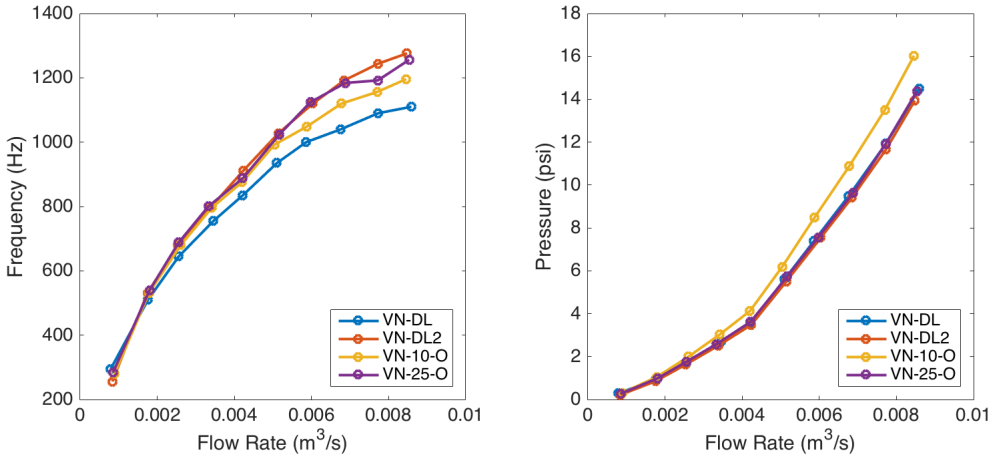

Figure 31 - Flow Rate vs. Frequency (left) Flow Rate vs. Pressure (right) for Nozzle Offsets: 0% (VN-DL), 0% (VN-DL2), 2.3% (VN-10-O), and 5.8% (VN-25-O)

Another aspect to consider when looking at nozzle symmetry is the jet profile. Figure 32 shows the normalized jet profile for the two offset nozzles and the nominal design at 0.00083 m^3/s flow rate and measured 8 mm from the FO. As can be seen, for the VN10-O nozzle there is little offset in the jet velocity profile indicating that an offset of 2.3% will not significantly affect the jet profile, whereas the VN-25N nozzle is skewed further to the left, which shows that a 5.8% offset does shift the jet noticeably. Additionally,

it can be seen that the nominal design has an offset jet velocity profile. This suggests that there are factors, other than an offset nozzle, which contribute to an offset jet profile. The effects of an offset jet profile are not fully known and wind tunnel tests would have to be conducted. In short, if a 2.3% tolerance is placed on the symmetry, there should be no significant effects to the jet profile when compared to the nominal design.

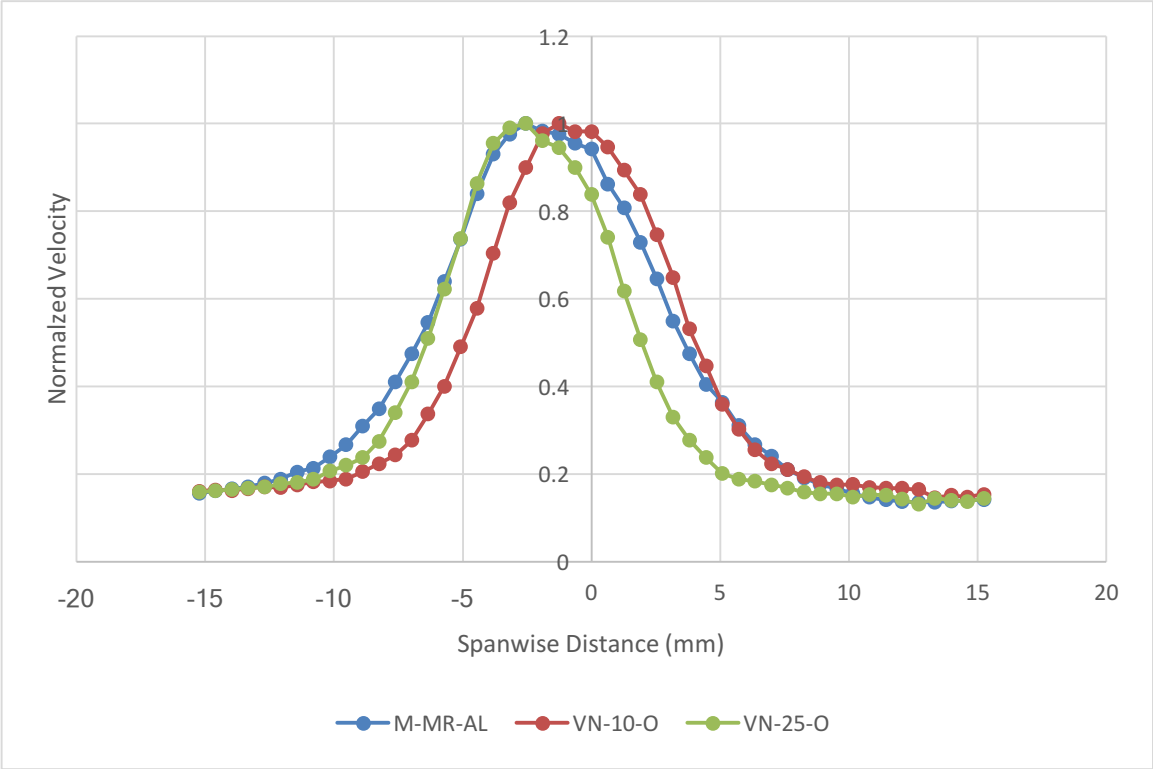

Figure 32 - Span-wise variation of the normalized jet speed along the exit plane for Nozzle Offsets: 0% (M-MR-AL), 2.3% (VN-10-O), and 5.8% (VN-25-O)

5.1.6 Nozzle Curvature

In Figure 33, the graph on the left plots the flow rate versus the oscillation frequency for nozzles with and without curvature. As can be seen, the nozzle without curvature lies between the two nozzles with curvature, indicating that this curvature has no effect on the oscillation frequency of the FO. This could be because the oscillation frequency largely

depends on the interaction within the interaction chamber, and hence the geometry outside the FO should not have an effect on the oscillation frequency.

The graph on the right in Figure 33 plots the relationship between flow rate and pressure. It can be seen that all of the oscillators have the same pressure. This indicates that the nozzle curvature has no effect on the pressure drop across the oscillators. This is expected as the nozzle width was found to be the governing factor and the geometry outside the oscillator should not affect the pressure.

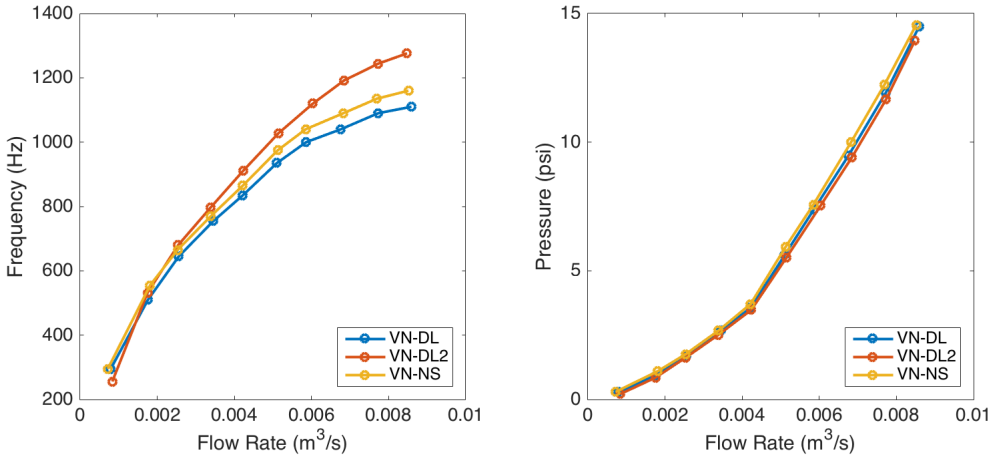

Figure 33 - Flow Rate vs. Frequency (left) Flow Rate vs. Pressure (right) for Nozzle Curvatures: nominal (VN-DL), nominal (VN-DL2), and none (VN-NS)

Figure 34 plots the normalized jet profiles for the nozzles with and without curvature at 0.00083 m^3/s flow rate and measured 8 mm away from the FOs. It can be seen that the jet profile for the two different nozzles are almost identical. This suggests that the curvature does not need to be controlled when manufacturing the FO, as it will not affect

the performance of the FO. There is a variation in the jet profile away from the center, but that does not have a significant effect on the performance of the oscillator and can be ignored. It is likely caused by manufacturing defects.

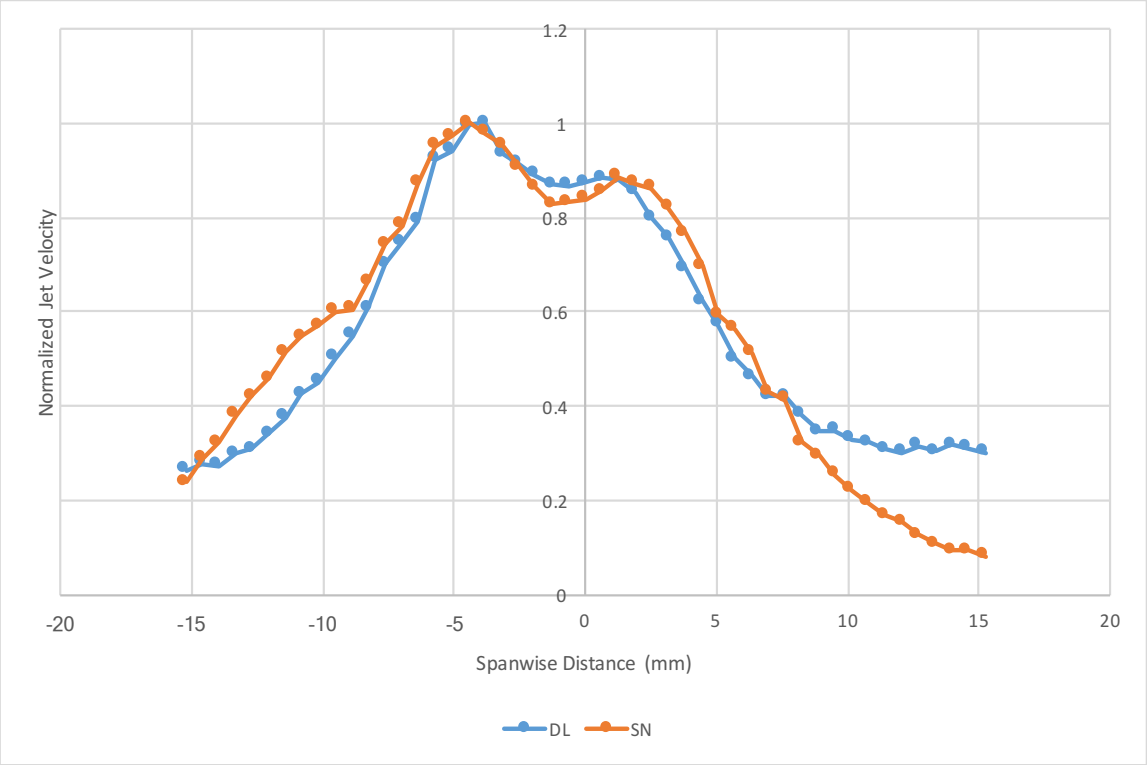

Figure 34 - Span-wise variation of the normalized jet speed along the exit plane for Nozzle Curvatures: nominal (VN-DL) and none (VN-SN)

5.2 Statistical Study

This section covers the statistical analysis that was conducted to determine which of the geometric variations affected the oscillation frequency and jet oscillation. Analysis of variance (ANOVA) was used to perform the analysis. The first step involved categorizing the dimensions into a high or low value. The numeral 1 (one) represents a low value while the numeral 2 (two) represents a high value. This was done for all of the variables except

nozzle width, which was divided into three categories, where “1” is a low value, “2” is a middle value, and “3” is a high value. Table 4 shows the categories into which each FO was divided.

Table 4 - Categorized Geometric Measurement of all FOs

Identifier	Nozzle Width	Nozzle Length	Interaction Chamber Width	Shoulder Radius	Nozzle Radius
M-MR-AL	2	1	2	1	1
M-IR-AL	2	2	2	2	2
M-MR-CF	2	1	2	2	1
SLS-NR-CF	3	1	2	2	2
SLA-N	3	1	2	2	2
AL1	2	1	2	1	1
AL2	2	1	2	1	1
AL3	2	2	2	1	1
M-AL-VND	2	2	1	1	1
M-AL-VNDL2	2	2	1	1	1
M-AL-VN50S	3	1	1	1	1
M-AL-VN25S	3	1	1	1	1
M-AL-VN25L	2	2	1	1	1
M-AL-VN50L	2	2	1	1	1
M-AL-VNS	2	2	1	1	1
M-AL-VN20N	1	1	1	1	1
M-AL-VN20W	3	1	1	1	1
M-AL-VNSRN	2	1	1	1	2
M-AL-VNLRN	2	2	1	1	2
M-AL-VN10-O	1	1	1	1	1
M-AL-VN25-O	2	1	1	1	1

To perform the analysis, a MATLAB script was used and is presented in Appendix A1.2. Type II sum of squares analysis is used as it is assumed there are no significant interactions between the input variables. For example, the nozzle width does not affect the

nozzle radius. The study was performed using the input variables that affect flow: nozzle width, nozzle length, interaction chamber width, shoulder radius, and nozzle radius.

5.2.1 Pressure Drop

Table 5 shows the results of the ANOVA study conducted on pressure. The results show that there is 99.8% probability that the nozzle width affects the pressure and 98.6% probability that the nozzle radius affects the pressure. In addition, there is 54.5% probability that the interaction chamber width affects the pressure, 0.74% probability that the nozzle length affects the pressure, and 6.3% probability that the shoulder radius affects the pressure.

Table 5 - Analysis of Variance for Pressure Drop

Source	Sum of Sq.	d.f.	Mean Sq.	F	Prob > F
Nozzle Width	6.2657	2	3.13283	10.16	0.0022
Nozzle Length	0	1	0.00003	0	0.9926
Inter. Chamber Width	0.1824	1	0.1824	0.59	0.4555
Shoulder Radius	0.002	1	0.00197	0.01	0.9374
Nozzle Radius	2.4551	1	2.45511	7.96	0.0144
Error	4.0071	13	0.30824		
Total	20.4503	19			

This is expected from the observations in the previous section where the results showed changes in pressure when the nozzle width and radius were varied. It also confirms that the other variables do not have an effect on the pressure drop and are not considered critical dimensions when controlling the pressure drop across the FO. It is likely that the controlling factor is the area of the orifice rather than the width of the interaction chamber; however, the height is not varied in this study, hence there are no data to support this claim.

Based on these data, the model that will be developed to predict the pressure drop across the FO will include the nozzle area and the nozzle radius as inputs.

5.2.2 Oscillation Frequency

Table 6 shows the results of the ANOVA study conducted on oscillation frequency. The results show that there is 92.7% probability that the nozzle width affects the oscillation frequency, 99.9% probability that the interaction chamber width affects the oscillation frequency, and 97.8% probability that the nozzle radius affects the oscillation frequency. In addition to this, there is 51.8% probability that the nozzle length affects the pressure and 25.3% probability that the shoulder radius affects the pressure.

Table 6 - Analysis of Variance for Oscillation Frequency

Source	Sum of Sq.	d.f.	Mean Sq.	F	Prob > F
Nozzle Width	8403.3	2	4201.66	3.22	0.073
Nozzle Length	683.5	1	683.5	0.52	0.4819
Inter. Chamber Width	27287	1	27286.96	20.93	0.0005
Shoulder Radius	141.2	1	141.17	0.11	0.7473
Nozzle Radius	8810.6	1	8810.61	6.76	0.022
Error	16947.7	13	1303.67		
Total	78129.8	19			

These results provide insight into the factors that affect oscillation frequency. It confirms that interaction chamber width, nozzle width, and the nozzle radius do affect the oscillation frequency of the FO. Therefore, the model that will be developed to predict the oscillation frequency of the FO includes the interaction chamber width, nozzle width, and nozzle radius as inputs.

This section looked at the variables that are critical in determining the pressure drop and the oscillation frequency of the FO. The nozzle area and nozzle radius are critical dimensions in determining the pressure drop across the FO. The interaction chamber width, nozzle width, and nozzle radius are critical dimension in determining the oscillation frequency of the FO. The shoulder radius and nozzle length are not critical dimensions for these two output variables.

5.3 Model Development

To provide the FO designer a method to understand the effect of varying the critical dimensions, numerical models were created based on the data collected during testing. These models include the critical dimensions and flow rate as the inputs. One model is used to predict the pressure drop while the other is used to predict the oscillation frequency. This section describes how the models were developed and presents them. The models are least squares fit to the data that were collapsed into to a linear relationship. Chapter 6 utilizes the models to determine critical values including knot point frequency.

5.3.1 Dimensionless Variables

After discussion with Dr. Michael DeSavlo of the Fluid Mechanics Research Laboratory (FMRL) at Georgia Institute of Technology (Georgia Tech), it was determined that utilizing dimensionless variables to develop the model would be beneficial. This is standard practice in the field of fluid mechanics. Four different variable were identified - dimensionless frequency, pressure ratio, Reynolds number, and Mach number.

The dimensionless frequency is used to scale the oscillation frequency to the size of the FO. This is calculated using Equation 2:

$$f+ = \frac{f * L_{sh} * A}{Q} \tag{2}$$

where $f+$ is the dimensionless frequency, f is the oscillation frequency in Hz, L_{sh} is the shoulder width in m, A is the nozzle area in m^2, and Q is the standard volumetric flow rate in m^3/s. The standard volumetric flow rate is a measure of the volumetric flow rate under standard temperature and pressure (STP) conditions. Multiplying this value by the density of air under standard conditions gives the mass flow rate. As this density is constant, the standard volumetric flow rate is directly proportional to the mass flow rate. The shoulder width is used here instead of the interaction chamber width after discussion with Dr. Michael DeSalvo as it was shown to be a better indicator of oscillation frequency instead of the interaction chamber width. Additionally, the interaction chamber width changes with changes in the nozzle width; whereas, the shoulder width does not. The shoulder width is the horizontal distance from the edge of the nozzle to the widest part of the interaction chamber. This can be seen in Figure 35 as the horizontal distance between the two points.

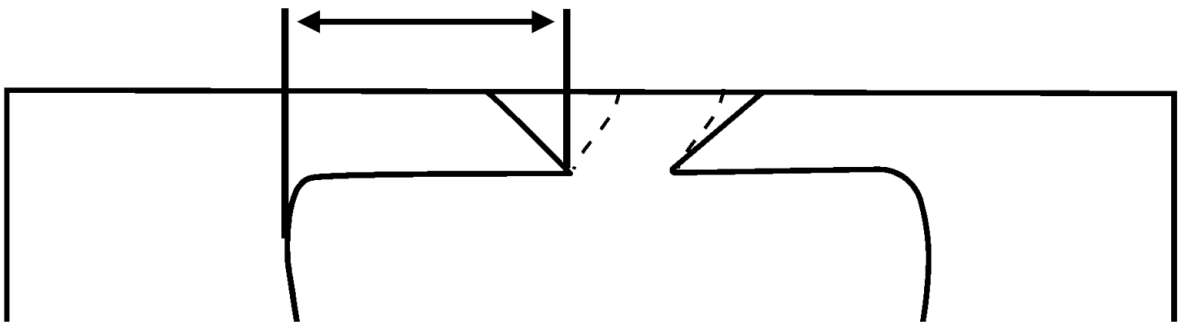

Figure 35 - Shoulder Width Dimension

The pressure ratio is used to scale the plenum pressure to the atmospheric pressure. Here, the pressure ratio is used to create the pressure drop across the FO dimensionless. The pressure ratio can be used to calculate the pressure drop across the FO, which is important in calculating the fluidic power requirements. The pressure ratio is calculated using Equation 3:

$$P_r = \frac{P_{pl}}{P_{atm}} \tag{3}$$

where P_r is the pressure ratio, P_{pl} is the absolute pressure in the plenum, and P_{atm} is the absolute pressure of the atmosphere. The units of P_{pl} and P_{atm} do not matter as long as they are the same.

The Mach number is used to scale the jet velocity to the speed of sound. This is calculated using Equation 4:

$$M = \frac{Q}{A\sqrt{\gamma RT}} \tag{4}$$

where M is the Mach number, γ is the specific heat ratio, R is the gas constant, and T is the temperature in K.

The Reynolds number is used to scale the jet velocity to the size of the FO. This is calculated using Equation 5:

$$Re = \frac{Q * L_{sh}}{A * \nu} \tag{5}$$

where Re is the Reynolds number and ν is the kinematic viscosity of the fluid in m^2/s. These variables can now be used to characterize the performance of the FO.

5.3.2 Pressure Model

To begin developing the model for pressure drop, the FO was treated as an orifice. This means that the flow rate squared is linearly proportional to the pressure drop and the gradient is determined by the orifice area. To remove the effect of this gradient, the Mach number is used instead of the flow rate as it accounts for the effect of the changing orifice area. This relation was plotted and can be seen in Figure 36. As can be seen, the curves collapse to a linear model, indicating that the relationship between these variables can be modeled with a first order polynomial. A model was generated using the data and a least squares fit was used to determine the relationship between the Mach number squared and the pressure ratio. It can also be seen that the line for the FOs with rounded nozzles have a lower slope. For this reason, two different models were developed - one for FOs with rounded nozzles and one for FOs with sharp edges. This is required as the losses are lower when the flow passes through a rounded orifice, therefore utilizing the same model for both would not be appropriate.

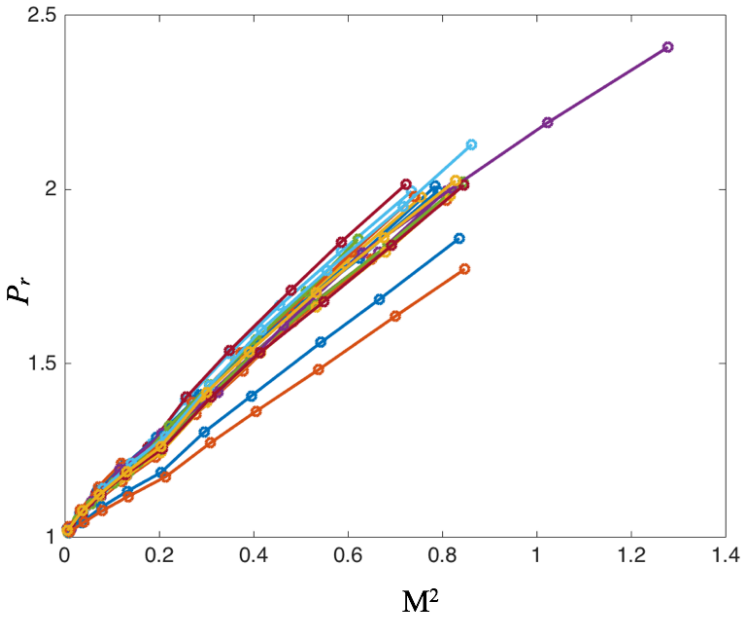

Figure 36 – Variation of Pressure Ratio (P_r) with Mach Number (M) for all machined aluminum FOs

The developed curve-fit can be characterized by Equation 6:

$$P_r = C_1 M^2 + C_2 \tag{6}$$

where C_1 and C_2 are non-dimensional constants that are dependent on whether or not the FO has a rounded nozzle. Table 7 lists the constants for the rounded and sharp FOs and were determined using lease square fit method. Figure 37 shows the best fit lines that correspond to the two different nozzles. The red line (upper) is for a sharp nozzle while the blue line (lower) is for a rounded nozzle.

Table 7 - Constants for Pressure Model

	C_1	C_2
Sharp Edges	1.222	1.0358
Rounded Edges	0.96257	1.000

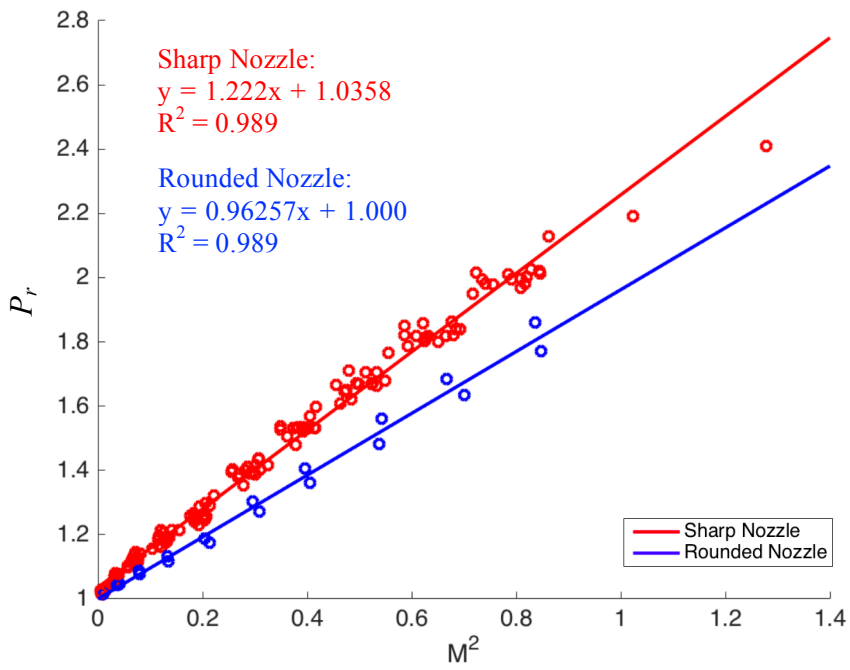

Figure 37 – Variation of Pressure Ratio (P_r) with Mach Number (M) for machined aluminum with curve-fits for sharp nozzle (red) and rounded nozzle (blue)

To verify this model, the pressure calculated using this model was compared to the measured pressure. The average difference for the model was calculated to be 5.95%. This is not a significant difference as variations of this magnitude were seen between the nominal designs that were tested. This difference was more prominent at higher flow rates and might be caused by changes in flow characteristics occurring near the knot point.

5.3.3 Frequency Model

Multiple approaches were tried when developing the model for the oscillation frequency. These included modeling the FO as a contraction and using that relationship to predict the frequency, linearizing the data using a semi-log or log-log relationship, and

modeling the relationship as a second order polynomial. Eventually, it was decided that piecewise linear regression model would provide a more meaningful relationship. A least squares fit was used to determine the initial trend line that passes through the data before the knot point of the piecewise linear regression and is shown in Equation 7. In chapter 6, the process of piecewise linear regression modeling will be explained and applied to the data after the knot point.

$$f + * M * \frac{L_{sh}}{L_{noz}} = \frac{3.11 * M * \frac{\sqrt{A}}{L_{noz}}}{\sqrt{Re}} - 0.0072757 \tag{7}$$

Initially, two different models were developed for a sharp nozzle and a rounded nozzle; however, it was discovered that measuring the shoulder width until the tangent point on the nozzle radius – as seen in Figure 35 - instead of the narrowest point, removed the need to have separate models. Figure 38 plots this relationship with the trend line.

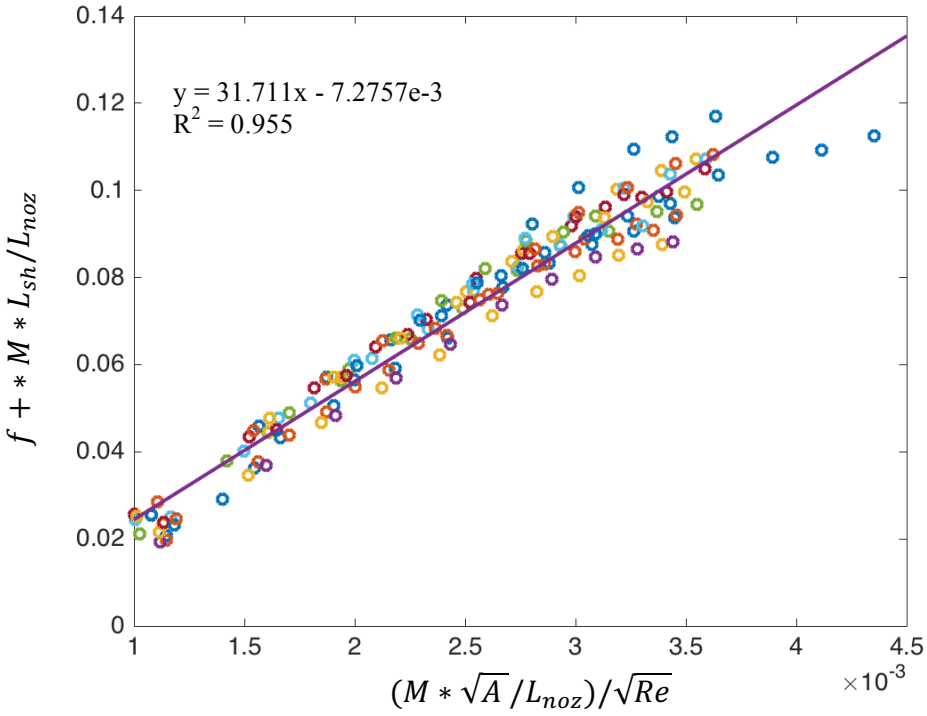

Figure 38 – Relationship between $(M * \sqrt{A}/L_{noz})/\sqrt{Re}$ and $f + * M * L_{sh}/L_{noz}$ machined aluminum FOs with curve-fit for before knot point

To verify this model, the oscillation frequency calculated using this model was compared to the measured oscillation frequency. The average difference for the model was calculated to be 7.41%. As a variation in oscillation frequency of 7.41% will not significantly affect the performance of the FO in the higher frequency regime, hence this model can be used with confidence in predicting the performance of the FO. This difference was more prominent at higher flow rates and is caused by changes in flow characteristics as the knot point is reached.

5.4 Chapter Summary

This chapter presented the results of tests that were conducted. First, the variations in the different dimensions were categorized. Increasing the nozzle width increased the oscillation frequency and decreased the pressure drop. Nozzle length does not have an effect on the oscillation frequency or the pressure drop, but it does affect the jet width. Adding a radius increases the oscillation frequency and reduces the pressure drop. Increasing the interaction chamber width reduces the oscillation frequency and has no effect on the pressure drop. Nozzle symmetry has no effect on the oscillation frequency or pressure drop; however, it does have an effect on the jet velocity profile. Finally, it was determined that the nozzle curvature has no effect on the oscillation frequency, pressure drop, or jet velocity profile.

An analysis of variance study was conducted to determine which factors affect the oscillation frequency and pressure drop. Nozzle width and nozzle radius were the primary contributors to variation in pressure drop and that nozzle width, nozzle radius, and the interaction chamber width were primary contributors to variation in oscillation frequency. This information was used to develop a model that used these variables as inputs and developed a relationship between flow rate and the output variables – pressure ratio and oscillation frequency.

CHAPTER 6. ANALYSIS AND DISCUSSION

This chapter discusses the effects of variations in critical dimensions, materials, and manufacturing processes. The model from the previous chapter is used to determine the knot frequency and the fluidic power. A sensitivity analysis for the critical dimension is presented. Also, the FOs manufactured with different materials and manufacturing processes are evaluated using the developed models.

6.1 Geometric Variation

6.1.1 Knot Point of Piecewise Linear Regression

Figure 38 plots the linear trend relating the oscillation frequency to the operating parameters of the fluidic oscillators tested. It shows that after a certain flow rate, the relationship between the x- and y-axes no longer follows the initial trend line. A piecewise linear function is used to describe the relationship and flowrate of a FO. This was done because two different linear relationships were observed in the data and fitting a single trend line through all the data did not provide an accurate representation of the data. A piecewise linear regression splits the data into two separate sets and fits a least squares fit through the two set of data. These trend lines intersect at the transition point referred to as the knot point. This is important as it signals a change in the flow characteristics of the FO. This could be due to either choking occurring at the orifice or internal flow separation. This splits the flow into two regimes, which is described by a piecewise linear regression. If this is indeed the choking point of the FO, the benefits of operating before this point include

the ability to achieve high oscillation frequency without requiring high fluidic power. However, if the flow is choked, sonic flow is achieved, which can positively benefit the coefficient of momentum. Hence, it is important to determine the location of this transition to allow the FO designer to pick the appropriate regime. If this is not caused by choking, the knot point provides the designer with the limit of the model.

Figure 39 plots the data from Figure 38 for the VN-20N nozzle as that is the only nozzle that had significant data in the region that deviated from the initial linear relationship developed in Chapter 5. It can be seen that the frequency data begin to deviate from the trend line at higher flow rates at the knot point, which was determined through the development of a piecewise linear regression model. In fluids, the Mach number is used to represent when the flow is choked; hence, it will be used to determine the point after with the model is no longer valid. The figure also plots the initial best-fit linear model and the observed trend line after the knot point. The knot point occurs at a Mach number of 0.72, for the limited set of data in this thesis. This could indicate that choking occurs at a Mach number of 0.72; however, more testing would be required to validate this. In addition to the Mach number, the pressure ratio is also an indicator of choking. The knot point corresponds to a pressure ratio of 1.67 indicating that the knot point of the FO occurs at that pressure ratio, for the limited set of data in this thesis. Further testing is required to conclude if the Mach number or the pressure ratio is the governing variable. Appendix A1.3 contains the MATLAB code that was used to determine the knot point of piecewise linear regression model of the FO.

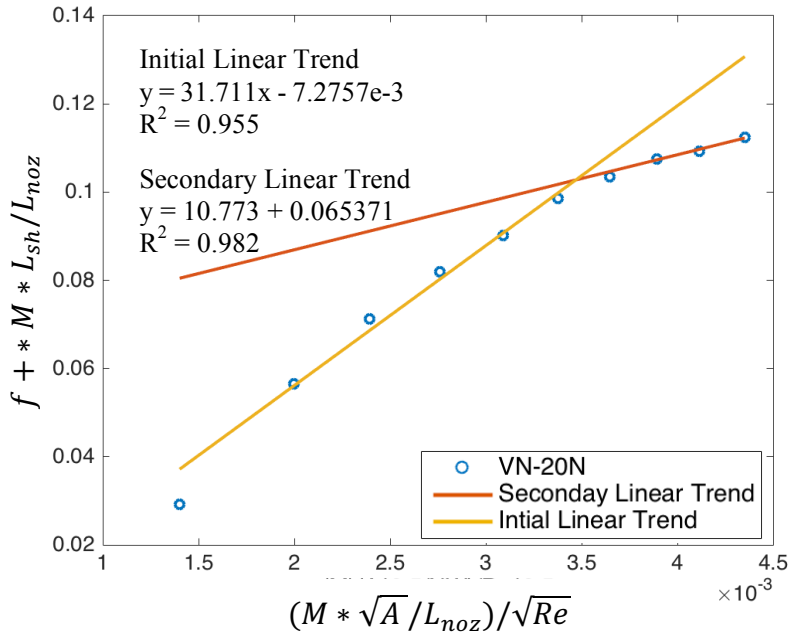

Figure 39 – Relationship between $(M * \sqrt{A}/L_{noz})/\sqrt{Re}$ and $f + * M * L_{sh}/L_{noz}$ for VN-20N nozzle with piecewise linear regression

It is also important to note that the atmospheric conditions will change as the altitude of the plane changes and as it travels to different locations. This means that knot point will occur at a lower mass flow rate at higher altitudes due to the reduced air pressure and colder temperatures. This means that the operating condition of the FO will change as the plane takes off and lands. The primary factor contributing to a change in the Mach number is the air temperature. A decrease in air temperature from 35°C to -10ºC will cause the Mach number to increase by 9.1%, causing the knot frequency to decrease by 8.3%. As the altitude of the plane increases from sea level to 2000m, there is a decrease in atmospheric air pressure from 14.7 psi to 11.53 psi, a 21.6% decrease. This will result in a 21.6% reduction in the minimum pressure required to change the regime of the flow. If this knot point is caused by choking, a 21.6% reduction in minimum pressure would significantly change when the flow is choked. If the FO is operated near this transition, it

is important to consider these effects; however, if the FO is not being operated near this transition, the variations caused by altitude changes or temperature should not affect the performance of the FO. To summarize, the knot point depends on the atmospheric conditions, which can vary significantly as the altitude and location of the plane changes. Although this is true, the change due to altitude can be negligible as the FOs may only be used during take-off and landing, thus the changes due to temperature differences will be more significant. However, changes due to the altitude of the airport may have an effect on the knot point.

6.1.2 Fluidic Power Requirements

Another important consideration for the FO system is its fluidic power requirement. This is because fluidic power on an airplane is limited. Hence, it is important to minimize the power requirement while achieving the same control authority. As the power requirement is governed by the mass flow rate and the pressure drop across the FO, reducing either of these will reduce the power requirement; however, reducing the mass flow rate would also reduce the momentum coefficient of the jet. Thus, it is beneficial to reduce the pressure drop across the FO while maintaining the mass flow rate. It was observed that rounding the nozzle reduced the pressure drop across the FO. This can be seen in Figure 36 as the two rounded nozzles have lower slopes than the sharp nozzles. This is likely due to reduced losses as the air flowed past the nozzle because the difference in nozzle area has been accounted for in the Mach number. This suggests that one way to reduce the power requirement of the system is to add a radius to the nozzle. The effects of adding a radius to the nozzle on the control authority of the FO are not known and wind tunnel tests are necessary to fully characterize the effects on control authority.

6.1.3 Critical Dimension Sensitivity

6.1.3.1 Nozzle Width

The nozzle width was found to be a critical dimension for both the pressure drop across the FO and the oscillation frequency of the FO. From the experimental data, increasing the nozzle width by 16.1% caused the pressure in the FO to decrease by 15.2%, while decreasing the nozzle width by 20.6% caused the pressure in the plenum to increase by 50.2%. Decreasing the nozzle width caused a much greater absolute value increase in pressure than the pressure reduction due to an increase in nozzle width. Also, an increase in pressure is unfavorable, which indicates that an asymmetric tolerance would be favorable in this situation. These values are significant because a 50.2% increase in the pressure would equate to a 50.2% increase in the fluidic power requirement. This could mean the system might not be able to provide the required power. However, it could also result in an increased jet momentum flux, negating the increased power requirements. Hence, wind tunnel tests are required to fully determine if this increase in plenum pressure, caused by a reduction in nozzle width, would affect the control authority of the FO.

The nozzle width also affects the changes in the oscillation frequency of the jet. A 16.1% increase in nozzle width caused the oscillation frequency in the FO to increase by 13.3%, while a 20.6% decrease caused the oscillation frequency in the FO to decrease by 11.0%. When compared to the asymmetry due to the change in pressure, this change in oscillation frequency is symmetric. If the FO is operated in the high frequency regime, these changes are not significant as the performance of the FO would be independent of the oscillation frequency. However, this is not an accurate representation of the effects of

nozzle width because the shoulder width was modified during these tests. Using the model developed in the previous chapter, Figure 40 plots the oscillation frequency of 16.1% wider and 20.6% narrower nozzles assuming that the shoulder width does not change. It shows that increasing the nozzle width decreases the flow rate. Before the knot point in the model, the wider nozzle experiences a 2.5% decrease in oscillation frequency while the narrower nozzle experiences a 2.7% increase in oscillation frequency. This suggests that although there was a large difference in oscillation frequency caused by changing the nozzle width, it was not due to a change in nozzle width. Appendix A1.4 contains a MATLAB code that can be used to predict the oscillation frequency and pressure drop of an oscillator.

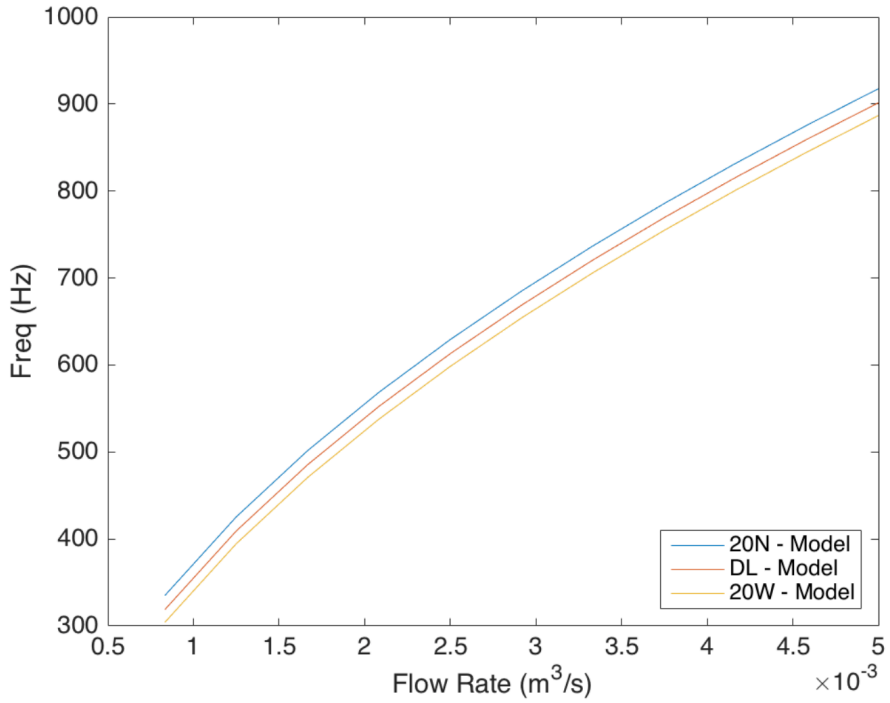

Figure 40 - Flow Rate vs. Frequency Model for Varying Nozzle Width

The knot point for the three nozzles was also calculated. The default nozzle had a knot frequency of 1106 Hz. The wider nozzle had a knot frequency of 1187 Hz, which is a

7.3% increase in knot frequency. The narrower nozzle had a knot frequency of 997 Hz, which is a 9.9% decrease in knot frequency. This is different from the measured knot point of 926 Hz, which indicates that nozzle width is not the only factor that affects the knot point of the oscillator. These changes would be significant if the FO is being operated near the transition boundary.

Table 8 shows the typical tolerance for the different manufacturing processes and the expected variations in the pressure drop and oscillation frequency. The positive (+) values represent the results of the addition of the tolerance to the nominal value (e.g., adding 0.001 inches to the nominal value) and the negative value represents the subtraction. As noted in the background, a tolerance of 0.001 inches is achievable by machining processes, 0.004 inches for injection molding, and 0.005 inches for an additive manufacturing process. It is important to note that holding a tolerance tighter than 0.01 inches can greatly increase the cost of the part. “Exp. Pressure Range” refers to the variation in pressure that would be observed based on the data that were collected using the VN-DL, VN-20N, and VN-20W nozzles. “Exp. Freq. Range” refers to the variation in oscillation frequency that would be observed based on the data that were collected using the VN-DL, VN-20N, and VN-20W nozzles. “Model Freq. Range” refers to the variation in oscillation frequency that would be expected had the shoulder width stayed the same and the nozzle width was the only variable that had changed and was calculated using the model that was developed. Lastly, the “Model knot Freq. Range” is the variation in the frequency at the knot point based on the model that was developed. To conclude, the main reason to tightly control the nozzle width dimension is to control the pressure drop across the FO because the pressure drop is significantly affected by the nozzle width, especially

when the nozzle width is reduced. This could be significant as it affects the fluidic power requirements of the system, which are often limited; however, the effect of this on the momentum coefficient of the jet are not known and wind tunnel tests are required to fully understand the effects of this variation. If the FO is operated in the high frequency regime, the variation in the oscillation frequency are not significant as the performance of the FO would be independent of the oscillation frequency. Also, the knot frequency would only be important if the FO is being operated near that transition.

Table 8 – Ranges of variation in Performance Characteristics based on Nozzle Width Tolerance

Process	Tolerance (in)	Exp. Pressure Range	Exp. Freq. Range	Model Freq. Range	Model Knot Freq. Range
Machining	±0.001	+2.1% -0.8%	+0.7% -0.5%	+0.1% -0.5%	+0.4% -0.4%
Injection Molding	±0.004	+4.8% -3.0%	+2.65% -1.8%	+0.5% -0.5%	+1.6% -1.6%
Additive Manufacturing	±0.005	+10.5% -3.8%	+3.3% -2.3%	+0.6% -0.6%	+2.0% -2.0%
Cost Effective Tolerance	±0.01	+21.0% -7.6%	+6.6% -4.6%	+1.3% -0.13%	+3.9% -4.0%

6.1.3.2 Shoulder Width

Another critical dimension that was identified in the previous chapter is the shoulder width because it contributes to the variation in oscillation frequency. Although the shoulder width was not varied during the testing, varying the nozzle width effectively changed the shoulder width of the oscillator. A 3% decrease in the shoulder width correlated to a 13.3% increase in oscillation frequency. A 3% increase in the shoulder width correlated to an 11.0% increase in the oscillation frequency. Again, this is not an accurate representation of the effect of a change in shoulder width because the nozzle width was

modified during these tests and hence the large changes. Using the model, Figure 40 plots the oscillation frequency of a 3% narrower and 3% wider shoulder assuming the nozzle width does not change. Before the knot point, the narrower shoulder produced a 7.5% increase in oscillation frequency whereas the wider shoulder produced an 8.0% decrease in oscillation frequency. If the FO is operated in the high frequency regime, these percentages are not significant as the performance of the FO would be independent of the oscillation frequency.

The knot point for the three nozzles was also calculated using the model. The default nozzle had a knot frequency of 1106 Hz. The narrower shoulder had a knot frequency of 1195 Hz, which is an 8.0% increase in knot frequency. The wider shoulder had a knot frequency of 1023 Hz, which is a 7.5% decrease in knot frequency. These changes would be significant if the FO is being operated near the transition boundary.

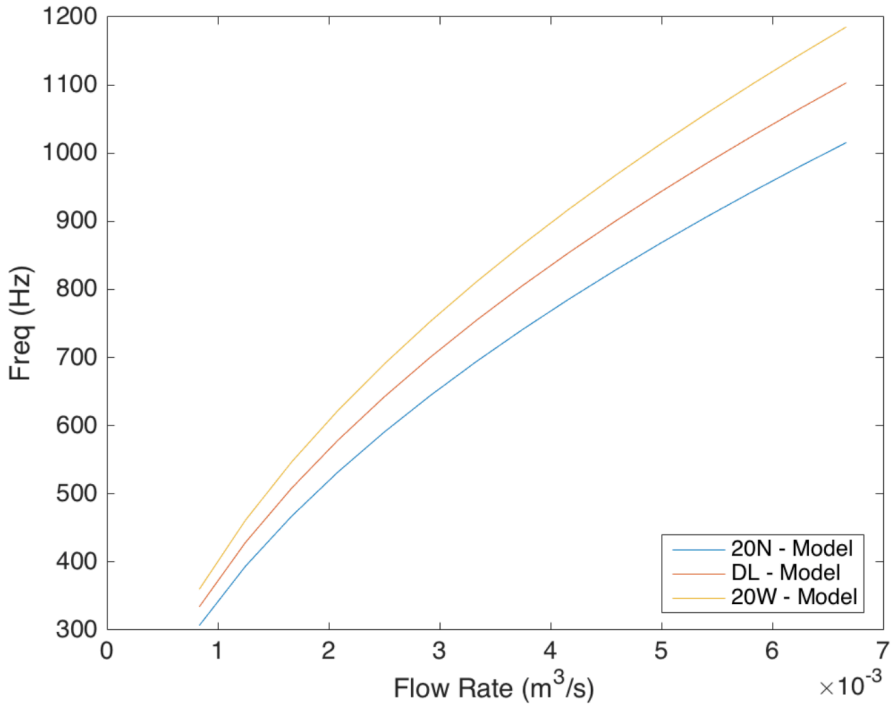

Figure 41 - Flow Rate vs. Frequency Model for Varying Shoulder Width

Table 9 shows the typical tolerance for the different manufacturing processes and the expected variation is oscillation frequency. The positive (+) values represent the results of the addition of the tolerance to the nominal value (e.g., adding 0.001 inches to the nominal value) and the negative value represents the subtraction. "Exp. Freq. Range" refers to the variation in oscillation frequency that would be observed based on the data that were collected using the VN-DL, VN-20N, and VN-20W nozzles. "Model Freq. Range" refers to the variation in oscillation frequency that would be expected had the nozzle width stayed the same and the shoulder width was the only variable that had changed and was calculated using the model that was developed. Lastly, the "Model knot Freq. Range" is the variation in the frequency at the knot point based on the model that was developed. It can be seen that the effect of the shoulder width on the oscillation frequency was less if the nozzle width was fixed. This suggests that although nozzle width and shoulder width do not

significantly impact the oscillation frequency; however, due to their coupled nature, increasing one and decreasing the other leads to a much larger change in oscillation frequency. Therefore, when manufacturing the FO, it might be more beneficial to control the nozzle width and the shoulder width, than to control the nozzle width and the width of the interaction chamber. However, if the FO is operated in the high frequency regime, the variation in the oscillation frequency are not significant as the performance of the FO would be independent of the oscillation frequency. Also, the knot frequency would only be important if the FO is being operated near that transition.

Table 9 – Ranges of variation in Performance Characteristics based on Shoulder Width Tolerance

Process	Tolerance (in)	Experimental Freq. Range	Model Freq. Range	Model Knot Freq. Range
Machining	±0.001	+1.2% -0.9%	+0.7% -0.7%	+0.7% -0.7%
Injection Molding	±0.004	+4.8% -3.7%	+2.7% -2.7%	+2.7% -2.7%
Additive Manufacturing	±0.005	+6.0% -4.6%	+3.4% -3.3%	+3.4% -3.3%
Cost Effective Tolerance	±0.01	+12.0% -9.1%	+6.8% -6.7%	+6.8% -6.7%

6.1.3.3 Nozzle Radius

The nozzle radius was identified as a critical dimension in the previous chapter because adding a radius to the nozzle increases the oscillation frequency and decreases the pressure drop across the FO. It was determined that adding a 1/32" radius increased the oscillation frequency by 6.5% and adding a 1/16" radius increased the oscillation frequency

by 4.1%. This is due to the reduction in shoulder width that is experienced as a radius is added. Additionally, it was determined that adding a 1/32" radius reduced the pressure drop frequency by 19.9% and adding a 1/16" radius reduced the pressure drop frequency by 26.1%. This suggests that it is important to control the nozzle radius as it has a significant effect on the pressure drop across the FO and ultimately the fluidic power requirement of the FO. However, adding a radius increases the oscillation frequency and reduces the pressure drop. This could mean that it might be beneficial to round the nozzle.

6.1.4 Non-Critical Dimensions

6.1.4.1 Nozzle Length

In the previous chapter, it was determined that the nozzle width does not have an effect on the oscillation frequency or the pressure drop across the FO. Hence it is not considered to be a critical dimension during the manufacturing of the FO. However, a change in the jet width was observed when the nozzle length was increased from 36% shorter than the nominal nozzle length to the nominal nozzle length. Also, there is no further increase after increasing the nozzle length past the nominal nozzle length, indicating that if this minimum length is achieved, then there will be no effect on the jet profile. Kolku (2016) showed that a wider jet profile allowed for similar control authority at a lower momentum coefficient; however, this was for a feedback fluidic oscillator. The effect of changing the jet width is not fully understood. Therefore, wind tunnel tests are necessary to fully characterize this relationship.

6.1.4.2 Nozzle Symmetry

In the previous chapter, it was determined that the nozzle symmetry does not have an effect on the oscillation frequency or the pressure drop across the FO. Hence it is not considered to be a critical dimension during the manufacturing of the FO. However, a change in the jet velocity profile was observed when the offset was 5.8%. There was no significant change in the jet velocity profile for a 2.3% offset, suggesting that if the 2.3% tolerance is met, then there will be no significant impact on the control authority of the oscillator. The effect of a skewed jet velocity profile is not fully understood. Therefore, wind tunnel tests are necessary to fully characterize this relationship.

6.1.4.3 Nozzle Curvature

In the previous chapter, it was found that the nozzle curvature does not have an effect on the oscillation frequency, pressure drop, or the jet profile of the oscillator. This leads to the conclusion that this is not a critical dimension and does not need to be controlled when manufacturing the FO.

In summary, the knot frequency is dependent on the Mach number of the jet, which is a function of the flow rate, nozzle area, and the atmospheric conditions. The knot point occurs at a Mach number of 0.72 for one set of data. Also, rounding the nozzle helps to reduce the fluidic power requirements of the FO. The nozzle width, shoulder width, nozzle radius, and nozzle symmetry were found to be critical dimensions, whereas the nozzle length and nozzle curvature had no effect on the performance.

6.2 Material

This section discusses the effects of material on the oscillation frequency, pressure drop, and jet profile of the fluidic oscillator. It is thought that the material should not affect the performance of the FO as long as it is stiff enough to resist significant deflection; however, the material may behave differently during the manufacturing process causing differences in dimensions and as a result, affect the performance of the FO. The experimental data of the FOs manufactured using different materials are evaluated. The data are then compared to the model developed in the previous chapter to see how well they match the model. The model that was developed in the previous chapter only utilized machined aluminum FOs; hence, any difference that is observed is likely due to the material.

6.2.1 Aluminum vs CF PEKK

To characterize the effect of the material on the performance of the FO, different test pieces were manufactured using the machining process that was used for Aluminum and CF PEKK. The graph on the left in Figure 42 shows the non-dimensional frequency model of both the aluminum and CF PEKK FOs. It shows that there are almost no differences in the no dimensional frequencies between the FOs, indicating that the material has no effect on the performance. The graph on the right plots the variation of pressure ratio with the Mach number of the FO. Again, there are almost no differences between the FOs, indicating that material has no effect on the pressure drop across the FO.

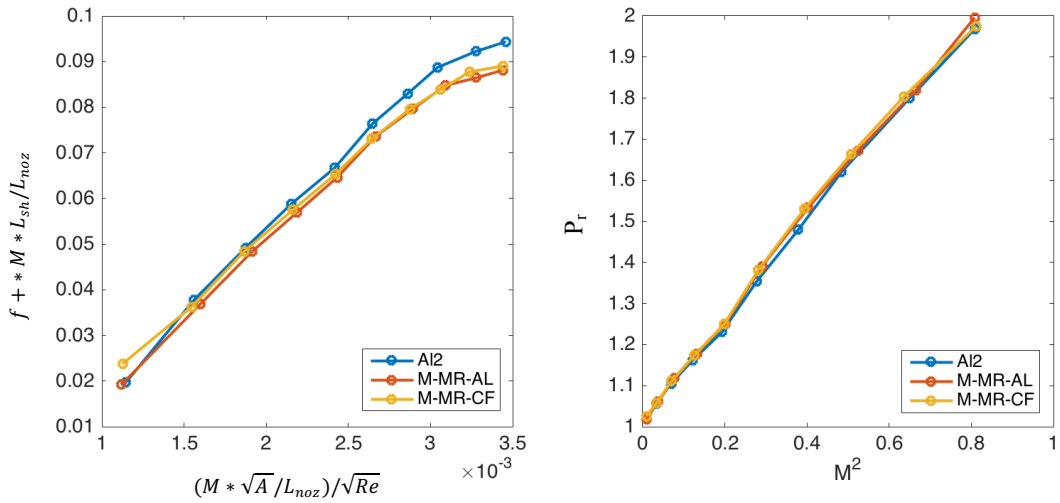

Figure 42 - Non-Dimensional Frequency Model (left) Pressure Ratio Model (right) for Materials: Aluminum (Al2, M-MR-AL) and CF PEKK (M-MR-CF)

Figure 43 compares the model with the experimental data. The graph on the left plots the frequency model. There is an average difference of 7.5% up to the knot point. If the FO is operated in the high frequency regime, the variation in the oscillation frequency are not significant as the performance of the FO would be independent of the oscillation frequency. The graph on the right plots the pressure model and the sharp nozzle model matches the experimental data better than the rounded nozzle model. There is an average difference of 3.65% indicating the model closely follows the experimental data. This change is not significant to affect the fluidic power requirement of the AFC. This is expected as the machining process produces sharp corners, and, if the material has no effect, then it should match the model.

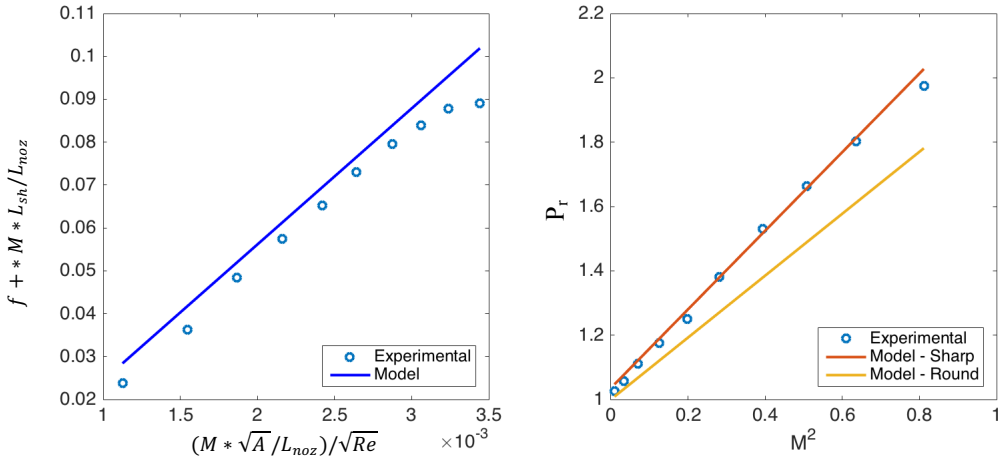

Figure 43 - Frequency Model Comparison (left) Pressure Ratio Model Comparison (right) for Machined CF PEKK FO

Figure 44 plots the normalized jet profile for the FOs manufactured using different materials at 0.00083 m^3/s flow rate and measured 8 mm from the FO. It can be seen that the aluminum M-MR-AL has a narrower jet profile than the M-MR-CF FO. However, the jet profile of Al 2, which should be identical to that of M-MR-AL, is just as wide as that of M-MR-CF. This suggests that the material does not affect the jet profile; however, the geometric variations do.

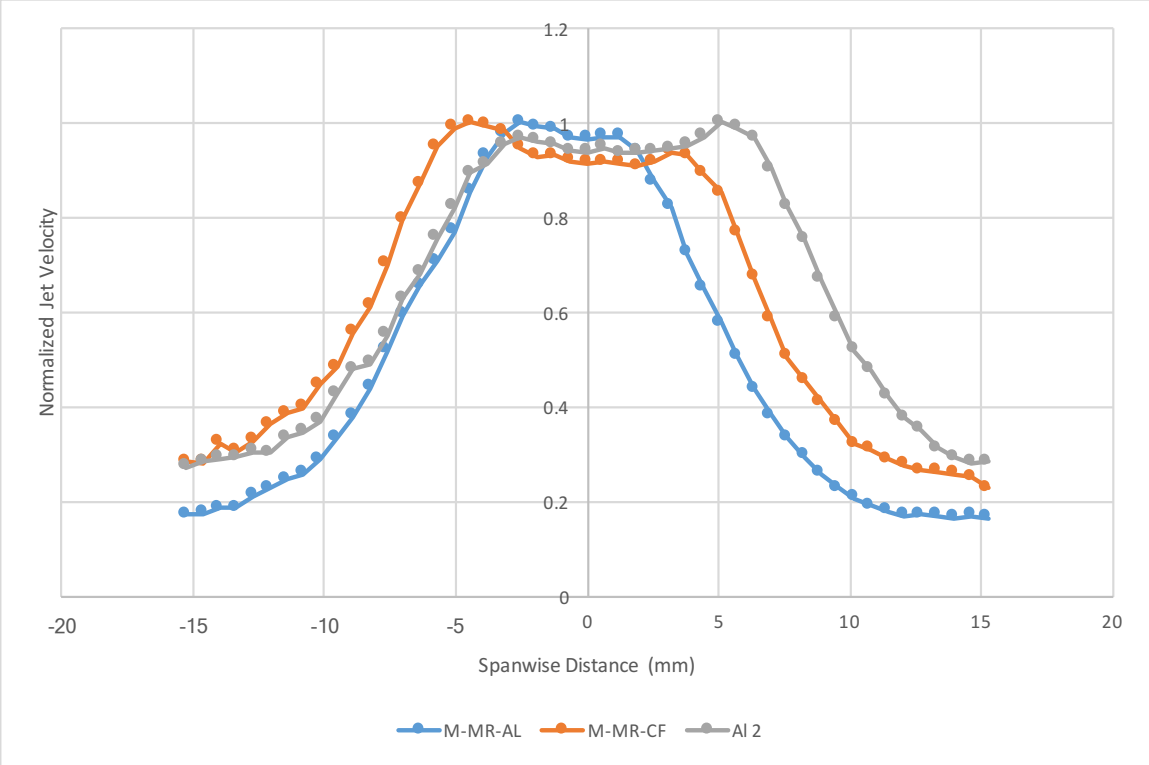

Figure 44 - Span-wise variation of the normalized jet speed along the exit plane for Materials: Aluminum (Al2, M-MR-AL) and CF PEKK (M-MR-CF)

6.2.2 Material Selection

Overall, the material does not matter when comparing the oscillation frequency, pressure drop and the jet profile of the fluidic oscillator. This is expected as the geometry is the main factor that is responsible for the performance of a feedback-free fluidic oscillator and that does not depend on the material. The surface roughness could affect the oscillation frequency, pressure drop, and jet profile of the fluidic oscillator. However, studies by Li (2016) showed no correlation between surface roughness and these characteristics. This means that FO designer is free to use any material as long as they are stiff enough to resist significant deflection and can be processed within the required

tolerances and surface finishes; however, there are other operational requirements that the designer must consider. These include the pressure, temperature, and humidity tolerance, density, and cost. CF PEKK looks to be an appropriate material for this due to the number of manufacturing processes with which it can be used, its temperature resistance, and its density; however, a drawback is its higher cost when compared to traditional materials. In the end, the designer is free to use any material that might serve the requirements.

6.3 Manufacturing Process

This section discusses the effects of the manufacturing process on the oscillation frequency, pressure drop, and jet profile of the fluidic oscillator. The experimental data of the FOs manufactured using different manufacturing process are evaluated. The data are then compared to the pre-knot point segment of the piecewise linear regression model shown in Figure 37 to determine its efficacy. The model only utilized machined aluminum FOs hence any different that is observed is likely due to the manufacturing process.

6.3.1 Process Comparison

To characterize the effect of the manufacturing process on the performance of the FOs, five different FOs were manufactured using different processes - two machined to tight tolerances, one machined each to mimic injection molding, and stereolithography and selective laser sintering. Their choice is detailed in Chapter 4. As it was determined that the material does not matter, these were manufactured using different materials.

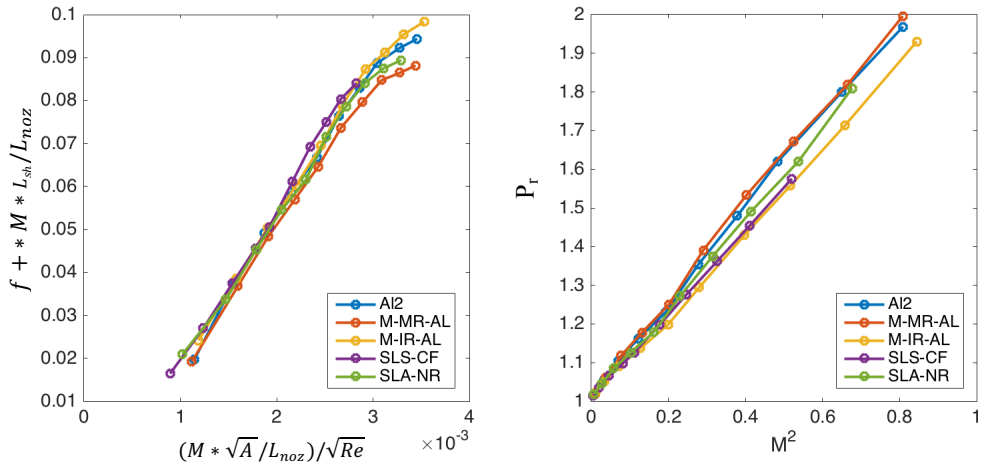

Figure 45 – Non-Dimensional Frequency Model (left) Pressure Ratio Model (right)for Processes: Machining (Al2, M-MR-AL), SLS (SLS-CF), SLA (SLA-NR), and Machined FO to mimic Injection Molding (M-IR-AL)

The graph on the left in Figure 45 plots the non-dimensional frequency model of the different FOs. It shows that there are almost no differences in the no dimensional frequencies between the FOs, indicating that the manufacturing process has no effect on the performance. The graph on the right plots the pressure ratio variation with the Mach number. It shows that the injection molding and SLS process have a slightly lower pressure ratio with the same Mach number. This was observed for the nozzles with rounded edges, which is expected as these process did not produce edges as sharp as those produced using machining. This shows that the injection molding and SLS process cannot produce the geometry to operate like machined FOs, which is the nominal FO design.

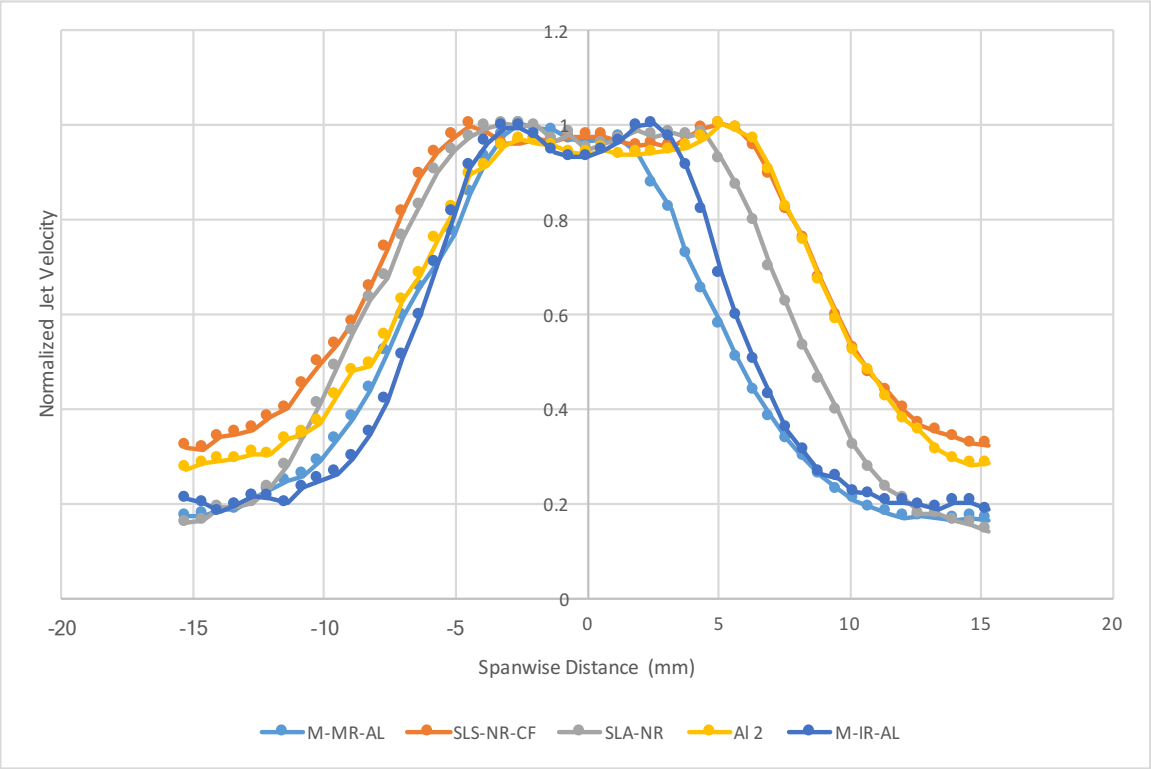

Figure 46 - Span-wise variation of the normalized jet speed along the exit plane for Processes: Machining (M-MR-AL), SLS (SLS-NR-CF), SLA (SLA-NR), and Machined FO to mimic Injection Molding (M-IR-AL)

Figure 46 plots the normalized jet profile for the FOs manufactured using the different manufacturing processes at 0.00083 m^3/s flow rate and measured 8 mm away from the FO. It can be seen that the SLS and SLA FOs have the widest jet profiles. This could be a result of the SLS and SLA FOs having a wider nozzle than the machined FO, resulting in a wider jet profile. This suggests that although the jet profile is affected by the process variation, it is because of the dimensional variation caused by the different processes.

6.3.2 Selective Laser Sintering

Figure 47 compares the model with the experimental data. The graph on the left plots the frequency model. There is an average difference of 5.95% indicating the model matches the experimental data well and effects due to process on oscillation frequency can be ignored if dimensional variations are accounted for. The graph on the right plots the pressure model and the experimental data fall between the sharp and round models. There is an average difference of 23.9% when compared to the sharp model and 15.2% when compared to the round model. This suggests that the SLS process did not produce sharp edges; however, the rounded edges that it produces do not have a radius that is as large as the VNSRN and VNLRN nozzles, which had a radius of 1/32 inches and 1/16 inches, respectively. Thus, if the designer intends to make the nominal design, the SLS process will not be appropriate.

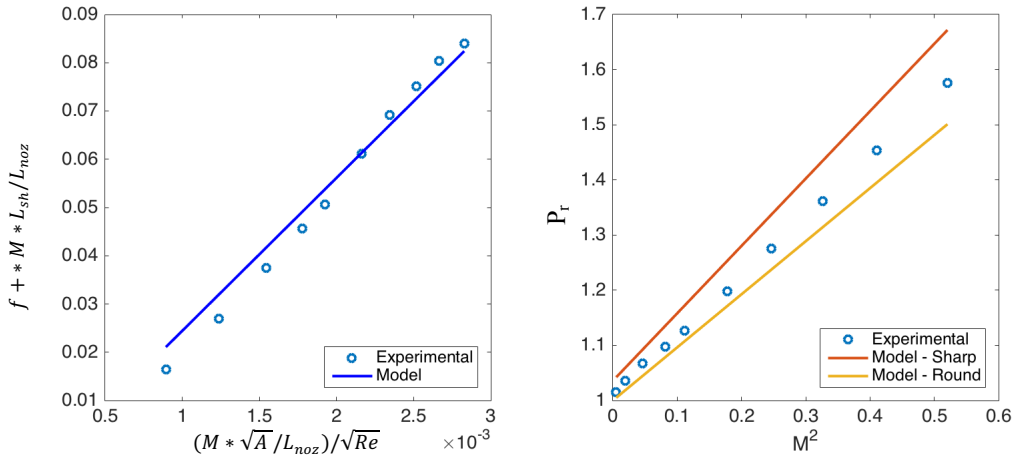

Figure 47 - Frequency Model Comparison (left) Pressure Ratio Model Comparison (right) for SLS CF PEKK FO

6.3.3 Stereolithography

Figure 48 compares the model with the actual experimental data. The graph on the left plots the frequency model. There is an average difference of 5.7% indicating the model matches the experimental data well and effects due to process on oscillation frequency can be ignored if dimensional variations are accounted for. The graph on the right plots the pressured model; the experimental data fall between the sharp and rounded models. There is an average difference of 14.1% when compared to the sharp model and 19.4% when compared to the round model. This suggests that the SLA process did not produce sharp edges; however, the rounded edges that it produces do not have a radius that is as large as the VNSRN and VNLRN nozzles, which had a radius of 1/32 inches and 1/16 inches, respectively. Additionally, the edges on the SLA part are sharper than those on the SLS FO as the error when compared to the sharp model is lower, while the error compared to the round model is greater. Thus, if the designer intends to make the nominal design, the SLA process will not be appropriate; however, it is more appropriate than the SLS process. In addition to this, the SLA FO holder experienced swelling and it is likely that an FO manufactured using the SLA process would also experience this, making it inappropriate for this application.

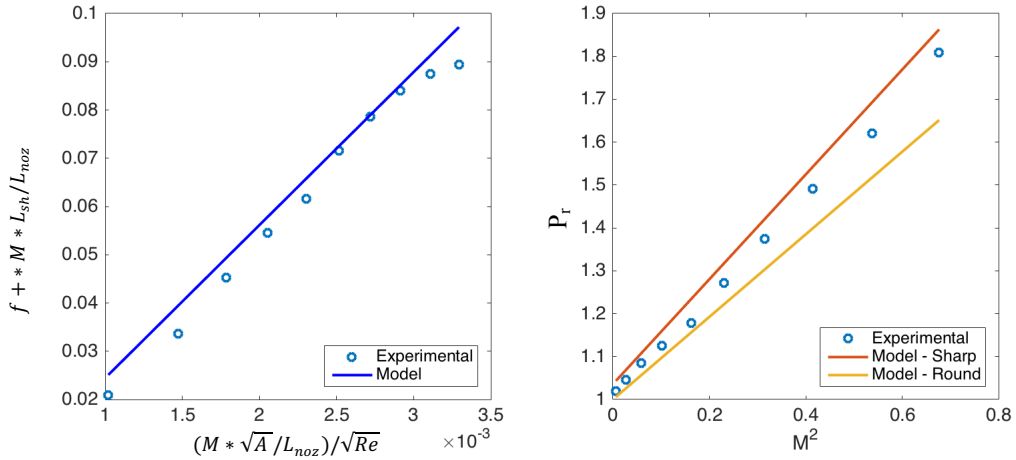

Figure 48 - Frequency Model Comparison (left) Pressure Ratio Model Comparison (right) for SLA Resin FO

6.3.4 Injection Molding

Figure 49 compares the model with the actual experimental data. The graph on the left plots the frequency model. There is an average difference of 4.3% indicating the model matches the experimental data well and effects due to process on oscillation frequency can be ignored if dimensional variations are accounted for. The graph on the right plots the pressure model and the experimental data fall between the sharp and round models. There is an average difference of 22.5% when compared to the sharp model and 11.7% when compared to the round model. This suggests that the injection molding process used did not produce sharp edges. Additionally, the edges on the injection molded part are similar to those produced using the SLS; however, they are not as sharp as those produced using

the SLA process. Thus, if the designer intends to make the nominal design, the injection molding process used here will not be appropriate.

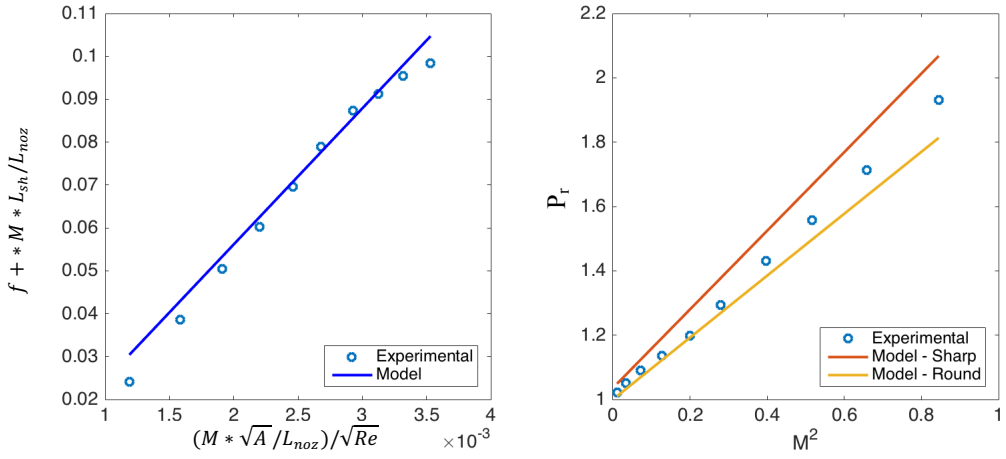

Figure 49 - Frequency Model Comparison (left) Pressure Ratio Model Comparison (right) for Machined Aluminum FO to mimic injection molded FO

6.3.5 Process Selection

In short, the nominal design of the FO can only be produced with the machining process as it features sharp edges. Thus, if the intention of the designer is to replicate this design for a full-scale manufacturing process, only machining will be appropriate. However, the results showed that rounding the nozzle of the FO reduced the pressure drop across the FO while achieving a higher oscillation frequency. This would enable the designer to achieve the same oscillation frequency for a lower fluidic power requirement. Thus, if the designer decides to integrate a rounded nozzle into the FO design, other manufacturing processes can be used to manufacture the FO. In this case, the injection

molding process will be the most appropriate due to lower cost and cycle time. The SLS process could also be used in the designer intends to vary the dimension of the FO depending on the location. Ultimately, wind tunnel tests are necessary to determine if rounding the nozzle with 1/32 inch radius would be beneficial.

6.4 Chapter Summary

To summarize, the knot frequency is dependent on the Mach number of the jet, which is a function of the flow rate, nozzle area, and the atmospheric conditions. The knot point of the piecewise linear regression model occurs at a Mach number of 0.72 for one set of data in this research and could be due to choking at the orifice; however, further testing is required to confirm this.

The nozzle width, shoulder width, and nozzle radius were found to be critical dimensions, whereas nozzle length and nozzle curvature had no effect on the performance of the FO. The nozzle width greatly affected knot point and the pressure drop across the FO. There was also a minor effect on the oscillation frequency. The shoulder width affected the oscillation frequency and the knot frequency equally. Additionally, if the interaction chamber width is controlled, an increase in the shoulder width would cause a decrease in oscillation frequency; however, the nozzle width would also increase, further decreasing the oscillation frequency. Hence, it is important to control both of these dimensions. Adding a radius to the nozzle changed the shoulder width and, as a result, affected the oscillation frequency; rounded edges reduced the flow loss, thereby reduced the pressure drop across the FO. The nozzle length had no effect on oscillation frequency and pressure

drop; however, decreasing the nozzle length narrowed the jet width. Lastly, the nozzle curvature did not have an effect the oscillation frequency, pressure drop or the jet profile.

The effects of materials and manufacturing process were also discussed. The material and how it responded to the manufacturing process did not affect the oscillation frequency, pressure drop or the jet profile, giving the designer the freedom to pick any material the fulfils the operational requirements, within the limits of the materials and processes utilized in this thesis. The manufacturing process did have an effect on the performance of the FO, due to the dimensional variation caused by the process. When these variations were input to the model, the model frequency closely matched the experimental frequency. The relationship between the flow rate did not match either model for the SLS, SLA, and injection molding, but instead fell between the two based on the sharpness of the edges. It was concluded, that if the nominal design was to be made with a process other than machining, then the SLA process would be most suitable as it had the sharpest edges. However, adding a radius to the nozzle reduced the pressure drop while increasing the oscillation frequency, which could be beneficial. Wind tunnel tests are necessary to quantify the effects of this change. In the next chapter, concluding remarks will be made for this entire work.

CHAPTER 7. CONCLUSIONS

Active flow control devices have gained popularity due to the potential benefits of applying active flow control to civil transport aircraft. McLean et al. (1998) reported that integrating flow control into aircraft flaps could lead reduction in the part count by 2.9%, empty weight by 3.3%, recurring manufacturing costs by 1.3%, and cruise drag due to weight by 1.9% when using a Boeing 737-700 aircraft as the reference. A further 1.3% reduction in cruise drag can be achieved due to the decrease in the size of fairings. Thus, integrating this technology would not only reduce the aircraft manufacturing costs but also reduce fuel consumption leading to lower emissions by the plane. Extensive research has been done on utilizing AFC to delay flow separation through a collaboration between Boeing and Georgia Tech to test the benefits of using this technology on trailing edge flaps (DeSalvo et al. 2011, Kuchan 2012, DeSalvo et al. 2014, Li 2016). They have quantified the benefits through bench and wind tunnel testing and evaluated the manufacturing and integration of this technology. However, work still needed to be done to fully quantify the effects of the material, manufacturing process and variation in geometry that are expected. Hence, that was the primary objective of this work.

After a review of AFC was conducted, the functional requirements of the FO were identified. They included the coefficient of momentum of the jet and the oscillation frequency of the oscillator. The coefficient of momentum was found to be a key factor in determining the control authority of the oscillator. Control authority refers to the ability of the FO to delay flow separation. There exists a minimum limit for the coefficient of momentum that must be reached to gain the benefits of using an FO. This limit changes

depending on the airfoil and would need to be determined using wind tunnel tests. The oscillation frequency also was found to affect the control authority of the oscillator. Two regimes exist for the frequency - the same order of magnitude as the shedding frequency and an order of magnitude greater than the shedding frequency. At frequencies an order of magnitude higher than the shedding frequency, the oscillator behaves independently of the frequency; hence, it is beneficial to operate in this region so dimensional variations do not affect the performance of the FO. The shedding frequency is dependent on the airfoil, and this would have to be calculated by the FO designer.

Operational requirements were also identified and include the fluidic power requirement, pressure in the system, temperature resistance, humidity resistance, and mass of the system. The fluidic power requirement is important as this is the amount of power that is required to drive the system. A large power requirement might negate the benefits that can be achieved by incorporating FOs, or it might not be physically possible to provide the required power. Hence, it is important to minimize the power requirement for a desired control authority. It is important to consider the pressure in the system and the FO; the air supply must be able to handle this pressure without failing or leaking. Temperature resistance is important as the FO can be exposed to large temperature fluctuations from the air source, heating by the engine exhaust, or cold temperatures at high altitudes. Humidity resistance is also important as the aircraft will be subject to many climates through its life and the FOs cannot fail due to swelling. Lastly, the weight is an important consideration, and an FO that has similar control authority while weighing less is preferred.

The materials that were studied were CF PEKK and aluminum. CF PEKK is advantageous due to the range of manufacturing processes that can be used and its ability

to withstand the expected temperatures and forces. It is also light; hence, it will not add a significant amount of mass to the system. Aluminum also has some of those benefits; however, due to its density, it might not be an appropriate material for this application. The material may respond differently to the manufacturing process hence the effect of this were quantified. Manufacturing processes that were considered included machining, injection molding, and additive manufacturing. Machining was identified as an ideal process for prototyping due to its tight tolerances and low cost, but can be expensive and slow for large-scale production. Injection molding is an ideal process for large-scale manufacturing; however, its ability to produce sharp edges needed to be characterized. Additive manufacturing is advantageous due to its ability to produce a single piece FO and change the FO geometry for different oscillators; however, it can be expensive and slow for large-scale production.

Critical dimensions were also identified and include the nozzle length, nozzle width, nozzle radius, nozzle symmetry, and interaction chamber width. Nozzle length was picked due to research done by Koklu (2016) suggested that lengthening the nozzle length positively affected the control authority. Nozzle width was picked as it was thought to affect the pressure drop across the orifice and to affect the oscillation frequency. Nozzle radius was picked as some manufacturing process cannot produce the sharp edges that are present on the nozzle. Additionally, this would affect the pressure drop across the orifice and might change the oscillation frequency of the jet as the nozzle geometry changes. Interaction chamber width was picked as a factor as the inside sharp edge present in the design cannot be manufactured using certain processes. This radius changes the size of the interaction chamber, which could affect the performance of the FO.

After the factors that could affect the FO performance were identified, test specimens were created to determine the effect of these factors. FOs were manufactured using Aluminum and Carbon Fiber PEKK using the same machining process to test the effect of the material. FOs were produced using machining, selective laser sintering, and stereolithography to test the effect of the manufacturing process. The dimensions were also varied to test the effect of dimensional variations.

To test these FOs, their tops were attached to their bodies using a cyanoacrylate glue. A FO holder was designed to hold the FO and seal the plenum so the only way for the air to leave the plenum was through the FO. Gaskets were used to seal the FO and the FO holder, which were inserted into the plenum. The flow rate, temperature, pressure, oscillation frequency, and jet profile were measured for the different FOs that were tested. In addition to measuring the operating parameters of the FO, the geometric dimensions of the FO were measured using multiple methods. A micrometer was used to measured external dimensions, while a phone camera and MATLAB setup was used to measure the internal dimensions.

Once the data were collected, the effects of variations in the different dimensions were categorized. Increasing the nozzle width increased the oscillation frequency and decreased the pressure drop. Nozzle length did not have an effect on the oscillation frequency or the pressure drop; however, increasing the nozzle length made the jet profile wider. Adding a radius increased the oscillation frequency and reduced the pressure drop. Increasing the interaction chamber width reduced the oscillation frequency and had no effect on the pressure drop. Nozzle symmetry has no effect on the oscillation frequency or

the pressure drop. Finally, it was determined that the nozzle curvature had no effect on the oscillation frequency or the pressure drop and that the jet profile was identical.

Next, an analysis of variance study was conducted to determine which factors affected the oscillation frequency and pressure drop. Nozzle width and nozzle radius were the primary contributors to variations in pressure drop. Nozzle width, nozzle radius, and the interaction chamber width were the primary contributors to variations in oscillation frequency.

Using this information, a dimensional analysis was developed to correlate the geometric dimensions and the operational characteristics of the FO to the oscillation frequency and pressure drop. The dimensionless variables that were used include the Mach number, Reynolds number, dimensionless frequency, and pressure ratio. These were used to create linear relationships; however, they were only valid until the knot point. It was identified that the FO model had knot point at a Mach number of 0.72 which corresponds to a pressure ratio of 1.67. This limit could have been caused by choking at the nozzle; however, further testing is required to make any conclusions.

A sensitivity analysis of the variation in critical dimensions was also conducted. It was found that the nozzle width significantly affects the pressure drop across the FO and the model knot point frequency of the FO, especially when the width is reduced. The shoulder width affected the oscillation frequency and the model knot point frequency of the oscillator. The nozzle radius affected pressure drop. The other dimensions had no effect on the oscillation frequency and the pressure drop. Hence, it is important to control these three dimensions. Although the oscillation frequency was affected, the imposed variation

was not large enough to affect the performance of the FO as it still operated in the same frequency regime. The nozzle length did affect the jet width; however, further testing would be required to correlate the effect of this on the control authority of the FO. Hence, it is important to control the nozzle width, shoulder length, and nozzle radius when manufacturing the FO.

The material has no effect on the performance of the FO, as long as it is stiff enough to prevent significant deflections that would change the dimensions and affect performance. The manufacturing process did have an effect on the performance of the FO due to the dimensional variation caused by the process. When these variations were input to the model, the model frequency closely matched the experimental frequency. The relationship between the flow rate and pressure drop matched neither the sharp nozzle nor the rounded nozzle models for SLS, SLA, and injection molding, but instead fell between the two based on the sharpness of the edges. It was concluded that if the nominal design was to be made without using machining, then the SLA process would be most suitable as it had the sharpest edges. However, adding a radius to the nozzle reduced the pressure drop while increasing the oscillation frequency, which would be beneficial. Wind tunnel tests are necessary to quantify the effects of this change.

7.1 Future Recommendations

The focus of this work was to predict the effect of material, manufacturing process, and dimensional variation on the performance of the FO and to use this to develop a design tool that an FO designer can use to create an FO that has the desired performance. This tool

is only valid within the data range that was tested, so testing FOs of different sizes can help validate the model at different scales. Additionally, measuring the thrust of the jet can provide insight into the jet momentum coefficient and can be measured using a load cell. This can be beneficial in getting a better insight into the performance of a FO. Additionally, the effect of changes in the jet profile and adding a radius to the nozzle should be tested in the wind tunnel.

APPENDIX A1. MATLAB CODE

A1.1 Image Processing Code

```
% Reads the image and converts to grayscale
img = imread('10-O.jpg');
img = rgb2gray(img);

% Detects the edges on the image
BW = edge(img,'Canny',[0.1 0.5]);

% Displays the image
imtool(BW)
```

A1.2 ANOVA Analysis

```
% Reads the excel file data
data = xlsread('datalevels.xlsx');
range = [1:5 9:20]

% Extracts the data
nozzleWidth = data(range,1)
nozzleLength = data(range,2)
FOWidth = data(range,3)
shlRad = data(range,4)
nozRad = data(range,5)
frequency = data(range,6)
pressure = data(range,8)

% Names the variables
names = {'Nozzle Width'; 'Nozzle Length'; 'FO Width'; ...
    'Shoulder Radius'; 'Nozzle Radius'}

% Performs ANOVA for Frequency
[P,T,STATS,TERMS] = anovan(frequency,{nozzleWidth, nozzleLength, ...
    FOWidth,shlRad, nozRad}, 'model', 'linear', ...
    'sstype', 2, 'varnames',names)

% Performs ANOVA for Frequency
[P,T,STATS,TERMS] = anovan(pressure,{nozzleWidth, nozzleLength, ...
    FOWidth,shlRad, nozRad}, 'model', 'linear', ...
    'sstype', 2, 'varnames',names)
```

A1.3 Knot Point

```
function [flow, freq, pres] = chokePoint(sw,nw,nh,r)

sw = sw./1000;
nw = nw./1000;
nh = nh./1000;

temp = 20;

M = 0.72;
area = nw.*nh;

flow = M.*(area.*((1.4*287.01*(temp+273.15)).^0.5));

Re = flow.*sw./(area.*0.000015);
x = M.*(area.^0.5./nw)./(Re.^0.5);

y = 31.711.*x - 0.0072757;
fpl = y./(M.*(sw./nw));
freq = fpl./(sw.*area./flow);

if r == 1
    y2 = 1.222.*M.^2 + 1.0358;
else
    y2 = 0.96257.*M.^2 + 1;
end

pres = (y2-1).*14.2;

end
```

A1.4 Frequency and Pressure Predictor

```
function predictor(sw, nw, nh, r, flow)

% Converts to meters
sw = sw./1000;
nw = nw./1000;
nh = nh./1000;

% Sets Constants
temp = 20;
area = nw.*nh;

% Calculates dimensionless variables
M = flow./(area.*((1.4*287.01*(temp+273.15)).^0.5));
Re = flow.*sw./(area.*0.000015);
```

```
% Calculates the Frequency
x = M.*(area.^0.5./nw)./(Re.^0.5);
y = 31.711.*x - 0.0072757;

fpl = y./(M.*(sw./nw));
Cfreq = fpl./(sw.*area./flow);

% Calculates the Pressure
if r == 1
    y2 = 1.222.*M.^2 + 1.0358;
    Cpres = (y2-1).*14.2;
else
    y2 = 0.96257.*M.^2 + 1;
    Cpres = (y2-1).*14.2;
end

% Plots the Data
figure
subplot (1,2,1)
hold on
plot(flow,Cfreq,'LineWidth',2)
set(gca,'fontsize',14)
xlabel('Flow Rate (m^3/s)')
ylabel('Frequency (Hz)')
axis square

subplot (1,2,2)
hold on
plot(flow,Cpres,'LineWidth',2)
set(gca,'fontsize',14)
xlabel('Flow Rate (m^3/s)')
ylabel('Pressure (psi)')
axis square

set(gcf,'Units','inches','Position',[0 0 12 6])

end
```

REFERENCES

3D Systems. (2016). *General Tolerance Calculator*. Retrieved from http://www.3dsystems.com/quickparts/learning-center/tolerance-calculator

Adib, A., Baptista, C., Barboza, M., Haga, C., and Marques, C. (2007). Aircraft engine bleed system tubes: Material and failure mode analysis. *Engineering Failure Analysis, 14*, 1605–1617.

Amitay, M., Smith, D. R., Kibens, V., Parekh, D. E., and Glezer, A. (2001, March). Aerodynamic Flow Control over an Unconventional Airfoil Using Synthetic Jet Actuators. *AIAA Journal, 39*(3), 361 - 370.

Becker, H., and Gärtner, C. (2008). Polymer microfabrication technologies for microfluidic systems. *Anal Bioanal Chem, 390*, 89-111.

Cattafesta III, L. N., and Sheplak, M. (2011). Actuators for Active Flow Control. *Annu. Rev. Fluid Mech, 43*, 247-272.

DeSalvo, M. (2015). *Airfoil Aerodynamic Performance Enhancement by Manipulation of Trapped Vorticity Concentrations using Active Flow Control.* Atlanta, GA: Georgia Institute of Technology.

DeSalvo, M., Whalen, E., and Glezer, A. (2011). High-Lift Enhancment using Active Flow Control . *29th AIAA Applied Aerodynamics Conference* (pp. 1-16). Honolulu, HI: AIAA.

DeSalvo, M., Whalen, E., and Glezer, A. (2014). Enhancement of a Fowler Flap High-Lift System using Active Flow Control. *52nd Aerospace Sciences Meeting* (pp. 1-19). National Harbor, MD: AIAA SciTech Forum.

Dole, C. E., and Lewis, J. E. (2000). *Flight Theory and Aerodynamics.* New York, NY: John Wiley and Sons.

Gad-el Hak, M., Pollard, A., and Bonnet, J. (1998). *Flow Control: Fundamentals and Practices.* Berlin: Springer-Verlag Berlin Heidelberg.

Gokoglu, S. A., Kuczmarski, M. A., Culle, D. E., and Raghu, S. (n.d.). Numerical Studies of a Fluidic Diverter for Flow Control. *39th AIAA Fluid Dynamics Conference* (pp. 1-14). San Antonio, TX: AIAA.

Gologan, C. (2010). *A Method for the Comparison of Transport Aircraft with Blown Flaps.* München: Technische Universität München.

Goodfellow, S. D., Yarusevych, S., and Sullivan, P. E. (2013, March). Momentum Coefficient as a Parameter for Aerodynamic Flow Control with Synthetic Jets. *AIAA Journal, 51*(3), 623-631.

Greenblatt, D., and Wygnanski, I. J. (2000). The control of #ow separation by periodic excitation. *Progress in Aerospace Sciences, 36*, 487-545.

Gregory, J. W., and Raghu, S. (2009). Variable-Frequency Fluidic Oscillator Driven by a Piezoelectric Bender. *AIAA Journal, 47*(11), 2717-2725.

Gregory, J. W., and Tomac, M. N. (2013). A Review of Fluidic Oscillator Development and Application for Flow Control. *Fluid Dynamics and Co-located Conferences. 43rd Fluid Dynamics Conference* (pp. 1-17). San Diego, CA: AIAA.

Gregory, J. W., Gnanamanickam, E. P., Sullivan, J. P., and Raghu, S. (2009, November). Variable-Frequency Fluidic Oscillator Driven by a Piezoelectric Bender. *AIAA Journal, 47*(11), 2717-2725.

Gregory, J. W., Sullivan, J. P., Raman, G., and Raghu, S. (2004). Characterization of a Micro Fluidic Oscillator for Flow Control. *2nd AIAA Flow Control Conference* (pp. 1-14). Portland, OR: AIAA.

Kalpakjian, S., and Schmid, S. R. (2008). *Manufacturing Processes for Engineering Materials.* Upper Saddle River, NJ: Pearson Education, Inc.

Kegerisea, M., Cabellb, R., and Cattafesta III, L. (2007). Real-time feedback control of flow-induced cavity tones—Part 1: Fixed-gain control. *Journal of Sound and Vibration, 307*, 906–923.

Kirschner, J. M. (1966). *Fluid Amplifiers.* New York, NY: McGraw Hill.

Koklu, M. (2016, March). Effect of a Coanda Extension on the Performance of a Sweeping-Jet Actuator. *AIAA Journal, 54*(3), 1125-1128.

Kuchan, A. (2012). *The Integration of Active Flow Control Devices into Composite Wing Flaps.* Atlanta, GA: Georgia Institute of Technology.

Lan, E. C., and Roskam, J. (1981). *Airplane Aerodynamics and Performance.* Ottawa: Roskam Aviation and Engineering.

Li, J. (2016). *Design of Active Flow Control Device Integration into a Composite Wing Flap.* Atlanta, GA: Georgia Institute of Technology.

Lin, J. C., Andino, M. Y., Alexander, M. G., Whalen, E. A., Spoor, M. A., Tran, J. T., and Wygnanski, I. J. (2016). An Overview of Active Flow Control Enhanced Vertical Tail Technology Development. *54th AIAA Aerospace Sciences Meeting* (pp. 1-13). San Diego, CA: AIAA SciTech Forum.

Mason, W. (2012). *Powered High Lift Systems Class Presentation.* Retrieved from http://www.dept.aoe.vt.edu/~mason/Mason_f/HiLiftPresPt2.pdf

McLean, J. D., Crouch, J. D., Stoner, R. C., Sakurai, S., Seidel, G. E., Feifel, W. M., and Rush, H. M. (1999). *Study of the Application of Separation Control by Unsteady Excitation to Civil Transport Aircraft.* Hampton, VA: NASA.

Meyer, M., Machunze, W., and Bauer, M. (2014). Towards the Industrial Application of Active Flow Control in Civil Aircraft - An Active Highlift. *32nd AIAA Applied Aerodynamics Conference* (pp. 1-13). Atlanta, GA: AIAA AVIATION Forum.

Mixon, J. S., Schoenster, J. A., and Willis, C. H. (1975). Fluctuating pressures on aircraft wing and flap surfaces associaed with powered-lift systems. *AIAA Journal*, 1-10.

Munson, B. R., Okiishi, T. H., Huebsch, W. W., and Rothmayer, A. P. (2013). *Fundamentals of Fluid Mechanics.* Jefferson City: John Wiley and Sons, Inc.

Oxford Performance Materials. (2016). *OXFAB® Data Sheet*. Retrieved from http://www.oxfordpm.com/oxfab®-data

Rathay, N. W., Boucher, M. J., Amitay, M., and Whalen, E. (2014). Performance Enhancement of a Vertical Tail Using Synthetic Jet Actuators. *AIAA Journal, 52*(4), 810-820.

Schultz, R., Michael, R., Dagenais, P., Fripp, M., and Tucker, J. (2008). *US Patent No. 7,404,416 B2.*

Tomac, M. N. (2013). *Internal Fluid Dynamics and Frequency Characteristics of Feedback-Free Fluidic Oscillators.* Columbus, OH: The Ohio State University.

Tomac, M. N., and Gregory, J. W. (2012). Frequency Studies and Scaling Effects of Jet Interaction in a Feedback-Free Fluidic Oscillator. *50th AIAA Aerospace Sciences Meeting including the New Horizons Forum and Aerospace Exposition* (pp. 1-15). Nashville, Tennessee: AIAA.